DISSERTATION

A SELECTION OF NITRIC OXIDE-RELEASING MATERIALS INCORPORATING *S*-NITROSOTHIOLS

Submitted by

Alec Lutzke

Department of Chemistry

In partial fulfillment of the requirements

For the Degree of Doctor of Philosophy

Colorado State University

Fort Collins, Colorado

Spring 2017

Doctoral Committee:

Advisor: Melissa Reynolds

Charles Henry
Alan Kennan
Matthew Kipper

ABSTRACT

A SELECTION OF NITRIC OXIDE-RELEASING MATERIALS INCORPORATING *S*-NITROSOTHIOLS

Nitric oxide (NO) is a diatomic radical that occurs as a crucial component of mammalian biochemistry. As a signaling molecule, NO participates in the regulation of vascular tone and maintains the natural antithrombotic function of the healthy endothelium. Furthermore, NO is produced by phagocytes as part of the immune response, and exhibits both antimicrobial and wound-healing effects. In combination, these beneficial properties have led to the use of exogenous NO as a multifunctional therapeutic agent. However, the comparatively short half-life of NO under physiological conditions often renders systemic administration infeasible. This limitation is addressed by the use of NO-releasing polymeric materials, which permit the localized delivery of NO directly at the intended site of action. Such polymers have been utilized in the development of antithrombotic or antibacterial materials for biointerfacial applications, including tissue engineering and the fabrication of medical devices. NO release from polymers has most frequently been achieved through the incorporation of functional groups that are susceptible to NO-forming chemical decomposition in response to appropriate environmental stimuli. While numerous synthetic sources of NO are known, the *S*-nitrosothiol (RSNO) functional group occurs naturally in the form of *S*-nitrosocysteine residues in both proteins and small molecule species such as *S*-nitrosoglutathione. RSNOs are synthesized directly from thiol precursors, and their NO-forming decay has generally been established to produce the

corresponding disulfide as a relatively benign organic byproduct. For these reasons, RSNOs have been conscripted as practical NO donors within a physiological environment.

This dissertation describes the synthesis and characterization of RSNO-based NO-releasing polymers derived from the polysaccharides chitin and chitosan, as well as the development of amino acid ester-based NO-releasing biodegradable poly(organophosphazenes) (POPs). The broad use of chitin and chitosan in the development of materials for tissue engineering and wound treatment results in a significant overlap with the therapeutic properties of NO. NO-releasing derivatives of chitin and chitosan were prepared through partial substitution of the carbohydrate hydroxyl groups with the symmetrical dithiols 1,2-ethanedithiol, 1,3-propanedithiol, and 1,6-hexanedithiol, followed by *S*-nitrosation. Similarly, thiol-bearing polyphosphazenes were synthesized and used to produce NO-releasing variants. Polyphosphazenes are a unique polymer class possessing an inorganic backbone composed of alternating phosphorus and nitrogen atoms, and hydrolytically-sensitive POP derivatives with organic substituents have been prepared with distinctive physical and chemical properties. Although POPs have been evaluated as biomaterials, their potential as NO release platforms has not been previous explored. This work describes the development of NO-releasing biodegradable POPs derived from both the ethyl ester of L-cysteine and the 3-mercapto-3-methylbutyl ester of glycine. The NO release properties of all polymers were evaluated at physiological temperature and pH, and the results suggested potential suitability in future biomaterials applications.

TABLE OF CONTENTS

LIST OF TABLES

LIST OF FIGURES

CHAPTER 1

INTRODUCTION

1.1. The physiological role of nitric oxide

1980 is often marked as a crucial milestone in the pharmacological history of nitric oxide (NO), following the publication of work by Furchgott and Zawadzki that demonstrated the essential role of endothelial cells in the relaxation of vascular smooth muscle.[1] This work was the first to establish a clear link between regulation of vascular tone and a then-unknown endothelium-derived relaxing factor (EDRF). The subsequent effort to identify EDRF culminated in a seminal 1987 paper by Ignarro *et al.* that demonstrated the chemical equivalence of EDRF and the diatomic radical NO.[2] In the aftermath of this discovery, NO biochemistry became a burgeoning field of study, and the 1998 Nobel Prize in Physiology or Medicine was awarded jointly to Furchgott, Ignarro, and Murad for their work in identifying the physiological importance of NO.[3] It was through the contribution of the latter co-laureate that the 19th century roots of NO pharmacology were revealed. Murad and his colleagues had been among the first to propose that nitroglycerin exerted its vasodilatory function through the biocatalyzed release of NO.[4] Since these formative studies, a clearer picture of NO's role in physiology and both its mechanism of action and breadth of potential therapeutic applications has emerged.

It is now known that the broad bioactivity of NO spans neurotransmission, regulation of vasodilation (as observed by Furchgott, Zawadski, and others), and antimicrobial effects when produced by certain phagocytes as part of the immune response.[5] NO also functions as a signaling molecule in the control of platelet activity, suppressing aggregation and preventing

thrombus formation under normal physiological conditions.[6,7] In mammals, NO production proceeds through enzymatic conversion of the amino acid L-arginine to citrulline and NO through a family of NO synthase (NOS) enzymes.[8] These isoforms include the so-called constitutive Ca^{2+}-dependent neuronal (eNOS or NOS I) and endothelial NOS (nNOS or NOS III), as well as inducible NOS (iNOS or NOS II).[9,10] Additional physiological NO generation occurs as a product of the nitrate-nitrite-nitric oxide pathway, which has been established to proceed in a NOS-independent manner.[11] NO is poorly soluble in water, exhibiting a saturated concentration of 1.7×10^{-3} M at 25 °C (p_{NO} = 1 atm).[12] In organic solvent and hydrophobic biological media (*e.g.* low-density lipoprotein), the solubility is significantly greater.[13,14] The kinetic diameter of NO (0.317 nm) is smaller than other physiologically-relevant gases, including carbon dioxide (0.330 nm) and molecular oxygen (0.346 nm).[15] The combination of lipophilicity, small size, and charge neutrality allows NO to easily permeate biomembranes.[16] NO may react within a physiological environment to produce other bioactive products, including both nitrite (NO_2^-) and nitrate (NO_3^-), as well as a multitude of reactive nitrogen species (RNS) such as peroxynitrite (ONO_2^-).[17] As a consequence, it may be difficult to distinguish between the direct effects of NO and those resulting from the action of physiological products of NO. As a comparatively stable radical, NO exhibits limited oxidative reactivity toward organic molecules and is typically incapable of hydrogen atom abstraction from hydrocarbons.[18] In a biological context, it has been observed that NO does not independently initiate lipid oxidation, and in fact inhibits propagation of lipid peroxidation through scavenging of lipid peroxyl radicals.[19] Cases of NO-related oxidative stress are therefore more accurately attributed to the formation of RNS such as peroxynitrite or nitrogen dioxide.

The mechanisms underlying the biological effects of NO are complex and subject to continuing study. In the NO-cGMP signaling pathway, binding of NO to NO-sensitive guanylyl cyclase activates the enzyme, which catalyzes the formation of cyclic guanosine 3',5'-monophosphate (cGMP) from guanosine triphosphate (GTP).[20] It is through the formation of cGMP and the influence of this effector on a variety of proteins that NO ultimately functions as a regulator of vascular tone and platelet activity.[21,22] During the normal function of the immune system, NO acts as a potent antimicrobial and tumoricidal agent. In macrophages, induction of iNOS activity by environmental stimuli (such as inflammatory cytokines) initiates production of NO.[23] This NO production is responsible for killing or inhibiting the replication of microbial pathogens and the destruction of tumor cells.[24] Although NO exhibits a degree of inherent toxicity, many of its effects are attributable to conversion of NO to peroxynitrite and other RNS through reaction with macrophage-produced superoxide (O_2^-).[25] Certain RNS are capable of inducing direct damage to microbial DNA through the chemical alteration of nucleobases, and may also impair the function of critical proteins through nitrosation and subsequent deamination of amino acid residues.[26,27] The collective effect of exposure to toxic, nitrosative RNS has been termed *nitrosative stress*, and is a major contributor to the antibacterial properties of NO.[28] It has been proposed that the ability of NO and NO-derived RNS to deleteriously affect bacteria through multiple, simultaneous chemical processes inhibits the development of meaningful resistance.[29]

NO has also been found to participate as an important factor in the wound healing process. By 1990, it had been demonstrated that supplemental L-arginine was capable of enhancing wound healing in healthy human subjects.[30] It was later observed by Bulgrin *et al.* that elimination of L-arginine from the diet of rats decreased the concentration of NO metabolites in

wounds.[31] This outcome was attributable to impaired NOS-mediated NO production as a consequence of L-arginine deficiency. In a murine model, the suppression of endogenous NO production by continuous intraperitoneal administration of NOS inhibitors lowered both the concentration of NO metabolites in wound exudate, and wound collagen accumulation.[32] Notably, Shi *et al.* found that impaired wound healing in diabetic rats could be improved by supplementation with L-arginine, suggesting the possibility of using NO to treat diabetes-related chronic wounds.[33]

Due to the numerous biological effects of endogenous NO, its conscription as a therapeutic agent was a logical progression. However, the effective physiological delivery of NO is limited by its reactivity. Although it can be safely transported and stored, administration of gaseous NO is complicated by its comparatively rapid reaction with atmospheric oxygen to form toxic nitrogen dioxide ($2\ NO + O_2 \rightarrow 2\ NO_2$).[34] Nevertheless, the direct use of inhaled gaseous NO is known as an FDA-approved treatment for pulmonary hypertension.[35] In other applications, the fundamental biochemistry of NO inhibits effective use by systemic administration. Although unreactive in deoxygenated aqueous solution, the physiological lifetime of NO is limited and dependent upon concentration.[36] Biological consumption of NO is partially attributable to reaction with molecular oxygen, a process which is generally believed to occur slowly at physiological NO concentrations, although this reaction may be accelerated in the hydrophobic regions of biological membranes.[37,38] In extravascular tissue, Thomas *et al.* estimated the half-life of NO to fall within the range of 0.09 to >2 s, depending on oxygen concentration.[38] In 1991, Borland used the known second-order rate constant for the *in vitro* reaction of NO with erythrocytes (167 $mM^{-1}\ s^{-1}$) to estimate an NO half-life of 4.6×10^{-4} s in blood.[39] Later, Liu *et al.* observed the relationship between erythrocyte concentration and consumption of NO in

phosphate buffered saline (PBS), leading to a calculated NO half-life of 1.8×10^{-3} s in whole blood.[40] In blood, the disappearance of NO is largely the outcome of reaction with oxyhemoglobin (and to a lesser extent, hemoglobin and methemoglobin), which occurs at a nearly diffusion-controlled rate.[41] A natural consequence of this bioreactivity is that the concentration of physiologically-produced NO (as in the case of generation by endothelial cells) decreases rapidly as it diffuses from the source.[42] For this reason, therapeutic NO is uniquely suited for localized delivery, where production or release of NO occurs in close proximity to the intended target site. Such an approach permits the exploitation of NO's antithrombotic, antibacterial, and wound-healing effects through the controlled administration of NO directly at biointerfaces. The pursuit of this strategy has led to the swift proliferation of NO-releasing biomaterials over the last several decades.

1.2. Applications of nitric oxide and nitric oxide donors

Identification of the biological activity of NO has led to the development of NO-releasing materials intended for a wide variety of therapeutic applications. Following implantation of a blood-contacting medical device (*e.g.* stents and catheters), the initial biological response to the presence of the foreign body includes deposition of hemostatic proteins on the surface of the device.[43] These proteins mediate a complex biochemical process that ultimately results in platelet adhesion, aggregation, and activation, leading to subsequent thrombus formation.[44,45] The clinical outcome of thrombus formation frequently includes medical complications such as obstruction or embolism, and may result in total failure of the device.[46] In the case of stents, the use of drug-eluting polymers incorporating anticoagulants such as heparin has been evaluated as one method of reducing the incidence of stent thrombosis.[47] Since NO functions as a platelet

inhibitor in a healthy, non-thrombogenic endothelium, the possibility of utilizing exogenous NO as a method of improving the blood compatibility of implantable biomaterials has been widely explored.[48] The performance of indwelling medical devices may also be compromised by bacterial infection, which is a significant source of severe complications and morbidity following implantation.[49] This process frequently results in the formation of adherent microbial biofilms that resist traditional antimicrobial treatments. During evaluation as a potential antimicrobial therapeutic, NO demonstrated potent antimicrobial effects against *Acinetobacter baumannii* (*A. baumannii*), *Escherichia coli* (*E. coli*), *Pseudomonas aeruginosa* (*P. aeruginosa*), and *Staphylococcus aureus* (*S. aureus*), among other bacterial species.[23,50] It has been observed that NO is utilized as a signaling agent in the regulation of biofilm formation in a variety of bacteria, and administered NO has been found to inhibit biofilm formation and disperse mature biofilms in species such as *P. aeruginosa*.[51] Collectively, the antithrombotic and antibacterial effects of NO have driven the pursuit of application-specific materials with NO-release capabilities. Such materials must demonstrate the ability to function as stores of releasable NO, and must consequently release that NO under an appropriate environmental stimulus.

While the adsorption and release of gaseous NO has been demonstrated with metal–organic frameworks (MOFs) and zeolites, incorporation of compounds that decompose to form NO remains the primary method of producing NO from biomaterials.[52,53] This process generally involves the blending of a suitable small molecule NO donor into a polymer, or the synthesis of a polymer that includes the donor as an integral, covalently-attached component. Certain compounds have proven more useful for this purpose than others. Although organic nitrates (such as nitroglycerin) and nitrites are known NO prodrugs, their metabolic activation requires the participation of enzymes such as mitochondrial aldehyde dehydrogenase (mtALDH).[54]

Incorporation of small molecule organic nitrates and nitrites within polymer matrices restricts this type of bioactivation, and enzymatic recognition of macromolecular equivalents cannot be assured. However, examples of topical preparations that generate NO through acidification of *inorganic* nitrites are known and have been utilized as treatments for bacterial infection.[55] In a physiological environment, sodium nitroprusside ($Na_2[Fe(CN)_5NO]$) decomposes spontaneously to form NO and has been utilized as a vasodilator since the late 1920s.[56] However, nitroprusside is metabolized to form cyanide, and has been infrequently utilized in biomaterials.[57,58] A variety of NO-releasing mesoionic heterocycles are known, including sydnonimines (such as molsidomine, a vasodilatory drug), 1,2,3,4-oxatriazolium-5-olates, and 1,2,3,4-oxatriazolium-imidates. In the case of the sydnonimines, the liberation of NO occurs through a relatively complex pathway that involves consumption of O_2 and the concomitant formation of O_2^{-}.[59] Other heterocyclic NO donors include the furoxans (1,2,5-oxadiazole-*N*-oxides) and their analogs, the 1,2,3-triazole-2-oxides. In general, the synthesis of these compounds is complex and requires multiple steps. Furthermore, their NO release is mechanistically complicated and may require biological activation (*e.g.* molsidomine) or reaction with endogenous thiols (*e.g.* furoxans).[60,61] As a consequence, these donors are rarely utilized in the development of NO-releasing materials.

In the early 1990s, work by Keefer *et al.* proposed that adducts of NO and certain secondary amines (earlier described by Drago) were capable of controlled NO release.[62] These *N*-diazeniumdiolates (NONOates) were found to exhibit vasorelaxant effects in an animal aortic ring model. By 1996, Keefer *et al.* had demonstrated the non-covalent incorporation of NONOates within polymer matrices, as well as the covalent attachment of the NO-donor group directly to the natural polysaccharide dextran and crosslinked poly(ethylenimine).[63] Grafts prepared from the latter material and poly(tetrafluoroethylene) were found to exhibit anti-platelet

effects in baboons. NONOates have subsequently been utilized as NO sources in a variety of polymer systems, ranging from polysaccharides like chitosan to biomedical grade polyurethanes.[64,65] However, the medical use of NONOate-based materials suffers from a critical drawback. The release of NO into oxygenated, aqueous solution has the potential to produce nitrosating agents such as HNO_2 or N_2O_3. In the case of NONOates, this NO release regenerates the parent secondary amine, which may subsequently react with nitrosating species to produce *N*-nitrosamines, compounds that have been identified as probable human carcinogens.[66,67] This concern has been directly addressed in the literature, where Keefer recommended restriction of *N*-bound NONOate use to compounds where the anticipated nitrosamine derivative is non-tumorigenic (*e.g. N*-nitrosoproline) or to non-biodegradable materials where toxic nitrosamines are not expected to enter physiological media.[68] In general, synthetic NO donors exhibit a wide range of useful NO release properties and have been successfully incorporated within a variety of polymers. However, examples of NO release are not solely constrained to synthetic functional groups, and one natural source in particular represents a promising and well-characterized alternative.

1.3. *S*-Nitrosothiols

S-Nitrosothiols (RSNOs) are NO-releasing compounds derived from thiols, and occur endogenously in both small molecule and protein-bound forms (primarily as *S*-nitrosated cysteine residues) (Figure 1.1).[69] RSNOs are known to decompose through thermal, photolytic, and transition metal-promoted pathways to form NO and the corresponding disulfide.[70] Among NO donors, RSNOs are unique as natural components of mammalian biochemistry. Subsequent to Ignarro's identification of NO as EDRF, Myers *et al.* argued that the behavior of EDRF was

more consistent with *S*-nitrosocysteine.[71] In 1992, Stamler *et al.* used chemiluminescence-based detection to determine an average RSNO concentration of 7 μM in human plasma, and suggested

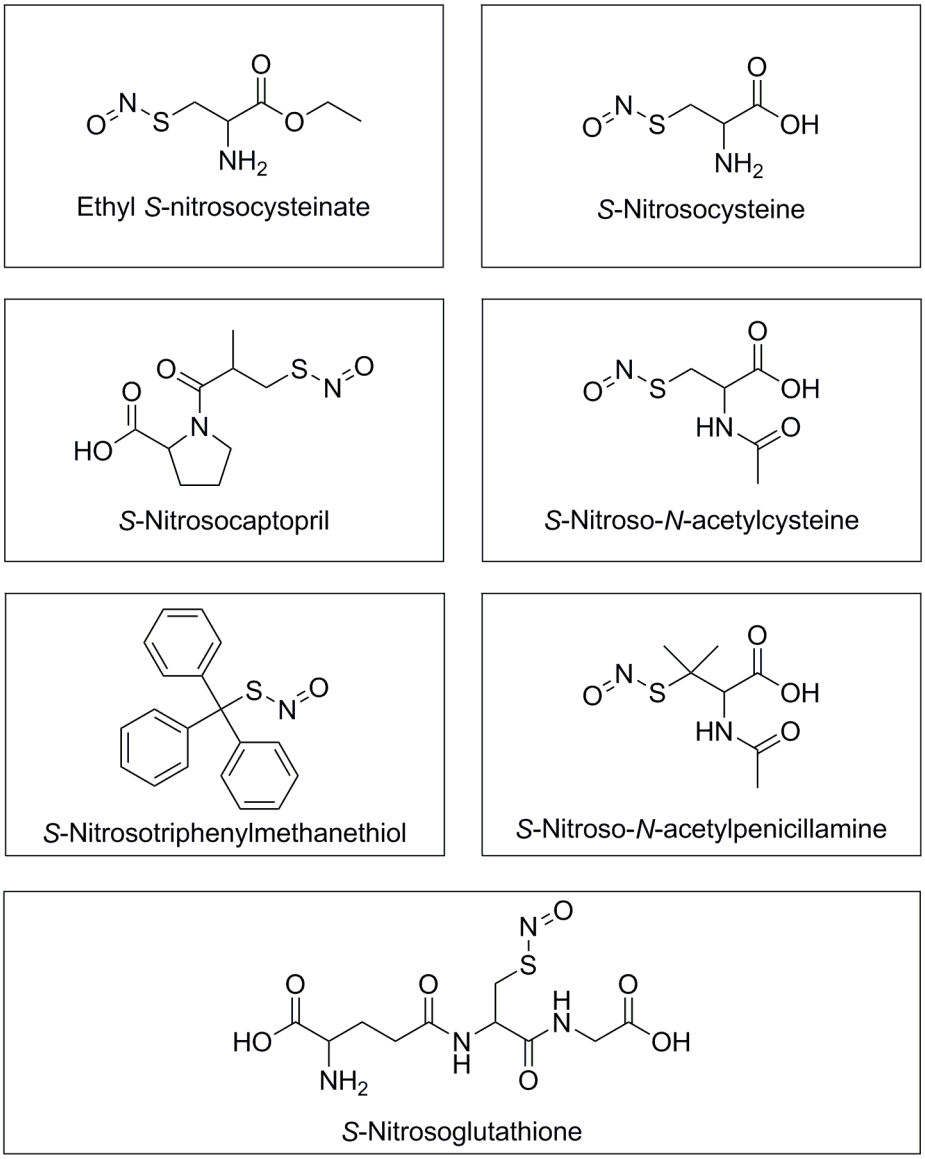

Figure 1.1 Examples of primary and tertiary *S*-nitrosothiols.

that *S*-nitrosoalbumin might serve as a physiological reservoir of NO in mammals.[72] It has since been established that RSNOs are common in mammalian physiology, primarily in the form of *S*-nitrosoalbumin and *S*-nitrosoglutathione (GSNO).[73] Nevertheless, it has proven challenging to

accurately quantify their physiological abundance, with reported concentrations that frequently range from low μM to nM.[74] Tsikas *et al.* determined an *S*-nitrosoalbumin concentration of approximately 200 nM in human plasma by GC-MS analysis of derivatized nitrite , while Tyurin *et al.* reported a significantly larger value of 4.2 μM through fluorometric assay.[75-77] More recently, Tsikas *et al.* utilized UPLC-MS/MS to quantify GSNO in human plasma, and concluded that the basal concentration was below 2.8 nM (limit of quantitation).[78] With the notable exception of reports from Stamler and Tyurin, the majority of studies indicate that basal physiological RSNO concentrations are below 1 μM, with certain methodologies yielding values below 1 *nM*.[76] Although accurate measurement of physiological RSNOs remains a developing field, their presence suggests the existence of an important biological function. In proteins, the reversible post-translational *S*-nitrosation of cysteine residues may alter their structure and activity.[79,80] It has also been proposed that endogenous RSNOs may act as storage and transport agents, through their ability to indirectly capture and later release NO.[72,81] Despite numerous studies that have examined the participation of RSNOs in various biochemical pathways, their physiological role has yet to be clearly elucidated. However, their potential biological significance and inherent physicochemical properties have led to the extensive characterization of both natural and synthetic RSNOs.

RSNOs are formed directly from thiols by the formal replacement of the proton with nitrosonium (NO^+), and have been known synthetically since a report from Tasker and Jones in 1909.[82] The conversion of thiols to RSNOs is generally rapid (approaching diffusion-limited, under certain conditions) in the presence of electrophilic nitrosating agents such as nitrous acid (HNO_2), nitrosyl chloride (NOCl), or dinitrogen trioxide (N_2O_3).[83] RSNOs may also be readily formed by the reaction of thiols with alkyl nitrites or nitrosonium tetrafluoroborate.[84] In the latter

case, the nitrosonium cation (NO^+) has been proposed as the active electrophilic species, and may also be formed during the use of other nitrosating agents under appropriately acidic conditions.[85] Morris *et al.* evaluated *S*-nitrosation kinetics for eight different thiols using sodium nitrite and perchloric acid (forming HNO_2 *in situ*), and first-order kinetics were observed with respect to thiol and acid concentration.[86] It has generally been shown that, under mildly acidic conditions, *S*-nitrosation follows the rate equation $k = [RSH][H^+][HNO_2]$, and that the nitrosating agent is $H_2NO_2^+$.[87] It is also the case that the addition of halide or pseudohalides such as thiocyanate catalyze *S*-nitrosations with HNO_2, likely through the formation of more reactive electrophiles.[86]

The RSNO group can be characterized by UV-Vis spectroscopy and exhibits a $\pi \rightarrow \pi^*$ transition centered near 330 nm, with typical molar extinction coefficients of approximately 1000 M^{-1} cm^{-1}.[87] A second, significantly less pronounced absorbance (20 M^{-1} cm^{-1}) assigned to the $n_N \rightarrow \pi^*$ transition occurs near 550 nm in primary and secondary RSNOs, and 600 nm in tertiary species. Bartberger *et al.* note that the weaker absorbance may be resolved as two distinct $n \rightarrow \pi^*$ bands with a separation of approximately 30 nm.[88] As a consequence of the visible range absorbance, RSNOs display either a red/pink (primary and secondary) or green (tertiary) color. Using IR spectroscopy, absorbance bands at approximately 1500 and 650 cm^{-1} were assigned by Arulsamy *et al*. to N=O and N-S vibrational modes.[89] Further characterization by ^1H, ^{13}C, and ^{15}N NMR spectroscopy has also been demonstrated, but is less routine and may require low temperature to improve stability of the analyte or clearly resolve certain peaks (particularly in the case of ^{15}N NMR).[89-91]

It has been proposed that the chemical behavior of RSNOs can be accurately described by three distinct resonance structures.[92] As shown in Figure 1.2, the zwitterionic structure II possesses an S-N double bond that has been calculated to significantly influence the overall

(a)

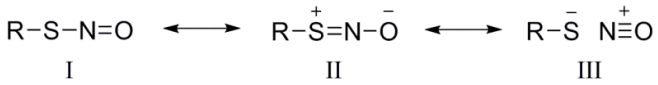

(b)

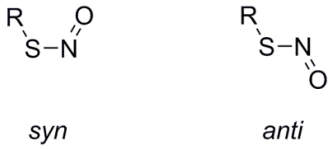

Figure 1.2 Structural characteristics of *S*-nitrosothiols. (a) Hypothesized resonance structures and (b) conformations of the *S*-nitrosothiol functional group.

character of the functional group. As predicted by this model, the RSNO group is essentially planar, and occurs in nearly isoenergetic *syn* or *anti* conformations arising from rotation around the S-N bond.[88,93] Interconversion is hindered (with an approximate 11 kcal mol^{-1} rotational barrier) and does not occur freely at room temperature, potentially supporting the argument for SNO delocalization.[88,89,92] Nevertheless, reported crystal structures generally indicate an S-N bond length of 0.18 nm, a value more consistent with S-N single bonds.[89,92] This elongation may be explained by structure III (Figure 1.2), where ion pairing is used to depict the S-N bond. The majority of computational studies support a small preference for the *syn* conformation in primary and secondary RSNOs. Yi *et al.* reported that the primary RSNO ethyl *S*-nitrosocysteinate

hydrochloride exists exclusively in the *syn* conformation, and Bartberger *et al.* observed the same behavior in *S*-nitrosocaptopril (also primary).[88,94] In contrast, the increased steric influence of the R group in tertiary RSNOs favors *anti*. As anticipated, X-ray crystallography of the tertiary RSNOs *S*-nitrosotriphenylmethanethiol and *S*-nitroso-*N*-acetylpenicillamine (SNAP) reveals an *anti* conformation in both compounds.[89,95,96]

The most commonly accepted pathway for thermal or photolytic RSNO decomposition involves scission of the S-N bond (approximately 20-32 kcal mol^{-1}) to form the corresponding thiyl radical and NO.[97] This pair may subsequently undergo unproductive geminate (or non-geminate) recombination, or two thiyl radicals may react to produce the corresponding disulfide (approximately 60 kcal mol^{-1}) and liberated NO, according to the overall equation 2 RSNO → 2 NO + RSSR.[98,99] This idealized description may not fully explain RSNO decomposition, particularly under oxygenated conditions. Notably, the disulfide-forming reaction may occur between a thiyl radical and an RSNO molecule, given the greater abundance of the latter species.[97] Furthermore, Zhao *et al.* noted that the gas phase homolytic BDEs of RSNOs typically fall within the upper end of the reported range (approximately 32 kcal mol^{-1}), predicting half-lives of years at room temperature.[100] This calculation is frequently contradicted by the experimental decomposition of many RSNOs within minutes or hours. To explain this phenomenon, Grossi *et al.* proposed that the decomposition of solution-phase RSNOs is autocatalytic and dependent upon the concentration of O_2 and NO (and therefore N_2O_3).[101] This notion was supported experimentally by the observation that the rate of decomposition was reduced by removal of either O_2 or NO from solution and enhanced by sparging with NO, leading the authors to suggest that N_2O_3 may act as a chain carrier during the decomposition process. Similarly, Zhao *et al.* proposed an autocatalytic decomposition mechanism based on

reaction with NO^+.[100] In general, inconsistent (and occasionally non-integer) kinetic observations of RSNO decomposition support a more complex pathway than the straightforward equation provided previously.

While GSNO can be readily isolated as a relatively stable solid, the majority of primary RSNOs are thermally unstable and rapidly decompose (particularly when concentrated).[102] In contrast, several isolable tertiary RSNOs have been reported to be essentially stable at ambient temperature in the absence of light. *S*-Nitroso-*N*-acetylcysteine (SNAC) and SNAP differ only by the presence of the *gem* dimethyl group in the latter compound. However, SNAP exhibits indefinite stability when isolated as a solid, while SNAC rapidly decomposes and cannot be isolated.[88,95] The explanation for the difference in stability between primary and tertiary RSNOs has been pursued by multiple researchers. Bainbrigge *et al.* utilized differential-scanning calorimetry (DSC) and thermogravimetric analysis (TGA) to observe that both SNAP and GSNO experience an NO-forming decomposition at 148 °C.[102] This result may indicate a similar S-N bond strength for both compounds. Furthermore, Grossi *et al.* found that the thermal stability of tertiary RSNOs was generally *lower* than their less substituted equivalents.[103] It was therefore reasoned that the remarkable stability of tertiary RSNOs may arise from an alternative explanation, such as the manifestation of steric effects during dimerization of thiyl radicals bearing a proximal *gem* dimethyl group. This argument was supported computationally by the calculation of an unusually high-energy, sterically congested conformation during formation of the disulfide bond.[102] It was observed by de Oliveira *et al.* that RSNO concentration influences the rate of decomposition in a complex manner.[104] When evaluating the stability of *S*-nitrosocysteine, SNAC, and GSNO in aqueous solution, it was found that a ten-fold increase in RSNO concentration (from 1×10^{-4} to 1×10^{-3} M) decreased the rate of decomposition by an

order of magnitude for all three substrates. This result was attributed to an increase in the rate of non-geminate radical recombination at elevated concentration. A final increase in concentration to 6.1×10^{-2} M significantly *accelerated* the decomposition, which was argued to be a consequence of the autocatalytic reaction $RS\cdot + RSNO \rightarrow RSSR + NO$. However, the outcome of many kinetic studies of RSNO decomposition must be evaluated with the knowledge that experimental conditions (particularly with respect to O_2/NO or transition metal ion concentration) may significantly influence the data. In the mid-1990s, Williams proposed that solution-phase RSNO decomposition was primarily induced by the presence of trace copper ions at concentrations as low as 10^{-6} M.[98] This reasoning was supported by the observation that the addition of ethylenediaminetetraacetic acid (EDTA) to aqueous RSNO inhibited or entirely prevented decomposition. It is now understood that copper readily catalyzes the NO-forming decomposition of RSNOs. Use of selective copper(I) chelators such as neocuproine demonstrate that Cu^+ is the active species, which may be formed from copper(II) salts by reduction in the presence of trace thiol.[98] The susceptibility of RSNOs to metal-accelerated decompositon is by no means limited to copper ions. It has been observed that Fe^{2+} exerts a small, but detectable, effect on both the formation and decomposition of RSNOs.[105] Furthermore, both mercury (Hg^{2+}) and silver (Ag^+) ions have been found to greatly accelerate RSNO decomposition in a non-catalytic fashion.[106] It has been shown that coordination of transition metals to the sulfur atom of the RSNO functional group decreases the S-N bond strength, thereby promoting homolytic dissociation. However, the precise mechanism through which transition metals are operative as RSNO decomposition catalysts remains unknown.

1.4. Reactivity considerations in the development of *S*-nitrosated polymers

A wide variety of RSNO-based NO-releasing biomaterials have been proposed for antithrombotic, antibacterial, and wound-healing applications. In 2000, Bohl and West reported the polymeric incorporation of the amino acid cysteine within a poly(ethylene glycol)-based hydrogel.[107] The subsequent *S*-nitrosation of this hydrogel using $NaNO_2$ at low pH produced an NO-generating material with reported antiplatelet effects. In a second early example, cysteine was conjugated to both polyethylene terephthalate and medical grade polyurethane and converted to the corresponding RSNO by treatment with $NaNO_2$/HCl, producing surfaces with reduced platelet adhesion relative to controls.[108] Later reports of RSNO-based materials have included NO-releasing polysiloxanes and polysaccharides with antibacterial activity, as well as numerous biodegradable polyesters proposed for applications ranging from the fabrication of erodible medical devices to tissue engineering.[109-114] Furthermore, macromolecular RSNOs have been demonstrated to improve outcomes in wound-healing applications.[115] It has generally been shown that the use of RSNO-based biomaterials produces effective platforms for the controlled release of NO for therapeutic purposes. However, the attachment of covalently-bound thiols to polymers and their subsequent conversion to RSNO derivatives results in several unique synthetic considerations. Thiol groups are readily oxidized to disulfide, and this process may result in crosslinking that alters the physical and chemical properties of polymers.[116,117] Several oxidants are known to effect this transformation, including molecular oxygen and iodine, while copper and iron ions are known to catalytically accelerate the reaction.[118-120] In the case of molecular oxygen, disulfide formation may occur more rapidly in DMF under basic conditions.[121] Moreover, disulfide may be produced through simple heating of thiols in the presence of DMSO.[122]

In the case of structurally complex polymers containing multiple functional groups, it cannot be presumed that nitrosating agents will selectively produce *S*-nitrosation. Exposure of primary aromatic amines to nitrous acid will result in the formation of unstable diazonium salts.[123] Primary aliphatic amines undergo diazotization followed by the rapid elimination of nitrogen gas, as exploited in the Demjanov and Tiffeneau-Demjanov rearrangements.[124,125] In the case of secondary aliphatic amines, stable (and potentially carcinogenic) *N*-nitrosamines are directly formed, while tertiary aliphatic amines slowly react in a dealkylative process that generates a secondary *N*-nitrosamine, carbonyl compound, and nitrous oxide.[66,126,127] Even subsequent to RSNO formation, certain structures (*e.g.* *S*-nitrosocysteine) may undergo transnitrosation reactions that result in diazotization of the amine group.[128] *N*-Nitrosation is not confined to amines, but also occurs in amides and other weakly nucleophilic nitrogen-containing functional groups.[129-132] Hydroxyl groups react in the presence of nitrous acid and other nitrosating species to form alkyl nitrites, which are independently capable of further nitrosation chemistry.[83,133] Notably, this brief list encompasses functional groups that are reasonably expected to occur in polyesters, polysaccharides, polyurethanes, and many other polymers used to develop RSNO-based NO delivery platforms. Because there is a significant possibility that alternative nitrosation reactions may occur, it is critical to employ all practical characterization techniques in evaluating RSNO-based materials to ensure the retention of structure.

1.5. Measurement of nitric oxide from *S*-nitrosothiol decomposition

Characterization of the NO release properties of small molecule RSNOs is a crucial step in evaluating their pharmacological activity. In the case of RSNO-based polymeric biomaterials, quantification of the total amount of releasable NO is used to determine

their NO storage capabilities. Furthermore, measurement of NO release as a function of time permits assessment of the material's performance as a source of therapeutic NO. To improve the biological relevance of such measurements, RSNOs are frequently incubated at physiological temperature and pH during the NO release period. The decomposition of RSNOs themselves may be measured spectrophotometrically, and has been related to the formation of NO through the equation 2 RSNO → 2 NO + RSSR.[134] As described previously, it is possible to directly monitor the decay of RSNOs using characteristic absorptions occurring at 330 ($\pi \rightarrow \pi^*$) and 550-600 nm ($n_N \rightarrow \pi^*$), with respective molar extinction coefficients of approximately 1000 and 20 M^{-1} cm^{-1}.[87] In certain examples, it has been observed that this decay is accompanied by the appearance of an absorbance at approximately 250 nm that arises from disulfide bond formation.[135] The RSNO absorbance centered near 330 nm is subject to interference from other species, including inorganic nitrite, nitrous acid, alkyl nitrites, and *N*-nitroso compounds.[81,136,137] The 50-fold weaker absorbance at 550-600 nm may not be resolved at low concentrations. Moreover, the molar extinction coefficients of macromolecular RSNOs may differ significantly from small molecule counterparts, and must be independently determined.[138] Because the rate of RSNO decomposition is altered by dissolution, solution-phase UV-Vis measurements of macromolecular RSNOs are unlikely to correspond to their NO release properties as solids.[83] RSNO decomposition has also been shown to occur without the concomitant formation of NO in certain cases, particularly at high thiol concentration.[139,140] For this reason, it should not be presumed *a priori* that a useful relationship exists between RSNO decomposition and NO formation in the absence of independent verification.

In general, reliable measurement of NO release from RSNO decomposition requires detection of NO itself or the byproducts of NO decomposition (*e.g.* nitrite). Multiple NO measurement techniques have been developed, and the majority can be employed (with varying degrees of reliability) to quantify NO release from RSNOs. Although it is possible to observe NO directly with electron paramagnetic resonance (EPR), in practice it is necessary to utilize spin trapping to form stable adducts that are easier to observe and quantify.[141] Most commonly, the routine measurement of NO release from RSNOs relies on colorimetric/fluorometric, electrochemical, or chemiluminescence-based methods. Since NO decomposes to form nitrite under aqueous, oxygenated conditions, nitrite quantification has frequently been used to indirectly measure the amount of NO formed within a solution. The Griess assay is a common colorimetric method of quantifying nitrite, and proceeds through acidification of nitrite to form nitrous acid.[142,143] Reaction of nitrous acid with sulfanilic acid produces the corresponding diazonium compound, which is coupled to a suitable aromatic amine to generate an azo dye. This technique may also include a *nitrate* (another NO oxidation product) reduction step to fully quantify NO release.[144] In general, limits of detection of approximately 500 nM are reported for the Griess assay.[145] The Griess assay is not selective, and will quantify nitrite from all sources, including that which is unrelated to the decomposition of RSNOs. Since RSNOs are almost exclusively synthesized using nitrite or nitrite-forming reagents, the potential for contamination and false positives is evident. Furthermore, certain functional groups besides RSNO (*e.g.* alkyl nitrites) can be expected to hydrolyze to form nitrite under the conditions of the Griess assay.[146] To permit improved discrimination between nitrite sources, the Saville-Griess assay has been employed to selectively decompose RSNOs. In 1958, Saville observed that the addition of mercury(II) or silver(I) salts to aqueous RSNO resulted in rapid hydrolysis to nitrite.[147] The

Saville-Griess assay exploits this phenomenon through the reaction of RSNOs with mercury, followed by the generation of an azo dye as in the traditional Griess assay.[148] The amount of nitrite arising from RSNO decomposition has therefore been calculated as the difference between the Saville-Griess and standard Griess protocols. Fluorescent probes have also been utilized in the indirect fluorometric measurement of NO at concentrations as low as the nM range.[145] These probe molecules are typically derived from 4,5-diaminofluorescein (DAF), and rely on the reaction of NO oxidation products (*e.g.* N_2O_3) to form a fluorescent triazole.[149] Since these techniques typically require expensive reagents and are uniquely suited to the detection of intracellular NO, they are not generally used to characterize NO-releasing materials.

The indirect colorimetric or fluorometric determination of NO does not permit the active monitoring of NO formation as it occurs. In contrast, real-time measurement of NO release is achievable using electrochemical or chemiluminescence-based methods. Typically, electrochemical NO measurement proceeds through the electrooxidation of NO to nitrite, according to the equations shown below.[150]

$$NO \rightarrow NO^+ + e^-$$

$$NO^+ + OH^- \rightarrow HNO_2$$

$$HNO_2 + H_2O \rightarrow NO_3^- + 2e^- + 3H^+$$

Electrochemical techniques are generally reported to have limits of detection in the pM to low nM range, and the *theoretical* measurement of as little as 10^{-20} mol NO has been previously

proposed for a porphyrinic microsensor with a detection limit of 10 nM.[151,152] Common interferences include anionic species such as ascorbate and nitrite, however these species may be excluded from the electrode by the use of selective membranes.[153] The electrochemical measurement of NO is possible within living tissue, and has been utilized to evaluate biological production of NO *in vivo*.[154,155] It has been established that RSNOs themselves may be detected by electrochemical reduction, although this method does not result in the production of NO at physiological pH.[156,157] Despite the established performance of electrochemical detection methods, quantification of NO by chemiluminescence is more frequently used to characterize NO release from RSNO-based materials. The chemiluminescent reaction between NO and ozone ($NO + O_3 \rightarrow NO_2^* + O_2$) was originally reported in 1949 by Tanaka and Shimayu, and later characterized by Greaves and Garvin in 1958.[158,159] The broad emission arising from the relaxation of excited-state NO_2 occurs primarily in the red/infrared range, with a short wavelength limit of 590 nm, as described by Clyne *et al.*[160] The chemiluminescent intensity is proportional to the pressures of NO and O_3, and inversely proportional to total pressure (resulting from collisional deactivation), requiring the use of partial vacuum within the reaction chamber for reliable detection.[161] In a typical procedure, an inert carrier gas is used to transfer NO from an external cell containing the sample to the reaction chamber within the instrument, which is maintained at reduced pressure. This chamber is supplied with ozone, and photons from the resulting chemiluminescent reaction pass through a filter (eliminating higher frequency light from potential side reactions) before reaching the detector. The transduction of this light emission has been widely used to measure NO from the decomposition of RSNOs under a variety of conditions, including directly within biological media such as plasma and whole blood at concentrations in the low nM range.[162] Nitrite formed by the prior decomposition of RSNOs

may be reduced to NO using iodide or vanadium(III) under acidic conditions and detected by chemiluminescence.[163-164] Furthermore, the *real-time* NO-forming decomposition of RSNOs may be monitored. In the case of overall NO determination, this decomposition can be accelerated through photolytic cleavage of the S-N bond by irradiation with UV light, or with the addition of copper ions.[165,166] In all examples, the detection of RSNOs suffers from the notable drawback that it must be conducted under anaerobic conditions to avoid the premature consumption of NO. The absence of molecular oxygen and the fact that NO is continuously purged by inert gas from sample solutions containing dissolved or suspended RSNO may exert a considerable influence on the observed decomposition kinetics.[101,103] Nevertheless, chemiluminescence-based analysis has been described as the gold standard in NO measurement, and remains a widely used approach to the characterization of NO release from RSNOs.[167]

1.6. Dissertation overview

This dissertation focuses on the synthesis and characterization of multiple RSNO-based NO-releasing polymers obtained from the polysaccharides chitin and chitosan, as well as from synthetic polyphosphazenes. Chitin is a biopolymer that primarily consists of *N*-acetylglucosamine units, and occurs naturally in structures as diverse as the shells of crustaceans and the cell walls of fungi.[168,169] Chitosan is produced from the amine-forming deacetylation of chitin and has been widely utilized as a biomaterial for its hemostatic and antimicrobial properties.[168,170] Preparation of NO-releasing chitosan has largely been confined to the conjugation of NO donor groups to the primary amine groups of oligosaccharidic forms, which have been explored for antibacterial applications.[171,172] In Chapter 2, the concept of modifying

the polysaccharides chitin and chitosan to include NO-donating RSNO moeities through replacement of *hydroxyl groups* is explored.

Polyphosphazenes are a unique class of polymers containing an inorganic phosphorus-nitrogen backbone, and are frequently substituted with variable organic pendant groups to confer new physical and chemical properties.[173] In the mid-1960s, Allcock and Kugel first described the preparation of amine-substituted polyphosphazenes, which led to the subsequent development of biodegradable polyphosphazenes with amino acid ester substituents by 1977.[174,175] Early examples included polymers bearing pendant groups derived from alkyl esters of glycine, alanine, and phenylalanine.[176] Allcock *et al.* proposed that such materials would undergo hydrolytic degradation to harmless or metabolizable products that could lead to their use as implantable biomaterials.[176,177] Biodegradable amino acid ester-based polyphosphazenes have since been subjected to a variety of *in vitro* and *in vivo* studies that demonstrate their potential utility for tissue engineering, drug delivery, and other biomedical applications.[178-180] Chapters 3 and 4 of this dissertation describe work toward the development of RSNO-based NO-releasing polyphosphazenes with amino acid ester substituents derived from cysteine and glycine.

REFERENCES

1. Furchgott, R. F.; Zawadzki, J. V. *Nature* **1980**, *288*, 373-376.
2. Ignarro, L. J.; Buga, G. M.; Wood, K. S.; Byrns, R. E. Chaudhuri, G. *Proc. Natl. Acad. Sci. USA* **1987**, *84*, 9265-9269.
3. SoRelle, R. *Circulation* **1998**, *98*, 2365-2366.
4. Katsuki, S.; Arnold, W.; Mittal, C.; Murad, F. *J. Cyclic Nucl. Res.* **1977**, *3*, 23-35.
5. Xu, W. M.; Liu, L. Z. *Cell Res.* **1998**, *8*, 251-258.
6. Wang, G.-R.; Zhu, Y.; Halushka, P. V.; Lincoln, T. M.; Mendelsohn, M. E. *Proc. Natl. Acad. Sci. USA* **1998**, *95*, 4888-4893.
7. Gkaliagkousi, E.; Ritter, J.; Ferro, A. *Circ. Res.* **2007**, *101*, 654-662.
8. Andrew, P. J.; Mayer, B. *Cardiovasc. Res.* **1999**, *43*, 521-531.
9. Förstermann, U.; Boissel, J. P.; Kleinert, H. *FASEB J.* **1998**, *12*, 773-790.
10. Kröncke, K.-D.; Fehsel, K.; Kolb-Bachofen, V. *Clin. Exp. Immunol*. **1998**, *113*, 147-156.
11. Weitzberg, E.; Hezel, M.; Lundberg, J. O. *Anesthesiology* **2010**, *113*, 1460-1475.
12. Bonner, F. T. *Methods Enzymol.* **1996**, *268*, 50-57.
13. Shaw, A. W.; Vosper, A. J. *J. Chem. Soc., Faraday Trans. 1* **1977**, *73*, 1239-1244.
14. Möller, M.; Botti, H.; Batthyany, C.; Rubbo, H.; Radi, R.; Denicola, A. *J. Biol. Chem.* **2005**, *280*, 8850-8854.
15. Rubel, A. M.; Stencel, J. M. *Energy Fuels* **1996,** *10*, 704-708.
16. Malinski, T.; Taha, Z.; Grunfeld, S. *Biochem. Biophys. Res. Commun*. **1993**, *193*, 1076-1082.
17. Kelm, M. *Biochim. Biophys. Acta* **1999**, *1411*, 273-289.

18. Darley-Usmar, V. M.; Hogg, N.; O'Leary, V. J.; Wilson, M. T.; Moncada, S. *Free Radic. Res. Commun.* **1992**, *17*, 9-20.

19. Hogg, N.; Kalyanaraman, B. *Biochim. Biophys. Acta*, **1999**, *1411*, 378-384.

20. Russwurm, M.; Koesling, D. *EMBO J.* **2004**, *23*, 4443-4450.

21. Archer, S. L.; Huang, J. M. C.; Hampl, V.; Nelson, D. P.; Shultz, P. J.; Weir, E. K. *Proc. Natl. Acad. Sci. USA* **1994**, *91*, 7583-7587.

22. Feil, R.; Kemp-Harper, B. *EMBO Rep.* **2006**, *7*, 149-153.

23. Schairer, D. O.; Chouake, J. S.; Nosanchuk, J. D.; Friedman, A. J. *Virulence* **2012**, *3*, 271-279.

24. Bogdan, C. *Nat. Immunol.* **2001**, *2*, 907-916.

25. Wink, D. A.; Mitchell, J. B. *Free Radic. Biol. Med*. **1998**, *25*, 434-456.

26. Fang, F. C. *J. Clin. Invest.* **1997**, *99*, 2818-2825.

27. Ohshima, H. *Toxicol. Lett.* **2003**, *140-141*, 99-104.

28. Heinrich, T. A.; da Silva, R. S.; Miranda, K. M.; Switzer, C. H.; Wink, D. A.; Fukuto, J. M. *Br. J. Pharmacol.* **2013**, *169*, 1417-1429.

29. Privett, B. J.; Broadnax, A. D.; Bauman, S. J.; Riccio, D. A.; Schoenfisch, M. H. *Nitric Oxide* **2012**, *26*, 169-173.

30. Barbul, A.; Lazarou, S. A.; Efron, D. T.; Wasserkrug, H. L.; Efron, G. *Surgery* **1990**, *108*, 331-337.

31. Bulgrin, J. P.; Shabani, M.; Smith, D. J. *J. Nutr. Biochem.* **1993**, *4*, 588-593.

32. Schaffer, M. R.; Tantry, U.; Gross, S. S.; Wasserburg, H. L.; Barbul, A. *J. Surg. Res.* **1996**, *63*, 237-240.

33. Shi, H. P.; Most, D.; Efron, D. T.; Witte, M. B.; Barbul, A. *Wound Repair Regen.* **2003**, *11*, 198-203.

34. Aga, R. G.; Hughes, M. N. *Methods Enzymol.* **2008**, *436*, 35-48.

35. Ichinose, F.; Roberts, J. D., Jr.; Zapol, W. M. *Circulation* **2004**, *109*, 3106-3111.

36. Ford, P. C.; Wink, D. A.; Stanbury, D. M. *FEBS Lett.* **1993**, *326*, 1-3.

37. Liu, X.; Miller, M. J. S.; Joshi, M. S.; Thomas, D. D.; Lancaster, J. R., Jr. *Proc. Natl. Acad. Sci. USA* **1998**, *95*, 2175-2179.

38. Thomas, D. D.; Liu, X.; Kantrow, S. P.; Lancaster, J. R., Jr. *Proc. Natl. Acad. Sci.* USA **2001**, *98*, 355-360.

39. Borland, C. *Br. Heart J.* **1991**, *66*, 405-407.

40. Liu, X.; Miller, M. J. S.; Joshi, M. S.; Sadowska-Krowicka, H.; Clark, D. A.; Lancaster, J. R., Jr. *J. Biol. Chem.* **1998**, *273*, 18709-18713.

41. Silaghi-Dumitrescu, R.; Scurtu, F.; Mason, M. G.; Svistunenko, D. A.; Wilson, M. T.; Cooper, C. E. *Inorg. Chim. Acta* **2015**, *436*, 179-183.

42. Ignarro, L. J., Ed. *Nitric Oxide: Biology and Pathobiology*, 2nd ed; Elsevier: Amsterdam, 2010; p 14.

43. Horbett, T. A. *Cardiovasc. Pathol.* **1993**, *2*, 137S-148S.

44. Ikeda, Y.; Handa, M.; Kawano, K.; Kamata, T.; Murata, M.; Araki, Y.; Anbo, H.; Kawai, Y.; Watanabe, K.; Itagaki, I. Sakai, K.; Ruggeri, Z. M. *J. Clin. Invest.* **1991**, *87*, 1234-1240.

45. Gorbet, M. B.; Sefton, M. V. *Biomaterials* **2004**, *25*, 5681-5703.

46. Hanson, S. R. *Cardiovasc. Pathol.* **1993**, *2*, 157S-165S.

47. Haude, M.; Konorza, T. F.; Kalnins, U.; Erglis, A.; Saunamäki, K.; Glogar, H. D.; Grube, E.; Gil, R.; Serra, A.; Richardt, H. G.; Sick, P.; Erbel, R. *Circulation* **2003**, *107*, 1265-1270.

48. Fleser, P. S.; Nuthakki, V. K.; Malinzak, L. E.; Callahan, R. E.; Seymour, M. L.; Reynolds, M. M.; Merz, S. I.; Meyerhoff, M. E.; Bendick, P. J.; Zelenock, G. B.; Shanley, C. J. *J. Vasc. Surg.* **2004**, *40*, 803-811.

49. Ribeiro, M.; Monteiro, F. J.; Ferraz, M. P. *Biomatter.* **2012**, *2*, 176-194.

50. De Groote, M. A.; Fang, F. C. *Clin. Infect. Dis.* **1995**, *21*, S162-S165.

51. Arora, D. P.; Hossain, S.; Xu, Y.; Boon, E. M. *Biochemistry* **2015**, *54*, 3717-3728.

52. Huxford, R. C.; Rocca, J. D.; Lin, W. *Curr. Opin. Chem. Biol.* **2010**, *14*, 262-268.

53. Fox, S.; Wilkinson, T. S.; Wheatley, P. S.; Xiao, B.; Morris, R. E.; Sutherland, A.; Simpson, A. J.; Barlow, P. G.; Butler, A. R.; Megson, I. L.; Rossi, A. G. *Acta Biomater.* **2010**, *6*, 1515-1521.

54. Chen, Z.; Zhang, J.; Stamler, J. S. *Proc. Natl. Acad. Sci. USA* **2002**, *99*, 8306-8311.

55. Ormerod, A. D.; Shah, A. A..; Li, H.; Benjamin, N. B.; Ferguson, G. P.; Leifert, C. *BMC Res. Notes* **2011**, *4*, 458.

56. Friederich, J. A.; Butterworth, J. F. IV *Anesth. Analg.* **1995**, *81*, 152-162.

57. Smith, R. P.; Kruszyna, H. *J Pharmacol. Exp. Ther.* **1974**, *191*, 557-563.

58. Yoon, J.; Wu, C.-J.; Homme, J.; Tuch, R. J.; Wolff, R. G.; Topol, E. J.; Lincoff, A. M. *Yonsei Med. J.* **2002**, *43*, 242-251.

59. Feelisch, M.; Ostrowski, J.; Noack, E. *J. Cardiovasc. Pharmacol.* **1989**, *14*, S13-S22.

60. Schönafinger, K. *Farmaco* **1999**, *54*, 316-320.

61. Gasco, A.; Fruttero, R.; Sorba, G.; Di Stilo, A.; Calvino, R. *Pure Appl. Chem.* **2004**, *76*, 973-981.

62. Maragos, C. M.; Morley, D.; Wink, D. A.; Dunams, T. M.; Saavedra, J. E.; Hoffman, A.; Bove, A. A.; Isaac, L.; Hrabie, J. A.; Keefer, L. K. *J. Med. Chem.* **1991**, *34*, 3242-3247.

63. Smith, D. J.; Chakravarthy, D.; Pulfer, S.; Simmons, M. L.; Hrabie, J. A.; Citro, M. L.; Saavedra, J. E.; Davies, K. M.; Hutsell, T. C.; Mooradian, D. L.; Hanson, S. R.; Keefer, L. K. *J. Med. Chem.* **1996**, *39*, 1148-1156.

64. Lu, Y.; Slomberg, D. L.; Schoenfisch, M. H. *Biomaterials* **2014**, *35*, 1716-1724.

65. Reynolds, M. M.; Hrabie, J. A.; Oh, B. K.; Politis, J. K.; Citro, M. L.; Keefer, L. K.; Meyerhoff, M. E. *Biomacromolecules* **2006**, *7*, 987-994.

66. Bartsch, H.; Montesano, R. *Carcinogenesis* **1984,** *5*, 1381-1393.

67. Tricker, A. R.; Preussmann, R. *Mutat. Res.* **1991**, *259*, 277-289.

68. Keefer, L. K. *ACS Chem. Biol.* **2011**, *6*, 1147-1155.

69. Zhang, Y.; Hogg, N. *Free Radic. Biol. Med.* **2005**, *38*, 831-838.

70. Singh, R. J.; Hogg, N.; Joseph, J.; Kalyanaraman, B. *J. Biol. Chem.* **1996**, *271*, 18596-18603.

71. Myers, P. R.; Minor, R. L., Jr.; Guerra, R., Jr.; Bates, J. N.; Harrison, D. G. *Nature* **1990**, *345*, 161-163.

72. Stamler, J. S.; Jaraki, O.; Osborne, J.; Simon, D. I.; Keaney, J.; Vita, J.; Singel, D.; Valeri, C. R.; Loscalzo, J. *Proc. Natl. Acad. Sci. USA* **1992**, *89*, 7674-7677.

73. Stamler, J. S. *Circ. Res.* **2004**, *94*, 414-417.

74. Wang, X.; Bryan, N. S.; MacArthur, P. H.; Rodriguez, J.; Gladwin, M. T.; Feelisch, M. *J. Biol. Chem.* **2006**, *281*, 26994-27002.

75. Tsikas, D.; Sandmann, J.; Gutzki, F. M.; Stichtenoth, D. O. Frölich, J. C. *J. Chromatogr B* **1999**, *726*, 13-24.

76. Tsikas, D.; Sandmann, J.; Frölich, J. C. *J. Chromatogr. B* **2002**, *772*, 335-346.

77. Tyurin, V. A.; Liu, S.-X.; Tyurina, Y. Y.; Sussman, N. B.; Hubel, C. A.; Roberts, J. M.; Taylor, R. N.; Kagan, V. E. *Circ. Res.* **2001**, *88*, 1210-1215.

78. Tsikas, D.; Schmidt, M.; Böhmer, A.; Zoerner, A. A.; Gutzki, F.-M.; Jordan, J. *J. Chromatogr. B* **2013**, *927*, 147-157.

79. Gaston, B. M.; Carver, J.; Doctor, A.; Palmer, L. A. *Mol. Interv.* **2003**, *3*, 253-263.

80. Sun, J.; Murphy, E. *Circ. Res.* **2010**, *106*, 285-296.

81. Wang, P. G.; Xian, M.; Tang, X.; Wu, X.; Wen, Z.; Cai, T.; Janczuk, A. J. *Chem. Rev.* **2002**, *102*, 1091-1134.

82. Tasker, H. S.; Jones, H. O. *J. Chem. Soc., Trans.* **1909**, *95*, 1910-1918.

83. Williams, D. L. H. *Nitrosation Reactions and the Chemistry of Nitric Oxide*; Elsevier: Amsterdam, 2004.

84. Carver, J.; Doctor, A.; Zaman, K.; Gaston, B. *Methods Enzymol.* **2005**, *396*, 95-105.

85. Ridd, J. H. *Adv. Phys. Org. Chem.* **1978**, *16*, 1-49.

86. Morris, P. A.; Williams, D. L. H. *J. Chem. Soc., Perkin Trans. 2* **1988**, 513-516.

87. Williams, D. L. H. *Acc. Chem. Res.* **1999,** *32*, 869-876.

88. Bartberger, M. D.; Houk, K. N.; Powell, S. C.; Mannion, J. D.; Lo, K. Y.; Stamler, J. S.; Toone, E. J. *J. Am. Chem Soc.* **2000**, *122*, 5889-5890.

89. Arulsamy, N.; Bohle, D. S.; Butt, J. A.; Irvine, G. J.; Jordan, P. A.; Sagan, E. *J. Am. Chem. Soc.* **1999**, *121*, 7115-7123.

90. Roy, B.; du Moulinet d'Hardemare, A.; Fontecave, M. *J. Org. Chem.* **1994**, *59*, 7019-7026.

91. Wang, K.; Hou, Y.; Zhang, W. Ksebati, M. B.; Xian, M.; Cheng, J.-P.; Wang, P. G. *Bioorg. Med. Chem. Lett.* **1999**, *9*, 2897-2902.

92. Timerghazin, Q. K.; Peslherbe, G. H.; English, A. M. *Org. Lett.* **2007**, *9*, 3049-3052.

93. Morakinyo, M. K.; Chipinda, I.; Hettick, J.; Siegel, P. D.; Abramson, J.; Strongin, R.; Martincigh, B. S.; Simoyi, R. H. *Can. J. Chem.* **2012**, *9*, 724-738.

94. Yi, J.; Khan, M. A.; Lee, J.; Richter-Addo, G. B. *Nitric Oxide* **2005**, *12*, 261-266.

95. Field, L.; Dilts, R. V.; Ravichandran, R.; Lenhert, P. G.; Carnahan, G. E. *J. Chem. Soc., Chem. Commun.* **1978**, 249-250.

96. Carnahan, G. E.; Lenhert, P. G.; Ravichandran, R. *Acta Crystallogr. Sect. B - Struct. Sci.* **1978**, *34*, 2645-2648.

97. Stamler, J. S.; Toone, E. J. *Curr. Opin. Chem. Biol*. **2002**, *6*, 779-785.

98. Williams, D. L. H. *Chem. Commun.* **1996**, 1085-1091.

99. Singh, R.; Whitesides, G. M. Chapter 13: Thiol-Disulfide Interchange. In *Sulphur-Containing Functional Groups*; Patai, S.; Rappoport, Z., Ed.; John Wiley & Sons, Ltd.: Chichester, 1993.

100. Zhao, Y.-L.; McCarren, P. R.; Houk, K. N.; Choi, B. Y.; Toone, E. J. *J. Am. Chem. Soc.* **2005**, *127*, 10917-10924.

101. Grossi, L.; Montevecchi, P. C.; Strazzari, S. *J. Am. Chem. Soc.* **2001**, *123*, 4853-4854.

102. Bainbrigge, N.; Butler, A. R.; Görbitz, C. H. *J. Chem. Soc., Perkin Trans. 2* **1997**, 351-353.

103. Grossi, L.; Montevecchi, P. C. *Chemistry* **2002**, *8*, 380-387.

104. de Oliveira, M. G.; Shishido, S. M.; Seabra, A. B.; Morgon, N. H. *J. Phys. Chem. A* **2002**, *106*, 8963-8970.

105. Vanin, A. F.; Malenkova, I. V.; Serezhenkov, V. A. *Nitric Oxide* **1997**, *1*, 191-203.

106. Swift, H. R.; Williams, D. L. H. *J. Chem. Soc., Perkin Trans. 2* **1997,** 1933-1935.

107. Bohl, K. S.; West, J. L. *Biomaterials* **2000**, *21*, 2273-2278.

108. Duan, X.; Lewis, R. S. *Biomaterials* **2002**, *23*, 1197-1203.

109. Riccio, D. A.; Coneski, P. N.; Nichols, S. P.; Broadnax, A. D.; Schoenfisch, M. H. *ACS Appl. Mater. Interfaces* **2012**, *4*, 796-804.

110. Pegalajar-Jurado, A.; Wold, K. A.; Joslin, J. M.; Neufeld, B. H.; Arabea, K. A.; Suazo, L. A.; McDaniel, S. L.; Bowen, R. A.; Reynolds, M. M. *J. Control. Release* **2015**, *217*, 228-234.

111. Lu, Y.; Shah, A.; Hunter, R. A.; Soto, R. J.; Schoenfisch, M. H. *Acta Biomater.* **2015**, *12*, 62-69.

112. Seabra, A. B.; da Silva, R.; de Oliveira, M. G. *Biomacromolecules* **2005**, *6*, 2512-2520.

113. Seabra, A. B.; da Silva, R.; de Souza, G. F.; de Oliveira, M. G. *Artif. Organs* **2008**, *32*, 262-267.

114. Damodaran, V. B.; Joslin, J. M.; Wold, K. A.; Lantvit, S. M.; Reynolds, M. M. *J. Mater. Chem.* **2012**, *22*, 5990-6001.

115. Li, Y.; Lee, P. I. *Mol. Pharm.* **2010**, *7*, 254-266.

116. Chong, S. F.; Chandrawati, R.; Städler, B.; Park, J.; Cho, J.; Wang, Y.; Jia, Z.; Bulmus, V.; Davis, T. P.; Zelikin, A. N.; Caruso, F. *Small* **2009**, *5*, 2601-2610.

117. Yoon, J. A.; Kamada, J.; Koynov, K.; Mohin, J.; Nicolaÿ, R.; Zhang, Y.; Balazs, A. C.; Kowalewski, T.; Matyjaszewski, K. *Macromolecules* **2012**, *45*, 142-149.

118. Smith, M. B.; March, J. *March's Advanced Organic Chemistry: Reactions, Mechanisms, and Structure*, 5th ed.; John Wiley & Sons, Ltd: New York, 2001; pp 1543-1544.

119. Danehy, J. P.; Doherty, B. T.; Egan, C. P. *J. Org. Chem.* **1971**, *36*, 2525-2530.

120. Ehrenberg, L.; Harms-Ringdahl, M.; Fedorcsák, I.; Granath, F. *Acta Chem. Scand.* **1989**, *43*, 177-187.

121. Ruano, J. L. G.; Parra, A.; Alemán, *J. Green Chem.* **2008**, *10*, 706-711.

122. Wallace, T. J. *J. Am. Chem. Soc.* **1964**, *86*, 2018-2021.

123. Smith, M. B.; March, J. *March's Advanced Organic Chemistry: Reactions, Mechanisms, and Structure*, 5th ed.; John Wiley & Sons, Ltd: New York, 2001; pp 816-817.

124. Kirmse, W. *Angew. Chem. Int. Ed.* **1976**, *15*, 251-261.

125. Smith, P. A. S.; Baer, D. R. *Org. React.* **1960**, *11*, 157.

126. Fridman, A. L.; Mukhametshin, F. M.; Novikov, S. S. *Russ. Chem. Rev.* **1971**, *40*, 34-50.

127. Smith, P. A. S.; Loeppky, R. N. *J. Am. Chem. Soc.* **1967**, *89*, 1147-1157.

128. Peterson, L. A.; Wagener, T.; Sies, H.; Stahl, W. *Chem. Res. Toxicol.* **2007**, *20*, 721-723.

129. Lobl, T. J. *J. Chem. Educ.* **1972**, *49*, 730-734.

130. García-Río, L.; Leis, J. R.; Moreira, J. A.; Norberto, F. *J. Chem. Soc., Perkin Trans. 2* **1998**, 1613-1620.

131. Kanaya, H.; Takeda, Y. *Cancer Lett.* **1983**, *18*, 143-148.

132. Werner, E. A.; *J. Chem. Soc., Trans.* **1919**, *115*, 1093-1102.

133. Doyle, M. P.; Terpstra, J. W.; Pickering, R. A.; LePoire, D. M. *J. Org. Chem.* **1983**, *48*, 3379-3382.

134. Joslin, J. M.; Neufeld, B. H.; Reynolds, M. M. *RSC Adv.* **2014**, *4*, 42039-42043.

135. Shishido, S. M.; de Oliveira, M. G. *Photochem. Photobiol.* **2000**, *71*, 273-280.

136. Fischer, M.; Warneck, P. *J. Phys. Chem*. **1996**, *100*, 18749-18756.

137. Ungnade, H. E.; Smiley, R. A. *J. Org. Chem.* **1956**, *21*, 993-996.

138. Damodaran, V. B.; Joslin, J. M.; Wold. K. A.; Lantvit, S. M.; Reynolds, M. M. *J. Mater. Chem*. **2012**, *22*, 5990-6001.

139. Singh, S. P.; Wishnok, J. S.; Keshive, M.; Deen, W. M.; Tannenbaum, S. R. *Proc. Natl. Acad. Sci. USA* **1996,** *93*, 14428-14433.

140. Dicks, A. P.; Li, E.; Munro, A. P.; Swift, H. R.; Williams, D. L. H. *Can. J. Chem.* **1998**, *76*, 789-794.

141. Hogg, N. *Free Radic. Biol. Med.* **2010**, *49*, 122-129.

142. Griess, P. *Ber. Dtsch. Chem. Ges.* **1879**, *12*, 426.

143. Tsikas, D. *J. Chromatogr. B* **2007**, *851*, 51-70.

144. Giustarini, D.; Rossi, R.; Milzani, A.; Dalle-Donne, I. *Methods Enzymol.* **2008**, *440*, 361-380.

145. Hetrick, E. M.; Schoenfisch, M. H. *Annu. Rev. Anal. Chem. (Palo Alto Calif.)* **2009**, *2*, 409-433.

146. Iglesias, E.; García-Río, L.; Leis, J. R.; Peña, M. E.; Williams, D. L. H. *J. Chem. Soc., Perkin Trans. 2* **1992**, 1673-1679.

147. Saville, B. *Analyst* **1958**, *83*, 670-672.

148. Diers, A. R.; Keszler, A.; Hogg, N. *Biochim. Biophys. Acta* **2014**, *1840*, 892-900.

149. Kojima, H.; Sakurai, K.; Kikuchi, K.; Kawahara, S.; Kirino, Y; Nagoshi, H.; Hirata, Y.; Nagano, T. *Chem. Pharm. Bull.* **1998**, *46*, 373-375.

150. Privett, B. J.; Shin, J. H.; Schoenfisch, M. H. *Chem. Soc. Rev.* **2010**, *39*, 1925-1935.

151. Malinski, T.; Taha, Z. *Nature* **1992**, *358*, 676-678.

152. Bănică, F.-G. *Chemical Sensors and Biosensors: Fundamentals and Applications*; John Wiley & Sons, Ltd.: Chichester, 2012.

153. Pinsky, D. J.; Patton, S.; Mesaros, S.; Brovkovych, V.; Kubaszewski, E.; Grunfeld, S.; Malinski, T. *Circ. Res.* **1997**, *81*, 372-379.

154. Burlet, S.; Cespuglio, R. *Neurosci. Lett.* **1997**, *226*, 131-135.

155. Cha, W.; Meyerhoff, M. E. *Langmuir* **2006**, *22*, 10830-10836.

156. Peng, B.; Meyerhoff, M. E. *Electroanalysis* **2013**, *25*, 914-921.

157. Tanaka, Y.; Shimayu, M. *J. Sci. Res. Inst. (Tokyo)* **1949**, *43*, 241.

158. Greaves, J. C.; Garvin, D. *J. Chem. Phys.* **1959**, *30*, 348-349.

159. Clyne, M. A. A.; Thrush, B. A.; Wayne, R. P. *Trans. Faraday Soc.* **1964**, *60*, 359-370.

160. Bates, J. N. *Neuroprotocols* **1992**, *1*, 141-149.

161. Marley, R.; Feelisch, M.; Holt, S.; Moore, K. *Free Radic Res.* **2000**, *32*, 1-9.

162. Garside, C. *Mar. Chem.* **1982**, *11*, 159-167.

163. Samouilov, A.; Zweier, J. L. *Anal. Biochem.* **1998**, *258*, 322-330.

164. Ewing, J. F.; Janero, D. R. *Free Radic. Biol. Med.* **1998**, *25*, 621-628.

165. Alpert, C.; Ramdev, N.; George, D.; Loscalzo, J. *Anal. Biochem.* **1997**, *245*, 1-7.

166. Fang, K.; Ragsdale, N. V.; Carey, R. M.; MacDonald, T.; Gaston, B. *Biochem. Biophys. Res. Commun.* **1998**, *252*, 535-540.

167. Zajda, J.; Crist, N. R.; Malinowska, E.; Meyerhoff, M. E. *Electroanalysis* **2016**, *28*, 277-281.

168. Zargar, V.; Asghari, M.; Dashti, A. *ChemBioEng Rev.* **2015**, *2*, 204-226.

169. Lenardon, M. D.; Munro, C. A.; Gow, N. A. R. *Curr. Opin. Microbiol.* **2010**, *13*, 416-423.

170. Rinaudo, M. *Prog. Polym. Sci.* **2006**, *31*, 603-632.

171. Lu, Y.; Slomberg, D. L.; Schoenfisch, M. H. *Biomaterials* **2014**, *35*, 1716-1724.

172. Lu, Y.; Shah, A.; Hunter, R. A.; Soto, R. J.; Schoenfisch, M. H. *Acta Biomater.* **2015**, *12*, 62-69.

173. Rothemund, S.; Teasdale, I. *Chem. Soc. Rev.* **2016**, *45*, 5200-5215.

174. Allcock, H. R.; Kugel, R. L. *J. Am. Chem. Soc.* **1965**, *87*, 4216-4217.

175. Allcock, H. R.; Kugel, R. L. *Inorg. Chem.* **1966**, *5*, 1716-1718.

176. Allcock, H. R.; Fuller, T. J.; Mack, D. P.; Matsumura, K.; Smeltz, K. M. *Macromolecules* **1977**, *10*, 824-830.

177. Allcock, H. R.; Pucher, S. R.; Scopelianos, A. G. *Macromolecules* **1994**, *27*, 1071-1075.

178. Kumbar, S. G.; Bhattacharyya, S.; Nukavarapu, S. P.; Khan, Y. M.; Nair, L. S.; Laurencin, C. T. *J. Inorg. Organomet. Polym.* **2006**, *16*, 365-385.

179. Deng, M.; Kumbar, S. G.; Wan, Y.; Toti, U. S.; Allcock, H. R.; Laurencin, C. T. *Soft Matter* **2010**, *6*, 3119-3132.

180. Lakshmi, S.; Katti, D. S.; Laurencin, C. T. *Adv. Drug Deliv. Rev.* **2003**, *55*, 467-482.

CHAPTER 2

NITRIC OXIDE-RELEASING *S*-NITROSATED DERIVATIVES OF CHITIN AND CHITOSAN FOR BIOMEDICAL APPLICATIONS

2.1. Introduction

Nitric oxide (NO) is a biologically-active molecule with an important role in numerous physiological processes, most notably as a signaling agent in the regulation of vasodilation.[1] Moreover, NO is an active participant during several crucial stages of wound repair, modulating the severity of the inflammatory response and promoting cell proliferation and angiogenesis.[2,3] These properties have led to the extensive investigation of supplemental NO for wound-healing applications. This use of NO is of particular interest in cases where endogenous NO production has been impaired as a result of illness, a condition that has been implicated in the persistence of chronic wounds.[4,5] NO and NO prodrugs are currently utilized as therapeutic agents for the treatment of cardiovascular and pulmonary ailments, although the controlled administration of therapeutic NO for wound-healing applications is complicated by the fact that NO is a highly reactive radical species with a relatively short half-life under atmospheric or physiological conditions (0.09 to >2 s in extravascular tissue) and exhibits acute toxicity at higher concentrations.[6,7] As a result, there has been considerable interest in the development of NO-releasing materials for the localized delivery of NO at biological interfaces. One way this has

This chapter was adapted from:

Lutzke, A.; Pegalajar-Jurado, A.; Neufeld, B. H.; Reynolds, M. M. Nitric oxide-releasing *S*-nitrosated derivatives of chitin and chitosan for biomedical applications. *J. Mater. Chem. B* **2014**, *2*, 7449-7458. Adapted by permission of The Royal Society of Chemistry.

been achieved involves the coupling of NO donor groups such as *N*-diazeniumdiolates and *S*-nitrosothiols (RSNOs) to polymer systems to prepare materials that release NO as a result of the decomposition of the donor group under physiological conditions.[8,9]

More recently, derivatives of the naturally-occurring β-(1,4)-linked polysaccharide chitin have been investigated as NO-releasing materials. Chitin is an abundant biopolymer primarily consisting of *N*-acetyl-D-glucosamine units and is commercially derived from marine crustaceans, where it occurs as a major structural component of the exoskeleton.[10] The most significant derivative of chitin is chitosan, a polysaccharide produced through the deacetylation (≥50%) of the parent polymer to form primary amine groups.[11] This process confers solubility in aqueous acid, as well as enhanced mucoadhesive and hemostatic properties.[12] Both polymers have been employed in a variety of biological applications, including use in surgical sutures and wound dressings that exploit their well-established biocompatibility and biodegradability.[13,14] The concept of utilizing chitin and chitosan derivatives as platforms for the controlled delivery of pharmaceutical agents has received significant attention in literature, due to the versatility of the materials and their inherently low toxicity and unique interactions with biological systems.[15,16] In the case of NO delivery for wound repair, chitin and chitosan offer the advantage of exhibiting hemostatic properties that may balance the reported ability of NO to inhibit platelet adhesion and aggregation, potentially expanding the application of NO-releasing derivatives to acute hemorrhagic wound care.[17,18,19] Furthermore, chitin and chitosan have previously been observed to independently accelerate wound healing in animal models.[20,21]

Chitin and chitosan derivatives are often synthesized through modification or substitution of the C6 and C3 hydroxyl groups, while chitosan derivatives may also be prepared through modification of the C2 primary amine, as in the case of *N*-alkylation or amide-forming

reactions.[22] In previously reported NO-releasing materials developed from chitosan or chitosan oligosaccharides, the primary amine of the glucosamine units was either directly reacted with gaseous NO to form the *N*-diazeniumdiolate donor group or converted to a secondary amine prior to *N*-diazeniumdiolate synthesis.[23,24] An alternative strategy involving the conjugation of *N*-acetyl-DL-penicillamine to chitosan in an amide-forming reaction followed by *S*-nitrosation with $NaNO_2$/HCl has also been described.[25] In these prior examples, the inherent reactivity of the C2 amine was used to introduce the desired NO donor group. Herein, we report the first synthesis of NO-releasing *S*-nitrosated chitin and chitosan derivatives prepared through the substitution of the C6 hydroxyl group. This was accomplished through the reaction of tosylated intermediates with the symmetrical dithiols 1,2-ethanedithiol (EDT), 1,3-propanedithiol (PDT), and 1,6-hexanedithiol (HDT), which were subsequently *S*-nitrosated with *tert*-butyl nitrite (*t*-BuONO) to form the corresponding *S*-nitrosothiol NO donor group. In addition, this work represents the first reported synthesis of *S*-nitrosated chitin derivatives for biomedical applications. The *S*-nitrosothiol donor group was selected largely due to its role as an endogeneous NO transfer agent, as in the case of *S*-nitrosoglutathione, and its decomposition into neutral products (2 RSNO $\rightarrow$ 2 NO + RSSR) under mild thermal conditions.[26,27] In the case of chitosan derivatives, substitution of the C6 hydroxyl group leads to a retention of the primary amine that is frequently used for derivatization, permitting further modification of the polysaccharides. Moreover, the use of harsh concentrated acid (as in the case of $NaNO_2$/HCl) was avoided by employing an alkyl nitrite as the *S*-nitrosating agent under comparatively mild conditions.

The total NO content of each *S*-nitrosated material was determined through analysis of NO released during thermal decomposition of the *S*-nitrosothiol groups, and the NO release profiles under physiological conditions (pH 7.4 phosphate buffered saline, 37 °C) were recorded in real-

time for at least 24 h, depending on the release time of the material. To assess the suitability of the thiolated parent materials for biomedical applications, the *in vitro* cytotoxicity of each derivative was evaluated by extract test. MTS and LIVE/DEAD assays were used to determine the viability of the cells, and any changes in morphology were observed by morphological assays.

2.2. Materials and methods

2.2.1. Materials

Chitin, 1,2-ethanedithiol (EDT), 1,3-propanedithiol (PDT), 1,6-hexanedithiol (HDT), hydrazine monohydrate, lithium chloride, *p*-toluenesulfonyl chloride (TsCl), and triethylamine (TEA) were purchased from Alfa Aesar (Ward Hill, MA, USA). Chitosan (PROTASAN UP B 90/20, 80 kDa MW) was purchased from NovaMatrix (Sandvika, Norway). 5,5′-Dithiobis(2-nitrobenzoic acid) (DTNB), phthalic anhydride, *tert*-butyl nitrite (*t*-BuONO), and tris(2-carboxyethyl)phosphine hydrochloride (TCEP·HCl) were purchased from Sigma-Aldrich (St. Louis, MO, USA). Phosphate buffered saline (PBS) tablets were purchased from EMD Chemicals (Gibbstown, NJ, USA). DL-Dithiothreitol (DTT) was purchased from AMRESCO (Solon, OH, USA). Spectra/Por 7 dialysis membrane (8 kD molecular weight cut-off) was purchased from Spectrum Laboratories, Inc. (Rancho Dominguez, CA, USA). Human dermal fibroblasts (HDF) were purchased from ZenBio, Inc. (Durham, NC, USA). Amphotericin B, gentamicin, and Media 106 fetal bovine serum supplement were purchased from Gibco® (Grand Island, NY, USA). Alexa Fluor® 568 Phalloidin, DAPI, PBS, propidium iodide, SYTO9, and trypsin-EDTA (0.25%) were purchased from Life Technologies (Grand Island, NY, USA). (3-(4,5-dimethylthiazol-2-yl)-5-(3-carboxymethoxyphenyl)-2-(4-sulfophenyl)-2H-tetrazolium) (MTS) was obtained from Promega

(Madison, WI, USA). 75T tissue culture (TC) plates were obtained from VWR (Denver, CO, USA). TEA was distilled from calcium hydride before use.

2.2.2. Characterization techniques

^{1}H NMR spectra were acquired using a Varian Inova 400 MHz FT-NMR spectrometer (Varian NMR Systems, Palo Alto, CA, USA). ATR-FTIR spectra were collected between 4000 and 650 cm^{-1} using a Nicolet 6700 spectrometer (Thermo Electron Corporation, Madison, WI, USA) equipped with a Smart iTR ATR sampling accessory. UV-Vis analysis was carried out using a Nicolet Evolution 300 spectrophotometer (Thermo Electron Corporation) equipped with a Praying Mantis accessory (Harrick Scientific Products, Inc., Pleasantville, NY, USA) for diffuse reflectance studies.

Ellman's assay for thiol quantification. For all materials, the incorporation of unoxidized thiol was quantified using Ellman's assay under heterogeneous conditions.[28,29] Samples of each polymer ($n \geq 3$) were suspended in 100 mM phosphate buffer (pH 8) and treated with 100 µL of 10 mM DTNB in buffer. The samples were agitated for 1 h at room temperature, then centrifuged prior to the removal of 200 µL aliquots of sample solution for analysis. The aliquots were transferred to a 96-well microtiter plate and absorbance values were acquired at 450 nm using a BioTek Synergy 2 plate reader (BioTek, Winooski, VT, USA). Thiol content was calculated using cysteine standards.

Chemiluminescence-based NO analysis. NO release from *S*-nitrosated polymer samples was recorded in real-time using Sievers nitric oxide analyzers (NOA 280i, GE Analytical, Boulder, CO, USA). Calibration was performed with nitrogen (zero gas) and 45 ppm NO/nitrogen. NO loading was determined by heating polymer samples ($n \geq 3$) to at least 120 °C, resulting in the

NO-releasing thermal decomposition of the *S*-nitrosothiol groups.[28] The corresponding NO emission from this process was measured and used to calculate the amount of thermally releasable NO present in each material. For studies performed under physiological conditions, polymer samples ($n \geq 3$) were suspended in 10 mM PBS (pH 7.4) at 37 °C and the NO release was measured for at least 24 h.

2.2.3. Cell studies

For cell culture, human dermal fibroblasts were cultured in media 106 supplemented with 2% v/v fetal bovine serum, 1 µg/mL hydrocortisone, 10 ng/mL human epidermal growth factor, 3 ng/mL basic fibroblast growth factor, 10 µg/mL heparin, 125 µg/mL amphotericin B, and 5 mg/mL gentamicin on a 75T TC plate. HDF were incubated at 37 °C in a humid atmosphere with 5% CO_2. When confluent, the cells were collected from a 75T flask by adding 2 mL of a trypsin-EDTA (0.25%) solution, and re-suspended at different concentrations (cells/mL) depending on the specific experiment.

Preparation of extracts. All cytotoxicity experiments were performed according to ISO standards.[30] Extracts from the six thiolated polysaccharides were obtained at physiological temperature (37 °C). To prepare extracts, each material was incubated in regular cell culture media (concentration of 1 mg material/mL cell media) for 24 h. After 24 h, the resulting extracts were used for cell experiments.

Extract study. To perform experiments with extracts, 8,000 cells per well were seeded in a 96-well plate for MTS assay, 25,000 cells per well were seeded in a 24-well plate for LIVE/DEAD assay and 50,000 cells per well were seeded in a 24-well plate for assessing the morphology of the cells.

MTS assay. For MTS assay, cells were incubated for 48 h. Six wells containing only cell culture media were used as a blank, six wells were used as a positive control, six wells were used as a negative control, and six wells were used for each material. For negative control, cells were exposed to methanol to reduce viability. After 45 min of exposure, the methanol was replaced by PBS to rinse the wells. PBS was replaced by fresh warm cell culture media. A 20 µL aliquot of MTS solution was added to each well. After 2 h incubation at 37 °C, absorbance readings were measured with a plate reader (BioTek Synergy 2) at 490 nm.

LIVE/DEAD assay. To prepare the LIVE/DEAD solution, PI (to stain dead cells) and SYTO9 (to stain live cells) were added to PBS at concentrations of 3 µM and 0.5 µM, respectively. Each time, three wells were used for positive control, three were used for negative control, and three wells were used for each material. For negative control, cells were exposed to methanol. After 45 min of exposure, the methanol and the media in the other wells was replaced with PBS. The PBS was then removed and 500 µL of LIVE/DEAD solution was added to each well and incubated for 1 h at room temperature. Subsequently, the LIVE/DEAD solution was removed and PBS was added to each well. Fluorescence microscopy images were obtained using an Olympus IX73 fluorescence microscope. An excitation wavelength of 543 nm was used for PI (617 nm emission observed), and a wavelength of 488 nm was used for SYTO9 (500 nm emission observed). Images of cells used for LIVE/DEAD assay are composed of two overlayed images (PI and SYTO9), combined using the Olympus CellSens software.

Morphological observations. Staining solution consisted of DAPI and Alexa Fluor® 568 Phalloidin at concentrations of 7.60 µM and 6.60 µM, respectively, in PBS. Each time, three wells were used for positive control, three were used for negative control, and three wells were used for each material. For negative control, cells were exposed to methanol. After 45 min of

exposure, methanol was removed and all wells were rinsed twice with 150 mM PBS, and fixed with 3.7% methanol-free formaldehyde in PBS for 10 min at room temperature. All wells were rinsed twice with PBS and exposed to acetone cooled to 0 °C for 4 min, rinsed twice again with PBS, and stained using 0.5 mL of staining solution for 20 min at room temperature. All wells were finally rinsed three times with PBS and imaged. Fluorescence microscopy images were also taken using an Olympus IX73 fluorescence microscope. An excitation wavelength of 358 nm was used for DAPI (461 nm emission observed), and a wavelength of 578 nm was used for Alexa Fluor® 568 Phalloidin (600 nm emission observed). Images of cells are composed of two overlayed images (DAPI and Alexa), combined using the Olympus CellSens software.

2.2.4. Synthesis of materials

Chitin derivatives

6-*O*-Tosyl chitin (1). Tosylated chitin was prepared by modifying a previously reported method.[31] 1.00 g chitin and 2.00 g lithium chloride were stirred in 50 mL DMA overnight to swell the polymer. The mixture was cooled to 0 °C and 7.56 mL TEA was added, followed by 9.38 g of TsCl dissolved in 10 mL of DMA. The reaction was stirred for 24 h at 5 °C. The resulting solution was decanted into 200 mL acetone to precipitate the polymer and the mixture was stirred for 30 min. The material was filtered and washed with 200 mL methanol, 100 mL DI water, and 200 mL acetone, then placed under vacuum with constant stirring to evaporate residual solvent and homogenize the powder. IR ν_{max}/cm^{-1} 3600-3200 (O-H), 3281 (amide N-H), 1657 (amide I), 1598 (aromatic C-C), 1538 (amide II), 1174 (S=O), 811 (tosyl aromatic C-H).

Chitin-EDT (CH-EDT) (2a). 0.400 g of 6-*O*-tosyl chitin (**1**) and 0.750 g of lithium chloride were stirred in 15 mL DMA to form a viscous solution. 0.782 mL TEA and 0.427 mL of EDT

were added, and the mixture was stirred for 20 h at 60 °C under nitrogen. The solution that formed over the course of the reaction was decanted into 200 mL acetone to precipitate the polymer and stirred for 30 min. The polymer was filtered, washed with 200 mL methanol and 200 mL acetone, then vigorously stirred to homogenize the powder. The material was then suspended in 10 mL of 10 mM DTT and TEA in DMA and stirred for 1 h at room temperature. The product was recovered by filtration and washed with 200 mL methanol and 100 mL acetone, then placed under vacuum to remove residual solvent. IR ν_{max}/cm^{-1} 3600-3200 (O-H), 3277 (amide N-H), 1652 (amide I), 1548 (amide II), 1027 (C-O).

Chitin-PDT (CH-PDT) (3a). An analog was prepared following the general method provided for **2a**, using 0.511 mL of PDT. IR ν_{max}/cm^{-1} 3600-3200 (O-H), 3293 (amide N-H), 1653 (amide I), 1537 (amide II), 1028 (C-O).

Chitin-HDT (CH-HDT) (4a). An analog was prepared following the general method provided for **2a**, using 0.778 mL of HDT. IR ν_{max}/cm^{-1} 3600-3200 (O-H), 3280 (amide N-H), 1652 (amide I), 1541 (amide II), 1029 (C-O).

***S*-Nitrosated chitin-EDT (2b).** Chitin-EDT (**2a**) (40 mg/mL) was suspended in 80% DMA/methanol. 0.500 mL *t*-BuONO was added, and the mixture was stirred at RT for 14 h. After the reaction, the nitrosated polymer was briefly stirred in 100 mL methanol, then filtered and washed with 100 mL acetone and 25 mL diethyl ether. The material was placed under vacuum to evaporate any remaining solvent/*t*-BuONO, then immediately stored at -20 °C for future use. IR ν_{max}/cm^{-1} 3600-3200 (O-H), 3285 (amide N-H), 1652 (amide I), 1537 (amide II), 1028 (C-O). UV-Vis λ_{max}/nm 549 (*S*-nitrosothiol, $n_N \rightarrow \pi^*$).

***S*-Nitrosated chitin-PDT (3b).** An analog was prepared from CH-PDT (**3a**) following the general method provided for **2b**. IR ν_{max}/cm^{-1} 3600-3200 (O-H), 3282 (amide N-H), 1655 (amide I), 1544 (amide II), 1026 (C-O). UV-Vis λ_{max}/nm 552 (*S*-nitrosothiol, $n_N \rightarrow \pi^*$).

***S*-Nitrosated chitin-HDT (4b)**. An analog was prepared from CH-HDT (**4a**) following the general method provided for **2b**. IR ν_{max}/cm^{-1} 3600-3200 (O-H), 3272 (amide N-H), 1652 (amide I), 1546 (amide II), 1024 (C-O). UV-Vis λ_{max}/nm 551 (*S*-nitrosothiol, $n_N \rightarrow \pi^*$).

Chitosan derivatives

***N*-Phthaloyl chitosan (5).** *N*-Phthaloyl chitosan was prepared by adapting a method for the selective *N*-phthaloylation of chitosan.[32] 3.00 g chitosan was added to a solution of 8.28 g phthalic anhydride dissolved in 57 mL of anhydrous DMF. The mixture was stirred for 4 h at 120 °C, then briefly cooled below 100 °C and 3 mL DI water was added. After stirring for an additional 4 h at 120 °C, the solution was decanted into 1 L of cold DI water to precipitate the polymer, then filtered and washed with 200 mL methanol. The material was stirred overnight in 300 mL methanol, then filtered and washed with methanol and acetone. IR ν_{max}/cm^{-1} 3600-3200 (O-H), 1775 (C=O), 1704 (C=O), 1064 (C-O), 719 (aromatic C-H). ^{1}H NMR δ_H/ppm (400 MHz, DMSO-d_6, Me_4Si) 7.80 (s, *N*-phthaloyl), 7.45 (s, *O*-phthaloyl), 5.4 - 2.6 (m, carbohydrate).

6-*O*-Tosyl-*N*-phthaloyl chitosan (5b). The tosylation of 5 was carried out by stirring 1.00 g of the polymer and 1.4 g LiCl in 35 mL DMA to form a solution. This solution was cooled to 0 °C and 5.29 mL TEA was added, followed by 6.57 g TsCl in 5 mL DMA. The reaction was stirred for 24 h at 5 °C, then the solution was decanted into 200 mL acetone and stirred for 30 min. The precipitated polymer was washed with 200 mL methanol, 50 mL water, and 200 mL acetone, then stirred under vacuum to remove residual solvent and homogenize the powder. IR ν_{max}/cm^{-1}

3600-3200 (O-H), 1776 (C=O), 1711 (C=O), 1175 (S=O), 1066 (C-O), 813 (tosyl aromatic C-H), 720 (phthaloyl C-H).

Chitosan-EDT (CS-EDT) (6a). 0.800 g of **5b** was dissolved in 30 mL of DMA containing 1.5 g LiCl. 1.64 mL TEA was added, followed by 0.598 mL EDT. The mixture was stirred for 20 h at 60 °C under nitrogen, then decanted into 200 mL methanol and stirred for 30 min. The polymer was filtered, washed with 100 mL methanol, then briefly stirred in 100 mL water adjusted to pH 9 using TEA. This mixture was precipitated into methanol and the material was washed with 200 mL methanol and 50 mL diethyl ether. The polymer was then stirred overnight at RT in 95% DMA/water. The following day, the polymer was recovered by filtration and stirred in 5 mL of hydrazine monohydrate at 80 °C for 5 h under nitrogen, then decanted into 50 mL methanol and recovered by filtration. The material was suspended in 10 mL 1% acetic acid containing 30 mg TCEP·HCl, and the mixture was stirred at RT for 1 h. The material was purified by 1 day of dialysis against 1% NaCl, followed by 2 days of dialysis against DI water. In all cases, the dialysis medium was adjusted to pH 5 using 1% HCl. The final product was isolated by lyophilization. IR ν_{max}/cm^{-1} 3600-3200 (O-H), 3334 (N-H), 3258 (N-H), 1061 (C-O).

Chitosan-PDT (CS-PDT) (7a). An analog was prepared following the general method provided for **6a**, using 0.716 mL of PDT. IR ν_{max}/cm^{-1} 3600-3200 (O-H), 3334 (N-H), 3260 (N-H), 1063 (C-O).

Chitosan-HDT (CS-HDT) (8a). An analog was prepared following the general method provided for **6a**, using 1.09 mL of HDT. IR ν_{max}/cm^{-1} 3600-3200 (O-H), 3320 (amine N-H), 3242 (amine N-H), 1062 (C-O).

***S*-Nitrosated chitosan-EDT (6b). 6a** (5 mg/mL) was suspended in 70% methanol/water. 0.100 mL of 1 M hydrochloric acid was added, followed by 0.200 mL *t*-BuONO. The mixture was

stirred for 30 min at RT, then decanted into 25 mL of methanol. The polymer was briefly stirred in methanol, then filtered and washed with 100 mL methanol and 50 mL diethyl ether. The material was placed under vacuum to evaporate any remaining solvent/*t*-BuONO, then immediately stored at -20 °C for future use. IR ν_{max}/cm^{-1} 3600-3200 (O-H), 3335 (amine N-H), 3253 (amine N-H), 1055 (C-O). UV-Vis λ_{max}/nm 547 (*S*-nitrosothiol, $n_N \rightarrow \pi^*$).

***S*-Nitrosated chitosan-PDT (7b).** An analog was prepared from **7a** following the general method provided for **6b**. IR ν_{max}/cm^{-1}: 3600-3200 (O-H), 3341 (amine N-H), 3224 (amine N-H), 1058 (C-O). UV-Vis λ_{max}/nm 546 (*S*-nitrosothiol, $n_N \rightarrow \pi^*$).

***S*-Nitrosated chitosan-HDT (8b).** An analog was prepared from **8a** following the general method provided for **6b**. IR ν_{max}/cm^{-1}: 3600-3200 (O-H), 3344 (amine N-H), 3234 (amine N-H), 1053 (C-O). UV-Vis λ_{max}/nm 544 (*S*-nitrosothiol, $n_N \rightarrow \pi^*$).

2.3. Results and discussion

2.3.1 Synthesis and characterization of thiolated polymers

Thiolated chitin derivatives were prepared by synthesizing a 6-*O*-tosyl intermediate, followed by nucleophilic displacement with the symmetrical dithiols EDT, PDT, and HDT (Figure 2.1a). The tosylation reaction had been previously established by literature to occur preferentially at the C6 primary hydroxyl group over the less accessible C3 hydroxyl group.[33,34] Performing the reaction at low temperature further improves the selectivity and decreases the rate of undesirable side reactions.[35] Effective tosylation of the polymer was supported by the development of IR features at 1598 cm^{-1} (aromatic C-C stretch), 1174 cm^{-1} (sulfonyl), and 811 cm^{-1} (aromatic C-H out-of-plane bend), as well as a corresponding decrease in the feature at 3600-3200 cm^{-1} (O-H stretch) (Figure 2.2). The bands at 1657 cm^{-1} (amide I) and 1538 cm^{-1}

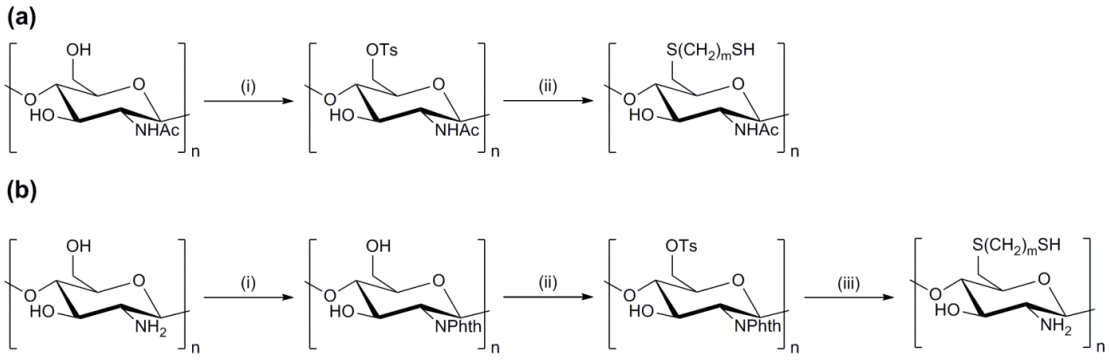

Figure 2.1 (a) Synthesis of thiolated chitin derivatives. (i) TsCl, TEA in DMA/LiCl, 24 h, 5 °C, (ii) $HS(CH_2)_mSH$ (where methylene units, *m*, are 2, 3, or 6), TEA in DMA/LiCl, 20 h, 60 °C, DTT, TEA in DMA, 1 h, RT. (b) Synthesis of thiolated chitosan derivatives. (i) Phthalic anhydride in DMF, 8 h, 120 °C, (ii) TsCl, TEA in DMA/LiCl, 24 h, 5 °C, (iii) $HS(CH_2)_mSH$, TEA in DMA/LiCl, $H_2NNH_2 \cdot H_2O$, 5 h, 80 °C, TCEP·HCl in 1% AcOH, 1 h, RT. Reproduced by permission of The Royal Society of Chemistry.

(amide II) confirmed the retention of the acetyl groups. The resulting 6-*O*-tosylated polymer exhibited high solubility in DMA/LiCl. Chitosan derivatives were prepared following a similar procedure, although it was necessary to protect the glucosamine units as the *N*-phthaloyl derivative to prevent the formation of sulfonamide during the tosylation step (Figure 2.1b). This was carried out by modifying a previously reported procedure for the selective *N*-phthaloylation of chitosan with phthalic anhydride in DMF.[32] The synthesis of *N*-phthaloyl chitosan was confirmed by the loss of IR bands at 3359 and 3295 cm^{-1} corresponding to the N-H stretches of the primary amine, and the appearance of bands at 1775 cm^{-1} (C=O), 1704 cm^{-1} (C=O), and 719 cm^{-1} (aromatic C-H out-of-plane bend) arising from the presence of the phthalimido moiety,while the band at 3600-3200 cm^{-1} (O-H) remained largely unchanged (Figure 2.3). ^1H NMR further supports the selective protection of the primary amine through the distinct signal from the aromatic protons at 7.80 ppm (*N*-phthaloyl), with the significantly smaller peak at 7.45 ppm corresponding to unhydrolyzed *O*-phthaloyl groups. Tosylation of the *N*-phthaloylated intermediate gave 6-*O*-tosyl-*N*-phthaloyl chitosan with distinguishing IR peaks at 1776

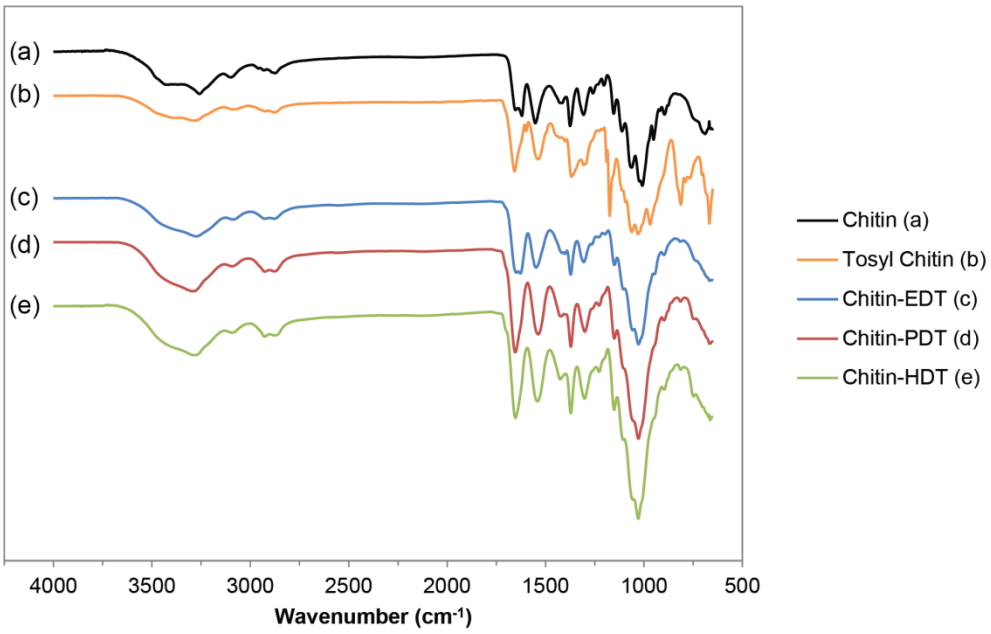

Figure 2.2 ATR-FTIR spectra of thiolated chitin derivatives. Reproduced by permission of The Royal Society of Chemistry.

(phthaloyl C=O), 1711 (phthaloyl C=O), 1175 (tosyl S=O), 813 (tosyl aromatic C-H), and 720 (phthaloyl aromatic C-H). Symmetrical dithiols were selected as a convenient method of thiolating the tosylated intermediates, since their symmetrical structure avoids chemoselectivity issues that would be present in a bifunctional nucleophile or additional protection/deprotection steps requiring harsh conditions. To avoid the formation of polydisulfides or extensive crosslinking, the thiolations were performed under a nitrogen atmosphere. For all polymers, inclusion of the dithiols was confirmed by thiol quantification with Ellman's assay (Table 2.1), and the diminished IR peak at 3600-3200 cm^{-1} that corroborated the expected loss of the C6 hydroxyl group. While the IR bands associated with sulfhydryl, thioether, and disulfide groups are too weak to be clearly identified in the ATR-FTIR spectra of the thiolated derivatives, displacement of the tosyl group was monitored by the reduction in the features at approximately 1600 cm^{-1}, 1175 cm^{-1}, and 815 cm^{-1}.[36] The weak feature retained at approximately 815 cm^{-1} in

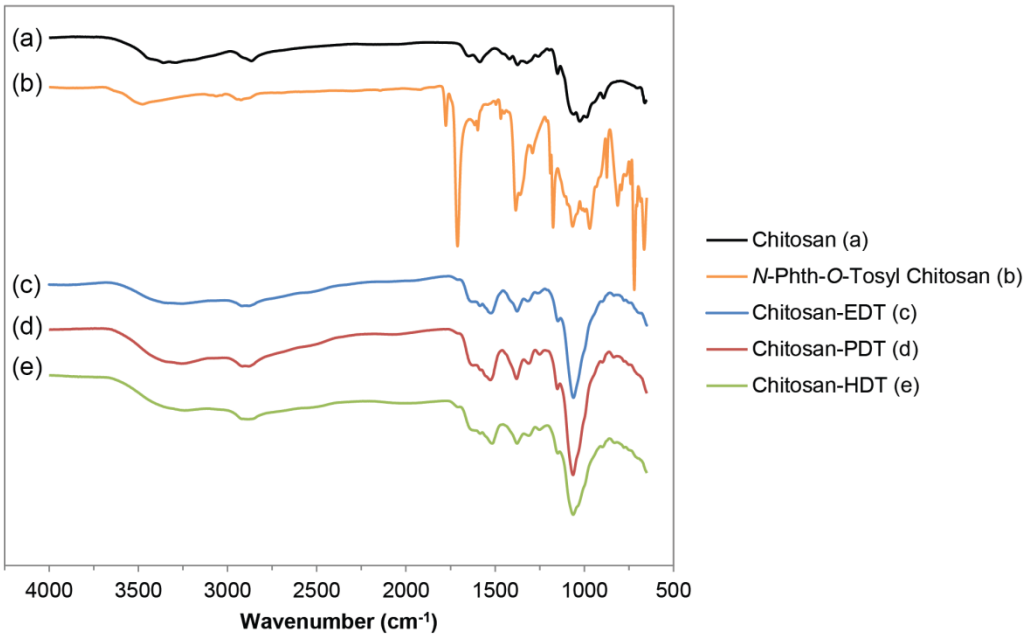

Figure 2.3 ATR-FTIR spectra of thiolated chitosan derivatives. Reproduced by permission of The Royal Society of Chemistry.

the IR spectra of all three thiolated chitin derivatives is attributable to formation of sulfonamide groups, which resulted from the reaction of glucosamine units with TsCl during the initial tosylation of chitin. This feature is not distinct in the spectra of the thiolated chitosan materials, where protection as the *N*-phthaloyl derivative may have prevented this reaction. Prior to thiol quantification, the primary amine groups of the chitosan derivatives were deprotected with aqueous hydrazine, which resulted in the reappearance of the characteristic N-H stretches at 3400-3200 cm^{-1} corresponding to the primary amine groups and the loss of the IR features associated with incorporation of the phthaloyl group. Since the materials were uniformly insoluble in pH 8 phosphate buffer, it was necessary to perform Ellman's assay under heterogeneous conditions, a method that had previously been employed to study other thiolated chitosan derivatives.[29] In all cases, the samples were allowed to react with DTNB for 1 h prior to removal of aliquots for spectroscopic analysis. Extension of the reaction period did not result in

Table 2.1 Summarized thiol and NO content data for chitin and chitosan derivatives. Data reported as mean ($n \geq 3$) ± SD. [a]Values determined by Ellman's assay. [b]Values determined by NOA via thermal decomposition of the *S*-nitrosothiol.

Material	Thiol content (mmol g^{-1})[a]	NO content (mmol g^{-1})[b]	Conversion (% NO/thiol content)
Chitin-EDT	0.547 ± 0.021	0.46 ± 0.081	84 ± 15
Chitin-PDT	0.288 ± 0.038	0.27 ± 0.052	94 ± 22
Chitin-HDT	0.216 ± 0.009	0.14 ± 0.028	62 ± 13
Chitosan-EDT	0.460 ± 0.056	0.40 ± 0.032	86 ± 13
Chitosan-PDT	0.107 ± 0.008	0.040 ± 0.004	37 ± 4
Chitosan-HDT	0.141 ± 0.025	0.11 ± 0.032	76 ± 26

increased chromophore concentration and higher apparent thiol content, indicating that 1 h was sufficient to complete the reaction with active sulfhydryl groups.

The thiolated chitin derivatives exhibited improved solubility in DMA/LiCl but did not dissolve to any appreciable extent in water, behavior that was consistent with the solubility characteristics of the parent polysaccharide.[37] In contrast, the chitosan derivatives CS-EDT and CS-PDT were soluble in dilute aqueous acid, but only following disulfide reduction with TCEP·HCl suggesting that partial oxidation of the thiol groups and crosslinking occurred during the synthesis. The water solubility of CS-EDT and PDT was maintained for the entire dialysis period (3 days), but the lyophilized materials exhibited poor water solubility (presumably a result of disulfide formation) and were largely insoluble after several days of storage, although treatment with additional TCEP·HCl restored the original solubility characteristics. CS-HDT could not be dissolved in water at any stage before or after reduction, potentially indicating increased hydrophobicity due to incorporation of the 6-carbon mercaptohexyl chain.

The thiolated chitosan derivatives exhibit uniformly lower thiol content than their chitin analogs, an outcome that is most directly attributable to the extended dialysis and lyophilization procedure used to purify the chitosan derivatives. This purification period may result in increased disulfide formation and consequently lower thiol content. While the thiolated chitin derivatives follow a predictable general trend where the increasing size of the dithiol results in a lower thiol content per unit of mass, in the case of the chitosan derivatives, lower thiol content was consistently observed for CS-PDT when compared to CS-HDT. This difference may be explained by the solubility of CS-PDT during the dialysis period (permitting the solution phase formation of disulfide linkages) and the tendency of the material to crosslink through disulfide formation, observed when the solubility of the polymer diminished rapidly following isolation. Since the chitin derivatives were stored at low temperature (-20 °C) immediately following reduction, no similar behavior was observed.

2.3.2 Synthesis and characterization of *S*-nitrosated polymers

Thiol groups were converted to the corresponding *S*-nitrosothiol via reaction with *t*-BuONO in 80% DMA/methanol for 14 h (chitin derivatives) or 70% methanol/water in the presence of acid for 30 min (chitosan derivatives) (Figure 2.4). The addition of methanol was not necessary to effect the *S*-nitrosation, but it was found to accelerate the reaction, potentially through a combination of solvent effects and the formation of an equilibrium concentration of dissolved methyl nitrite.[38] The formation of *S*-nitrosothiols leads to two characteristic UV-Vis absorptions, the first between 330-350 nm ($n_O \rightarrow \pi^*$) and the second in the approximate range of 550-600 nm ($n_N \rightarrow \pi^*$).[39] The latter feature was used to evaluate the success of the nitrosation reaction due to its greater diagnostic value, since alkyl nitrites and nitrosamines have no

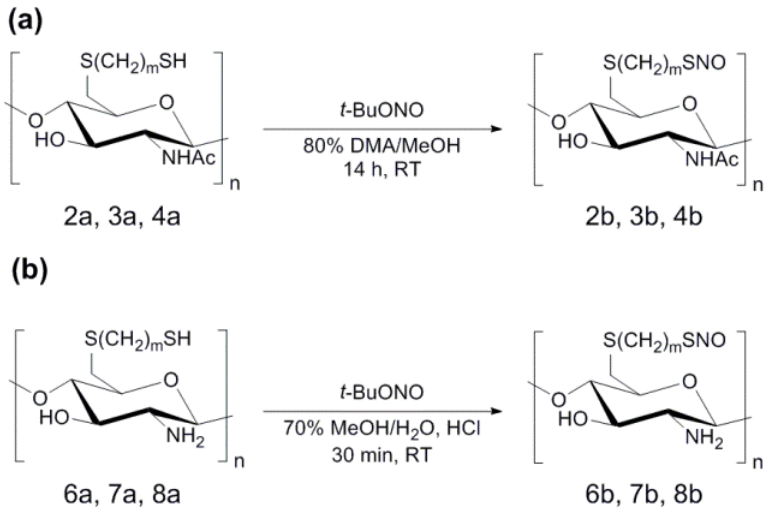

Figure 2.4 *S*-nitrosation of (a) thiolated chitin derivatives and (b) thiolated chitosan derivatives. Reproduced by permission of The Royal Society of Chemistry.

prominent absorption in this region.[40,41] The successful *S*-nitrosation of CH-EDT, PDT, and HDT was confirmed by the appearance of broad features at 549, 552, and 551 nm, respectively, in the DR UV-Vis spectra of the nitrosated materials (Figure 2.5). For CS-EDT, PDT, and HDT, these features appeared at 547, 546, and 544 nm. The development of the absorption near 550 nm resulted in the materials acquiring the distinctive red/pink color characteristic of *S*-nitrosothiols. For all polymers, preservation of the carbohydrate structure after the nitrosation was confirmed by the retention of characteristic IR peaks. The NO loading and release properties of each material were evaluated using NO-selective chemiluminescence-based NO analyzers, which rely on the gas-phase reaction of NO with ozone to produce excited state nitrogen dioxide ($NO + O_3 \rightarrow NO_2^* + O_2$).[42,43] The light emission from the relaxation of NO_2^* to the ground state is measured and used to quantify NO release. In all cases, measurements were performed in custom cells under deoxygenated conditions with a constant flow of nitrogen. The thermally-releasable NO content of each material was determined by heating samples of the polymers to at least 120 °C, producing NO emission as a result of *S*-nitrosothiol decomposition (Table 2.1). NO

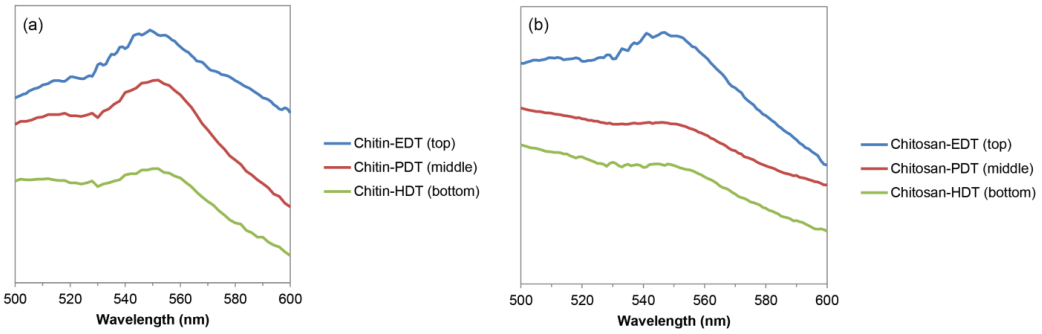

Figure 2.5 Diffuse reflectance UV-Vis spectra of *S*-nitrosated (a) chitin and (b) chitosan derivatives depicting the characteristic $n_N \rightarrow \pi^*$ transition of *S*-nitrosothiols. UV-Vis λ_{max}/nm 549 (chitin-EDT), 552 (chitin-PDT), 551 (chitin-HDT), 547 (chitosan-EDT), 546 (chitosan-PDT), and 544 (chitosan-HDT). Reproduced by permission of The Royal Society of Chemistry.

emission was monitored in real time and recorded until reaching baseline (Figure 2.6). In all cases, the prolonged heating resulted in visible degradation of the polymer itself, which became a blackened mass. This method was previously reported for similar NO-releasing polysaccharides, and permitted the calculation of NO content based on initial sample mass.[28] To ensure that the detected NO could be exclusively attributed to *S*-nitrosothiol decomposition and not collateral thermal degradation of the polymer backbone, control studies were performed using unmodified chitin/chitosan both before and after exposure to *t*-BuONO under identical conditions. For both polysaccharides, there was no detectable NO release from the controls within the temperature range used to promote thermal decomposition of the *S*-nitrosated derivatives.

The variation in total NO content is primarily attributable to differences in the amount of available thiol groups in each material. Differences in thiol conversion (defined as mol NO/mol thiol) between the three derivatives of each parent polysaccharide are most likely to be a consequence of both the rate of parallel *S*-nitrosothiol decomposition during the nitrosation process, as well as varying particle size and consistency between materials, leading to differences in the rate of solvent diffusion into the polymer. The former explanation may be a

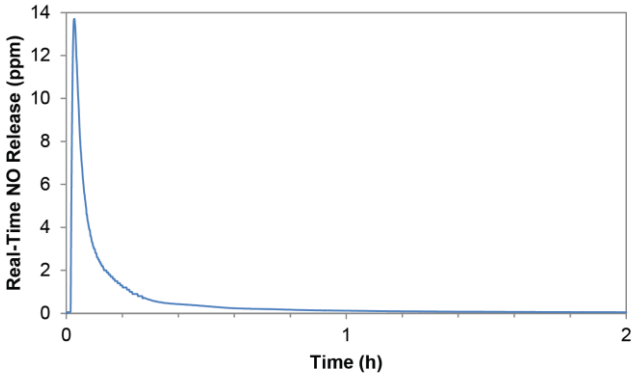

Figure 2.6 Representative thermal decomposition of chitosan-EDT. The material was heated to 120 °C under a nitrogen atmosphere and the resulting nitric oxide (NO) emission was measured by chemiluminescence-based detection until returning to baseline. This process caused accelerated decomposition of the *S*-nitrosothiol, liberating quantifiable NO, and resulted in the concomitant decomposition of the polysaccharide backbone. Reproduced by permission of The Royal Society of Chemistry.

more important factor in the nitrosation of chitin derivatives due to the extended nitrosation period (14 h), while the latter explanation may better account for differences in the chitosan derivatives. This process is demonstrated by the low level of conversion (% NO/thiol content) in the case of CS-PDT, which was denser than the EDT and HDT analogs (potentially due to crosslinking) and had larger particle sizes during the heterogeneous nitrosation.

To assess the NO loading characteristics of the materials relative to other *S*-nitrosated NO-releasing polysaccharides, the chitin and chitosan derivatives were compared with our previously reported *S*-nitrosated dextran derivatives. The NO content of the chitin and chitosan derivatives (as high as 0.46 ± 0.081 mmol NO/g polymer for CH-EDT) compares favorably with values for the dextran-based materials, where a maximum NO content of 0.205 mmol NO/g polymer was determined for an *S*-nitrosated dextran-cysteamine conjugate.[28] The NO content of the *S*-nitrosated chitin and chitosan derivatives may also be compared with existing NO releasing chitosan derivatives prepared through the formation of *N*-diazeniumdiolates, which have reported total NO content in the range of 0.200 mmol/g for chitosan-NO adducts synthesized

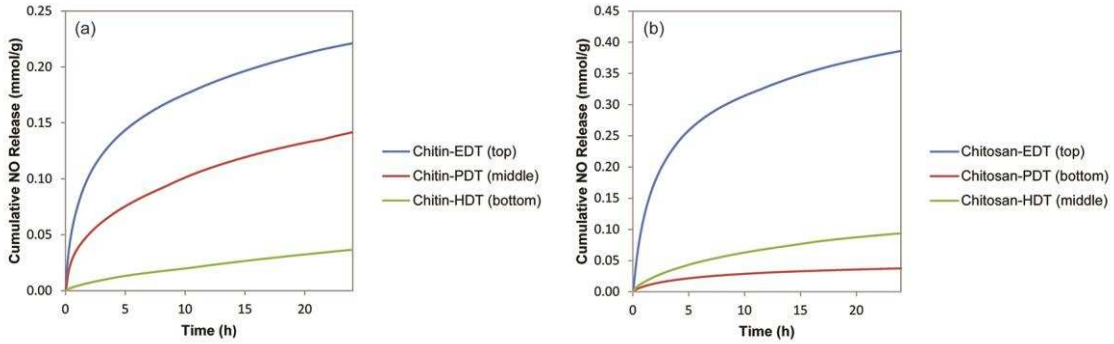

Figure 2.7 Cumulative NO release after 24 h from (a) *S*-nitrosated chitin derivatives and (b) *S*-nitrosated chitosan derivatives under physiological conditions (pH 7.4 PBS, 37 °C). Reproduced by permission of The Royal Society of Chemistry.

from the direct reaction of NO with chitosan to 0.87 mmol/g for water-soluble *N*-diazeniumdiolated chitosan oligosaccharides.[23,24] NO release under physiological conditions was evaluated by suspending samples of the polymers in deoxygenated 10 mM PBS (pH 7.4) at 37 °C under a nitrogen atmosphere and recording the resulting NO release profile for at least 24 h (Figure 2.7, Table 2.2).[44] CH-HDT was observed to release a lower proportion of the total NO content over a 24 h period than EDT and PDT derivatives, which may be attributable to impaired solvent diffusion due to the greater hydrophobicity of that material. For all chitin derivatives, detectable NO release continued for over 72 h, although the majority of the release occurred within a 6 h period (Figure 2.8a). In the case of the chitosan derivatives, NO recovery was nearly quantitative after 24 h, reflecting the greater hydrophilicity of the deacetylated variants when compared to their chitin analogs. As noted for the chitin derivatives, the *S*-nitrosated chitosan materials released the majority of the available NO within 6 h (Figure 2.8b).

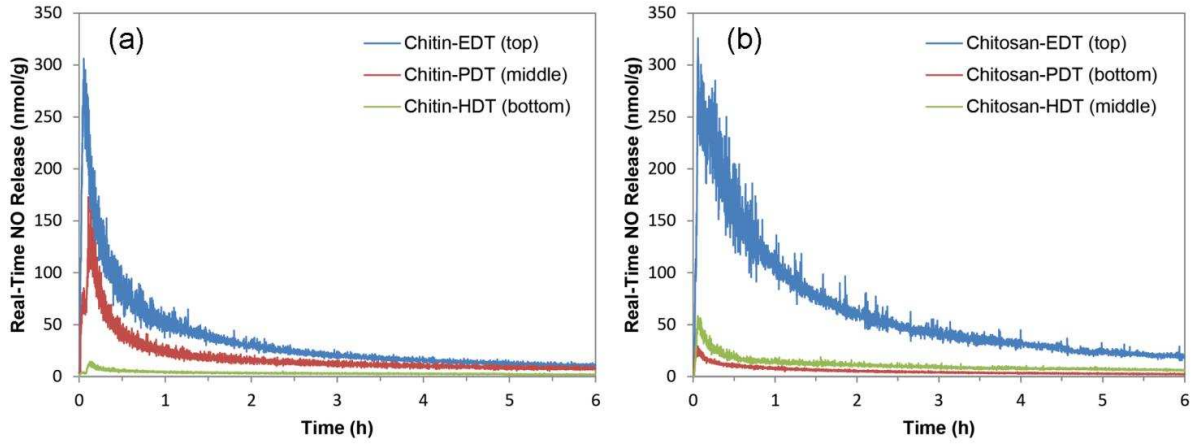

Figure 2.8 Initial real-time NO release profile (6 h). (a) *S*-nitrosated chitin and (b) chitosan (pH 7.4 PBS, 37 °C). Reproduced by permission of The Royal Society of Chemistry.

Table 2.2 Cumulative NO released over 24 h under physiological conditions. Data reported as mean ($n \geq 3$) ± SD. [a]Value determined by NOA in 10 mM pH 7.4 PBS, 37 °C.

Material	NO release (mmol g^{-1})[a]	NO recovery (% of NO content)
Chitin-EDT	0.19 ± 0.025	42 ± 9
Chitin-PDT	0.12 ± 0.017	45 ± 11
Chitin-HDT	0.042 ± 0.005	31 ± 7
Chitosan-EDT	0.39 ± 0.028	99 ± 11
Chitosan-PDT	0.042 ± 0.004	110 ± 14
Chitosan-HDT	0.087 ± 0.007	81 ± 25

2.3.3 Cytotoxicity studies

The relative biocompatibility of the six thiolated derivatives was evaluated using an extract approach based on the commonly accepted ISO regulation 10993 part 5.[30] Two cytotoxicity tests (MTS and LIVE/DEAD) and morphological observations were used to ensure their suitability for

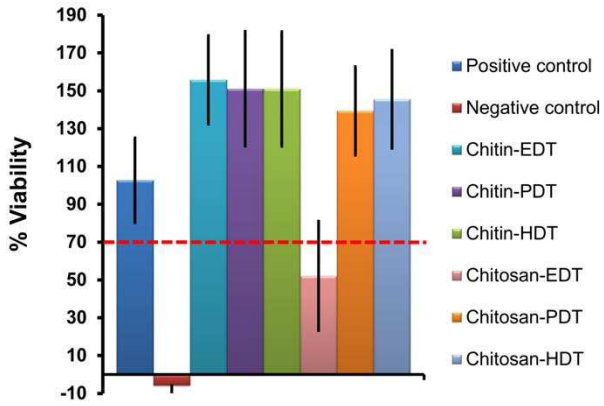

Figure 2.9 MTS assay results for cultured human dermal fibroblasts in the presence of cell culture media. Red line indicates viability of 70% below which the material is considered cytotoxic for human dermal fibroblasts. From left to right: (1) positive control, (2) negative control, (3) chitin-EDT, (4) chitin-PDT, (5) chitin-HDT, (6) chitosan-EDT, (7) chitosan-PDT, and (8) chitosan-HDT. Reproduced by permission of The Royal Society of Chemistry.

biomedical applications. MTS assay tests mitochondrial activity in live cells and is therefore an excellent indicator of the biocompatibility of new materials.[44] Figure 2.9 shows the results of MTS experiments for extracts from all of the thiolated chitin and chitosan derivatives. For the majority of the thiolated derivatives, there was no decrease in cellular viability (normalized with the control sample) when cells were exposed to the extracts. On the contrary, residual material present in the extract promoted cell proliferation as shown in Figure 2.9 (% viability > 100%). These results are not surprising as both chitin and chitosan have been used by other authors to enhance cell proliferation.[45-47] In addition, the results suggest that there were no toxic leachables (*i.e.* residual solvents/reagents or toxic hydrolysis products) at a cytotoxic concentration present in these five extracts. Only CS-EDT resulted in viability lower than 70%, and this polysaccharide is consequently the only thiolated derivative considered cytotoxic for human dermal fibroblasts, likely indicating the presence of toxic degradation products in the material that are released during the extract process.[30] Since CS-EDT is purified by dialysis, it is unlikely that solvent or

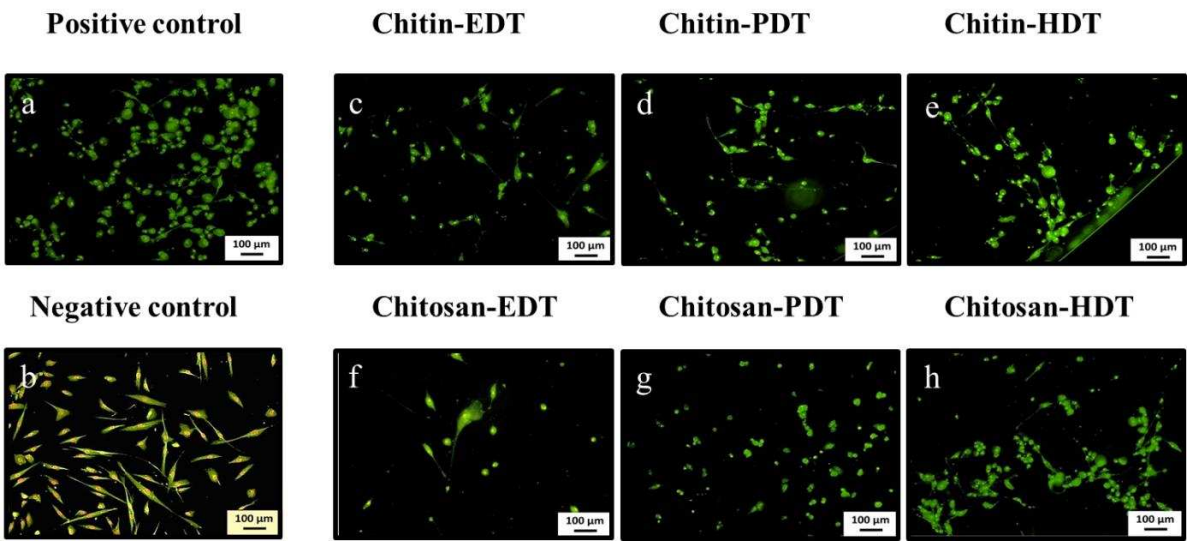

Figure 2.10 LIVE/DEAD studies. Overlaid fluorescence microscopy images of human dermal fibroblasts attached to a TC plate for 72 hours using: cell culture media or positive control (a), cell culture media and exposure to methanol prior staining or negative control (b) extract from chitin derivatives (c, d, e) and extract from chitosan derivatives (f, g, h). Green cells are considered alive and red cells are considered dead. Reproduced by permission of The Royal Society of Chemistry.

residual reagents such as TCEP remain present in the polymer, and any such contaminants were not detected by ATR-FTIR. It is more plausible that hydrolytic degradation of the polymer resulted in the release of trace thiolated (EDT) monomeric or oligomeric species that were cytotoxic. Since no cytotoxicity was observed for CH-EDT, this outcome may be explained by increased solvent permeation in the case of the chitosan derivative, increasing the extent of hydrolysis, or unique degradation products resulting from structural differences between the polymers (primarily in the form of *N*-acetylation in the case of CH-EDT).

Similar results to MTS assay were observed when the LIVE/DEAD assay was performed. Figure 2.10a shows HDF that have not been exposed to methanol or any extract. The green color indicates that the cell membrane is intact, therefore the cells are viable. Figure 2.10b shows cells exposed to methanol. In the case of this negative control, cells were fixed when exposed to

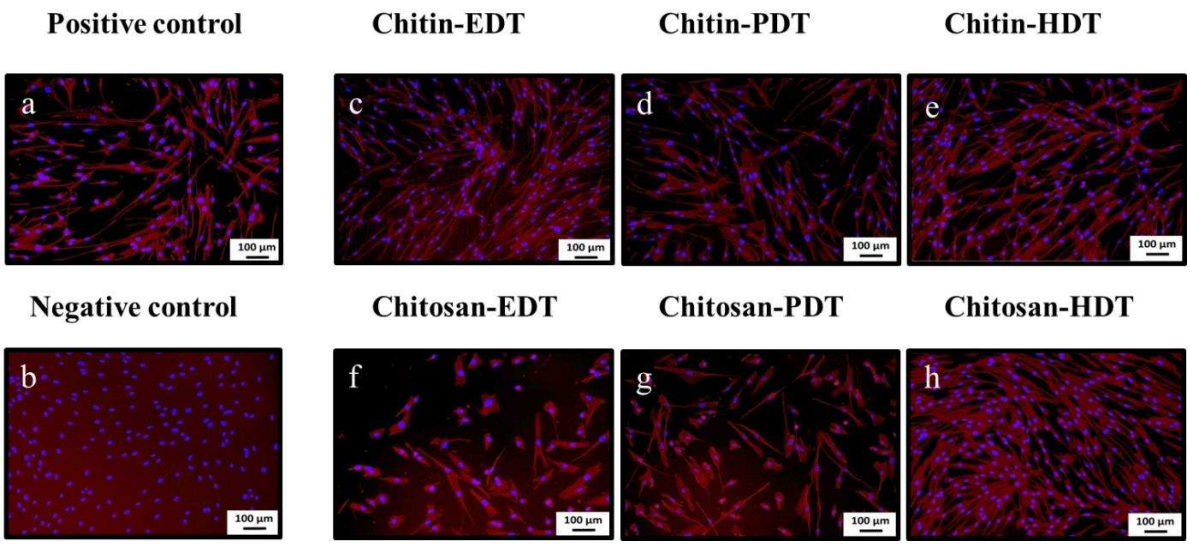

Figure 2.11 Morphological studies. Overlaid fluorescence microscopy images of human dermal fibroblasts attached to a TC plate for 72 hours using: cell culture media (a), cell culture media and exposure to methanol prior staining (b) extract from chitin derivatives (c, d, e) and extract from chitosan derivatives (f, g, h). Blue areas are cell nuclei and red areas are cell membranes. Reproduced by permission of The Royal Society of Chemistry.

methanol and the membrane was disrupted. As a consequence the color of the HDF is a mixture of the red and green staining. A comparable ratio of LIVE/DEAD cells was observed in the positive control sample and in all thiolated derivatives with the exclusion of CS-EDT. A lower number of viable cells were observed for cells cultured with CS-EDT extract and only isolated areas were covered with cells (Figure 2.10f), corroborating the lower viability. Therefore, it can be said that five out of the six thiolated derivatives are considered biocompatible with HDF.

In terms of cell morphological observations, Figure 2.11 revealed cells with normal morphology, spreading and growing to confluency for all thiolated derivatives except CS-EDT. When cells were cultured using the CS-EDT extract, a significant reduction in the area covered by HDF was observed. However, cells showed normal morphology and spreading as seen in Figure 2.11f, indicating that in the presence of the CS-EDT extract cell morphology is not

affected. This observation confirms that five out the six thiolated derivatives do not induce any changes in the HDF morphology, therefore, they are not considered cytotoxic to HDF.

2.4. Conclusions

NO-releasing derivatives of chitin and chitosan were prepared through conjugation of the symmetrical dithiols EDT, PDT, and HDT to the polysaccharides, followed by *S*-nitrosation of the resulting thiolated polymers with *t*-BuONO. In the case of chitin, this work is the first report of *S*-nitrosated derivatives for biomedical applications. For chitosan, a synthetic route to thiolated and *S*-nitrosated derivatives has been presented that results in the retention of the C2 primary amine, leaving it available for polyelectrolyte formation or further covalent derivatization. The free sulfhydryl content of the thiolated intermediates was assessed by Ellman's assay, and the NO loading and physiological release characteristics were evaluated using real-time NO chemiluminescence-based NO measurements. In all cases, the primary factor in the total NO content of each material was the quantity of unoxidized thiol present prior to the nitrosation procedure. All six materials released NO under physiological conditions, with continuous release occurring for at least 24 h. In the case of the chitosan derivatives, NO recovery from chitosan derivatives was nearly quantitative after the 24 h period, an outcome that was attributable to increased solvent permeation. Five of the thiolated derivatives presented cell viability higher than 70% and only CS-EDT was considered cytotoxic, as corroborated by MTS and LIVE/DEAD assays. In addition, no changes in morphology were observed in the presence of extracts from the thiolated derivatives, supporting the potential of the materials for biomedical applications.

Individual contributions and funding sources

Diffuse reflectance UV-Vis measurements obtained by B. H. Neufeld. Cytotoxicity studies performed by A. Pegalajar-Jurado, who was the primary author of section 2.3.3. All other work carried out by A. Lutzke. Funding for this research was provided by the Department of Defense Congressionally Directed Medical Research Program (W81XWH-11-2-0113). A.P.J also acknowledges support *via* the Camille and Henry Dreyfus Foundation Postdoctoral Program in Environmental Chemistry.

REFERENCES

1. Ignarro, L. J.; Buga, G. M.; Wood, K. S.; Byrns, R. E.; Chaudhuri, G. *Proc. Natl. Acad. Sci. USA* **1987**, *84*, 9265-9269.
2. Isenberg, J. S.; Ridnour, L. A.; Espey, M. G.; Wink, D. A.; Roberts, D. A. *Microsurgery* **2005**, *25*, 442-451.
3. Witte, M. B.; Barbul, A. *Am. J. Surg*. **2002**, *183*, 406-412.
4. Luo, J.; Chen, A. F. *Acta Pharmacol. Sin*. **2005**, *26*, 259-264.
5. Witte, M. B.; Thorton, F. J.; Tantry, U.; Barbul, A. *Metabolism* **2002**, *51*, 1269-1273.
6. Miller, M. R.; Megson, I. L. *Br. J. Pharmacol*. **2007**, *151*, 305-321.
7. Thomas, D. D.; Liu, X.; Kantrow, S. P.; Lancaster, J. R., Jr. *Proc. Natl. Acad. Sci. USA* **2001**, *98*, 355-360.
8. Seabra, A. B.; Duran, N. *J. Mater. Chem.* **2010**, *20*, 1624-1637.
9. Riccio, D. A.; Schoenfisch, M. H. *Chem. Soc. Rev.* **2012**, *41*, 3731-3741.
10. Hudson, S. M.; Smith, C. *Biopolymers from Renewable Resources*; Kaplan, D. L., Ed.; Springer-Verlag: Heidelberg, 1998; pp 96-115.
11. Jayakumar, R.; Menon, D.; Manzoor, K.; Nair, S. V.; Tamura, H. *Carbohydr. Polym.* **2010**, *82*, 227-232.
12. Dash, M.; Chiellini, F.; Ottenbrite, R. M.; Chiellini, E. *Prog. Polym. Sci.* **2011**, *36*, 981-1014.
13. Jayakumar, R.; Prabaharan, M. Sudheesh Kumar, P. T.; Nair, S. V.; Tamura, H. *Biotechnol. Adv.* **2011**, *29*, 322-337.
14. Ravi Kumar, M. N. V. *React. Funct. Polym.* **2000**, *46*, 1-27.
15. Hu, L.; Sun, Y.; Wu, Y. *Nanoscale* **2013**, *5*, 3103-3111.

16. Ravi Kumar, M. N. V.; Muzzarelli, R. A. A.; Muzzarelli, C.; Sashiwa, H.; Domb, A. J. *Chem. Rev.* **2004**, *104*, 6017-6084.

17. de Graaf, J. C.; Banga, J. D.; Moncada, S.; Palmer, R. M.; de Groot, P. G.; Sixma, J. J. *Circulation* **1992**, *85*, 2284-2290.

18. Homer, K. L.; Wanstall, J. C. *Br. J. Pharmacol.* **2002**, *137*, 1071-1081.

19. Gries, A.; Bode, C.; Peter, K.; Herr, S. A.; Böhrer, H.; Motsch, J.; Martin, E. *Circulation* **1998**, *97*, 1481-1487.

20. Prudden, J. F.; Migel, M.; Hanson, P. L.; Friedrich, L.; Balassa, L. *Am. J. Surg.* **1970**, *119*, 560-564.

21. Ueno, H.; Mori, T.; Fujinaga, T. *Adv. Drug Deliv. Rev.* **2001**, *52*, 105-115.

22. Rinaudo, M. *Prog. Polym. Sci* **2006**, *31*, 603-632.

23. Wan, A.; Gao, Q.; Li, H. *J. Appl. Polym. Sci.* **2010**, *117*, 2183-2188.

24. Lu, Y.; Slomberg, D. L.; Schoenfisch, M. H. *Biomaterials* **2014**, *35*, 1716-1724.

25. Tan, L.; Wan, A.; Li, H. *Langmuir* **2013**, *29*, 15032-15042.

26. Broniowska, K. A.; Diers, A. R.; Hogg, N. *Biochim. Biophys. Acta* **2013**, *1830*, 3173-3181.

27. Williams, D. L. H. *Chem Commun.* **1996**, 1085-1091.

28. Damodaran, V. B.; Place, L. W.; Kipper, M. J.; Reynolds, M. M. *J. Mater. Chem.* **2012**, *22*, 23038-23048.

29. Schmitz, T.; Grabovac, V.; Palmberger, T. F.; Hoffer, M. H.; Bernkop-Schnürch, A. *Int. J. Pharm* **2008**, *347*, 79-85.

30. International Organization for Standardization, Biological evaluation of medical devices - Part 5: Test for in vitro cytotoxicity, ISO 10993-5, Geneva, Switzerland, 2009, 1-34

31. Morita, Y.; Sugahara, Y.; Takahashi, A.; Ibonai, M. *Eur. Polym. J.* **1994**, *30*, 1231-1236.

32. Kurita, K.; Ikeda, H.; Shimojoh, M.; Yang, J. *Polym. J.* **2007**, *39*, 945-952.

33. Kurita, K.; Inoue, S.; Nishimura, S. *J. Polym. Sci. Part A: Polym. Chem.* **1991**, *29*, 937-939.

34. Kurita, K.; Yoshino, H.; Yokota, K.; Ando, M.; Inoue, S.; Ishii, S.; Nishimura, S. *Macromolecules* **1992**, *25*, 3786-3790.

35. Zou, Y.; Khor, E. *Biomacromolecules* 2005, **6**, 80-87.

36. Coates, J. *Encyclopedia of Analytical Chemistry*; Meyers, R. A., Ed.; John Wiley & Sons, Ltd.: Chichester, 2000; pp 10815-10837.

37. Austin, P. R. *Chitin, Chitosan, and Related Enzymes*; Zikakis, J. P., Ed.; Harcourt Brace Jovanovich: New York, 1984; pp 227-237.

38. Doyle, M. P.; Terpstra, J. W.; Pickering, R. A.; LePoire, D. M. *J. Org. Chem.* **1983**, *48*, 3379-3382.

39. Williams, D. L. H. *Acc. Chem. Res.* **1999,** *32*, 869-876.

40. Ungnade, H. E.; Smiley, R. A. *J. Org. Chem.* **1956**, *21*, 993-996.

41. Wang, P. G.; Xian, M.; Tang, X.; Wu, X.; Wen, Z.; Cai, T.; Janczuk, A. J. *Chem. Rev.* **2002**, *102*, 1091-1134.

42. Fontijn, A.; Sabadell, A. J.; Ronco, R. J. *Anal. Chem.* **1970**, *42*, 575-579.

43. Reynolds, M. M.; Hrabie, J. A.; Oh, B. K.; Politis, J. K.; Citro, M. L.; Keefer, L. K.; Meyerhoff, M. E. *Biomacromolecules* **2006**, *7*, 987-994.

44. Promega, CellTiter 96 Aqueous One Solution Cell Proliferation Assay Technical Bulletin, 2012.

45. Yusof, N. L.; Lim, L. Y.; Khor, E. *J. Biomed. Mater. Res.* **2001**, *54*, 59-68.

46. Chung, L. Y.; Schmidt, R. J.; Hamlyn, P. F.; Sagar, B. F.; Andrews, A. M.; Turner, T. D. *J. Biomed. Mater. Res.* **1994**, *28*, 463-469.

47. Risbud, M.; Hardikar, A; Bhonde, R. *J. Biosci.* **2000**, *25*, 25-30.

CHAPTER 3

NITRIC OXIDE RELEASE FROM A BIODEGRADABLE CYSTEINE-BASED POLYPHOSPHAZENE

3.1. Introduction

Biodegradable polymeric materials have been widely utilized in the development of medical devices such as sutures, bioabsorbable or drug-eluting stents, implants for tissue engineering, and numerous other products for a variety of biomedical applications.[1] The majority of existing synthetic biodegradable polymers are polyesters, a broad category that includes widely-utilized materials such as polyglycolic acid (PGA), polylactic acid (PLA), poly(lactic-*co*-glycolic acid) (PLGA), poly(ε-caprolactone) (PCL), and numerous others.[2] In addition to polyesters, other biodegradable polymers have been investigated for use in biomedical applications, ranging from natural polysaccharides such as chitosan to synthetic polymers like polyanhydrides, polyorthoesters, polyphosphoesters, and polyphosphazenes.[3-5] Polyphosphazenes are a promising class of synthetic polymers that have been extensively investigated for various applications, and consist of a polymeric inorganic backbone containing alternating phosphorus and nitrogen atoms.[6] Geminal substitution of the phosphorus atom to incorporate organic pendant groups yields poly(organophosphazenes) (POPs), a particularly diverse polymer class that includes hundreds of structurally distinct members with varying physicochemical properties determined by the nature of the organic substituents.[7] The use of side

This chapter was adapted from:

Lutzke, A.; Neufeld, B. H.; Neufeld, M. J.; Reynolds, M. M. Nitric Oxide Release From a Biodegradable Cysteine-Based Polyphosphazene. *J. Mater. Chem. B* **2016**, *4*, 1987-1998. Adapted by permission of The Royal Society of Chemistry.

groups derived from amino acids such as glycine, L-alanine, L-cysteine, and others results in hydrolytically-sensitive polymers that slowly hydrolyze to release the amino acid, with the polymer backbone degrading to form low-toxicity ammonia and phosphate products.[8-11] Such materials have been investigated for biomedical applications that range from tissue engineering to drug delivery.[12]

A critical concern in the development of any polymeric biomaterial has been the potential for adverse physiological responses that arise from the interaction of the material and the surrounding biological environment.[13] Implantation of a biomaterial or medical device initiates a complex sequence of biological responses at the biointerface that can lead to persistent inflammation, thrombosis, and fouling that may ultimately lead to unfavorable medical outcomes.[14,15] Efforts to improve the blood and tissue compatibility of biomaterials have frequently focused on the development of drug-elution systems that reduce thrombogenicity or otherwise mitigate adverse host responses.[16,17] Such materials have incorporated various anti-inflammatory drugs as well as anticoagulative therapeutics such as heparin and nitric oxide (NO).[18-20] NO is a promising therapeutic agent that occurs endogenously as a regulatory molecule in many physiological processes, including vasodilation, neurotransmission, and the immune response.[21-23] In addition, NO has a crucial role in maintaining the natural function of the endothelium.[24] Under normal conditions, vascular NO is produced by endothelial cells through enzymatic oxidation of L-arginine to citrulline.[25] This physiologically-produced NO exerts antithrombotic effects by contributing to the inhibition of platelet adhesion to the endothelium.[26] The disruption of endothelial function that occurs after the introduction of a vascular implant may subsequently lead to thrombosis.[27] For this reason, numerous authors have explored the antithrombotic properties of supplemental NO as a method of imitating the function

of the natural endothelium and improving the performance of blood-contacting implants.[28] Furthermore, it has been shown that NO exhibits antimicrobial properties that inhibit bacterial proliferation and may prevent the formation of biofilms that often lead to infection following the implantation of devices such as catheters.[29,30] It has also been shown that NO modulates wound repair, and exogenous supplementation with NO has been observed to result in improved wound healing time in the case of both soft tissue and bone fractures.[31-35]

Although inhaled NO has been utilized as a therapeutic for the treatment of pulmonary disorders, its short *in vivo* half-life (milliseconds to seconds) results in rapidly diminishing concentration as the distance from the point of origin increases.[36,37] As a consequence, NO supplementation as a method of improving biomaterial performance is best achieved through its localized delivery at biological interfaces. To effect the controllable administration of therapeutic NO at biological interfaces, NO prodrugs are employed in the form of molecules containing functional groups that decompose to release NO under physiological conditions. The most common NO donor groups of this type are *N*-diazeniumdiolates and *S*-nitrosothiols (RSNOs), which are respectively synthesized from secondary amines and thiols and have been conjugated to various polymer systems to confer NO release properties.[38] Additional direct, indirect, or conditional NO donor species include inorganic complexes such as sodium nitroprusside and Angeli's salt, as well as the heterocyclic sydnonimines and furoxans, among others.[39] One potential advantage to the use of *S*-nitrosothiols is their well-characterized decomposition through thermal, photolytic, or transition metal-catalyzed pathways to yield NO and relatively benign disulfide according to the equation $2\ RSNO \rightarrow 2\ NO + RSSR$.[40] In comparison, *N*-diazeniumdiolates decompose to form the parent secondary amine, which may subsequently react with NO oxidation products to form potentially carcinogenic *N*-nitrosamines.[41] *S*-

Nitrosothiols with diverse structures and release properties are easily synthesized from the parent thiols in a single step, while many alternative NO donor species may require comparatively complex syntheses. Furthermore, unlike wholly synthetic NO donors, *S*-nitrosothiols have been identified as endogenous species in the form of *S*-nitrosoalbumin and *S*-nitrosoglutathione (GSNO) and have been determined to occur naturally at concentrations in the pM-μM range.[42-45] For these reasons, the use of an *S*-nitrosothiol to impart NO release function to a polyphosphazene may represent a meaningful contribution to the field of NO-releasing biomaterials. Such a material may potentially serve in the traditional tissue engineering roles proposed for biodegradable polyphosphazenes and presents an alternative to more common polyester-based NO-releasing polymers.

In this work, we report the first synthesis of an NO-releasing poly(organophosphazene) containing *S*-nitrosothiol groups as NO donor moieties. The polymer was prepared by substitution of poly(dichlorophosphazene) with ethyl *S*-methylthiocysteinate, followed by partial cleavage of the disulfide linkages to provide free sulfhydryl groups for subsequent conversion to the *S*-nitrosothiol derivative using *tert*-butyl nitrite (*t*-BuONO). The resulting polymer was characterized by ^{1}H, ^{13}C, and ^{31}P NMR, ATR-FTIR, and UV-Vis spectroscopy. The free sulfhydryl content of the intermediate thiolated polymer was evaluated colorimetrically using a modified Ellman's assay protocol with bis(2,4-dinitrophenyl) disulfide and by ^{1}H NMR spectroscopy. The total NO content of the NO-releasing polymer (mmol NO g^{-1}) was determined by solution-phase UV decomposition of the *S*-nitrosothiol functional group and subsequent chemiluminescence-based quantification of the corresponding NO release. To demonstrate the ability of the material to deliver NO under physiological conditions, polymer samples were immersed in pH 7.4 phosphate buffered saline (PBS) at 37 °C for 24 h and the NO release was

continuously monitored. In addition, an extract-based approach was employed to evaluate the cytotoxicity of both the thiolated and *S*-nitrosated polymers with respect to human dermal fibroblasts (HDF). Our results indicate that poly(organophosphazenes) bearing *S*-nitrosothiol functional groups may be suitable as NO-releasing biomaterials.

3.2. Materials and methods

3.2.1 Materials

L-Cysteine ethyl ester hydrochloride (98+%), lithium bis(trimethylsilyl)amide (LiHMDS, 99%), sulfuryl chloride (97%), and triethylamine (TEA, 99+%) were purchased from Alfa Aesar (Ward Hill, MA, USA). 2-Mercaptoethanol (99%) was purchased from AMRESCO (Solon, OH, USA). Phosphate buffered saline (PBS) tablets were purchased from EMD Chemicals (Gibbstown, NJ, USA). *tert*-Butyl nitrite (*t*-BuONO, 90%) was purchased from Sigma-Aldrich (St. Louis, MO, USA). Phosphorus pentachloride (98%) and phosphorus trichloride (98+%) were purchased from Strem Chemicals, Inc. (Newburyport, MA, USA). *S*-Methyl methanethiosulfonate (MMTS, 97+%) was purchased from TCI America (Portland, OR, USA). Human dermal fibroblasts (HDF) were grown in the Ketul Popat lab at Colorado State University. High-glucose Dulbecco's modified Eagle's medium (DMEM) was purchased from Hyclone (Manassas, VA, USA) and supplemented with penicillin-streptomycin and fetal bovine serum. CellTiter-Blue was purchased from Promega (Madison, WI, USA). Trypsin-EDTA, propidium iodide (PI), SYTO 9, Alexa Fluor 568 Phalloidin, and DAPI were purchased from Life Technologies (Grand Island, NY, USA). TEA was distilled from calcium hydride. Sulfuryl chloride and phosphorus trichloride were distilled under nitrogen prior to use. All other reagents were used as received.

3.2.2 General characterization techniques

NMR spectra were acquired using an Agilent (Varian) Inova 400 MHz FT-NMR (Agilent Technologies, Inc., Santa Clara, CA, USA). For ^{1}H NMR spectra in D_2O, chemical shifts were referenced to maleic acid (δ_H = 6.2 ppm) and shifts for ^{31}P NMR spectra were referenced to triphenylphosphine (δ_P = -6 ppm). ATR-FTIR spectra were recorded in the range of 650-4000 cm^{-1} using a Nicolet 6700 spectrometer (Thermo Electron Corporation, Madison, WI, USA). UV-Vis absorption studies were performed using a Nicolet Evolution 300 spectrophotometer (Thermo Electron Corporation). Polymer molecular weight was characterized by gel permeation chromatography (GPC) using a Waters University 1500 GPC instrument (Waters, Milford, MA, USA). Thermal properties of the polymer were evaluated by differential scanning calorimetry with a TA Instruments DSC 2920 and the decomposition temperature was determined using a TA Instruments TGA 2950 (TA Instruments, New Castle, DE, USA). For cell viability studies, absorbance measurements were obtained using a BioTek Synergy 2 microplate reader (BioTek, Winooski, VT, USA). LIVE/DEAD assay and morphological cell images were taken with an Olympus IX73 inverted fluorescence microscope at 10X magnification and processed using Olympus CellSens software (Olympus, PA, USA).

Nitric oxide content determination by UV decomposition. The total NO content of the *S*-nitrosated polymer (mmol g^{-1}) was determined using a Sievers chemiluminescence-based NO analyzer (NOA 280i) (GE Analytical Instruments, Boulder, CO, USA). Prior to use, the NO analyzer was calibrated with UHP nitrogen zero gas and 45 ppm NO/nitrogen. Polymer samples ($n \geq 3$, data reported as mean ± SD) were dissolved in DMF (1 mg mL^{-1}) and varying concentrations were prepared by serial dilution. The UV-Vis absorption

spectrum (200-600 nm) was acquired for each dilution and 100 µL aliquots of the polymer solutions were injected into customized glass gas-flow cells containing deoxygenated DMF with a nitrogen flow/purge gas. The photolytic decomposition of the *S*-nitrosothiol functional group was induced by irradiation with 365 nm light using a 100 W Blak-Ray B-100AP UV lamp (UVP, Upland, CA, USA). Released NO was continuously purged from the DMF solution and transported into the NO analyzer with nitrogen flow gas (200 mL min^{-1}). The output concentration as a function of time was related to total NO release using a calibration constant (mol NO ppb^{-1} s^{-1}) previously determined by reduction of sodium nitrite and verified by decomposition of the *S*-nitrosothiol GSNO. This process was used to calculate the total quantity of releasable NO present in a given mass of polymer. In addition, the NO release resulting from the injection of each aliquot of polymer solution was used to establish a linear relationship between releasable NO and the UV absorbance feature at 337 nm, and the molar extinction coefficient for the polymer-bound *S*-nitrosothiol was calculated.

Nitric oxide release. To assess the NO release properties under physiological conditions, *S*-nitrosated polymer samples (n = 3, data reported as mean ± SD) were suspended as insoluble coarse powders (0.2 mg mL^{-1}) in 5 mL deoxygenated 10 mM pH 7.4 PBS at 37 °C and protected from ambient light for the duration of the experiment. Released NO was purged from the buffer solution and monitored over 24 h by NO analyzer as described previously. At the end of each experiment, the polymer was exposed to 365 nm UV light at 40 °C to decompose remaining *S*-nitrosothiol. Similar procedures were used to evaluate NO release from the polymer at 25 °C in pH 7.4 PBS, 37 °C in pH 5.0 acetate buffer (10 mM sodium acetate/acetic acid), and 37 °C under anhydrous, solvent-free conditions. In the latter experiment, the polymer was

dissolved with 2 mL deoxygenated DMF prior to UV decomposition. Statistical differences were evaluated by single-factor ANOVA analysis and Tukey's range test ($p < 0.05$).

Polymer degradation study. 20.00 mg samples (n = 5) of both the thiolated and *S*-nitrosated polymers were incubated in 5 mL of 10 mM pH 7.4 PBS at 37 °C for 6 weeks. During this period, the samples were continuously agitated and protected from exposure to ambient light. At the end of each week, the buffer was removed and the samples were washed with Millipore water and lyophilized. The dry weight of each sample was subsequently recorded.

3.2.3 Precursor and polymer synthesis

Ethyl *S*-methylthiocysteinate hydrochloride (1). 4.00 g (21.5 mmol) L-cysteine ethyl ester hydrochloride was dissolved in 80 mL ethanol and 2.24 mL (23.7 mmol, 1.1 eq.) MMTS was added. The mixture was stirred overnight at RT, followed by reduction of the solvent volume to approximately 20 mL by rotary evaporation. The product was precipitated by the addition of 100 mL diethyl ether, then filtered and washed with 3 × 50 mL diethyl ether. Residual solvent was removed by vacuum to yield 3.01 g (60%) of fine white crystals. ^{1}H NMR δ_H/ppm (400 MHz, D_2O): 4.34 (dd, -CH-), 4.18-4.07 (m, -OCH_2-), 3.20-3.09 (m, -$SSCH_2$-), 2.25 (s, -$SSCH_3$), 1.12 (t, -CH_3).

Trichloro(trimethylsilyl)phosphoranimine (2). 16.6 g (99 mmol) of LiHMDS was suspended in 200 mL of anhydrous diethyl ether under an inert nitrogen atmosphere and cooled to 0 °C. 8.70 mL (99 mmol, 1 eq.) of phosphorus trichloride was slowly added to the mixture over 30 min. The reaction was allowed to warm to RT and was stirred for 1 h, then cooled to 0 °C and 7.98 mL (99 mmol, 1 eq.) sulfuryl chloride was added over 30 min. The mixture was stirred for 1 h at 0 °C and warmed to RT and stirred for an additional 30 min. The resulting solution was

filtered and the solvent was removed under vacuum to isolate the crude product. The purified compound was collected by vacuum distillation (21 °C, 1 Torr) as a colorless liquid and was stored at -20 °C prior to use. The final recovery was 15.0 g (67%). ^{1}H NMR δ_H/ppm (400 MHz, $CDCl_3$): 0.18 ppm (d, -Si(CH_3)$_3$). ^{31}P NMR δ_P/ppm (162 MHz, $CDCl_3$): -55 ppm (s).

Poly(dichlorophosphazene) (PDCP) (3). 1.5 g of phosphoranimine **2** was dissolved in 5 mL of dichloromethane containing 3.5 x 10^{-2} M phosphorus pentachloride as initiator. The mixture was stirred under nitrogen for 2.5 h and the resulting polymer was isolated under vacuum. ^{31}P NMR δ_P/ppm (162 MHz, $CDCl_3$): -18 ppm (s).

Poly(bis(ethyl *S*-methylthiocysteinyl)phosphazene) (POP-EtCys) (4). A typical synthesis proceeded from **3** (0.795 g) as follows: 3.50 g (15.1 mmol, 2.2 eq. relative to dichlorophosphazene units) of **1** was suspended in 50 mL dry THF. 5.26 mL (37.8 mmol, 2.5 eq. relative to ethyl *S*-methylthiocysteinate) of TEA was added, and the mixture was stirred under nitrogen at 40 °C for 24 h. The mixture was cooled to room temperature and filtered into a solution of **3** dissolved in 10 mL dry THF. The resulting cloudy solution was stirred at 40 °C under nitrogen for 28 h, then filtered to remove solids and slowly decanted into 400 mL hexanes to precipitate the polymer. The polymer was washed with 5 × 100 mL hexanes and placed under vacuum to remove residual solvent to recover 1.81 g (61%) of poly(bis(ethyl *S*-methylthiocysteinyl)phosphazene) as a coarse powder. ^{1}H NMR δ_H/ppm (400 MHz, $CDCl_3$): 4.6-4.0 (-CH-, -OCH_2-), 3.29 (-$SSCH_2$-), 2.43 (-$SSCH_3$), 1.31 (-CH_3).

Poly(ethyl *S*-methylthiocysteinyl-*co*-ethyl cysteinyl phosphazene) (POP-EtCys-SH) (5). The disulfide groups of **4** were partially cleaved by treatment with 2-mercaptoethanol. In a typical protocol, the polymer from the previous step was dissolved in a mixture of 60 mL ethanol/30 mL DCM and 1.47 mL (5 eq.) of 2-mercaptoethanol was added. The resulting solution was stirred

under nitrogen at 40 °C for 48 h, then reduced to approximately half the original volume under vacuum. This solution was filtered and decanted into 400 mL hexanes to precipitate the polymer, which was subsequently washed with 5 × 100 mL hexanes. The polymer was then dissolved in 10 mL DCM, washed with 3 × 5 mL water to remove remaining 2-mercaptoethanol, then dried with anhydrous $MgSO_4$, filtered, and isolated under vacuum. To ensure the removal of water, the polymer was frozen with liquid nitrogen and lyophilized for 24 h. The final recovered yield was 1.14 g. ^{1}H NMR δ_H/ppm (400 MHz, $CDCl_3$): 4.6-4.0 (-CH-, -OCH_2-), 3.29 (-$SSCH_2$-), 2.43 (-$SSCH_3$), 1.83 (-SH), 1.31 (-CH_3). ^{13}C NMR δ_C/ppm (100 MHz, $CDCl_3$): 173 (-CO_2-), 61 (-OCH_2-), 54 (-CH-), 43 (-$SSCH_2$-), 23 (-$SSCH_3$), 14 (-CH_3). ^{31}P NMR δ_P/ppm (162 MHz, $CDCl_3$): -2.6 (s). IR ν_{max}/cm^{-1}: 3320, 2980, 2914, 1732, 1417, 1367, 1295, 1180, 1117, 1026, 948, 853, 792, 760, 698. UV-Vis λ_{max}/nm (DMF): 267 (disulfide).

***S*-Nitrosation of poly(ethyl *S*-methylthiocysteinyl-*co*-ethyl cysteinyl phosphazene) (POP-EtCys-NO) (6)** 10% v/v *t*-BuONO in ethanol was prepared at 0 °C and used to suspend **5** at a concentration of 125 mg/mL. The resulting solution was agitated at room temperature for 15 min, then evaporated under vacuum to yield the *S*-nitrosated polymer. IR ν_{max}/cm^{-1}: 3300, 2977, 2915, 1732, 1520, 1367, 1296, 1180, 1117, 1024, 950, 920, 853, 794, 763, 750, 699. UV-Vis λ_{max}/nm (DMF): 267 (disulfide), 337 (*S*-nitrosothiol, $\pi \rightarrow \pi^*$, $\varepsilon = 810 \pm 20$ M^{-1} cm^{-1}), 547 (*S*-nitrosothiol, $n \rightarrow \pi^*$).

3.2.4 Cell studies

HDF were cultured in Hyclone high-glucose DMEM until reaching approximately 90% confluency within the growth flasks. The cells were subsequently removed from the

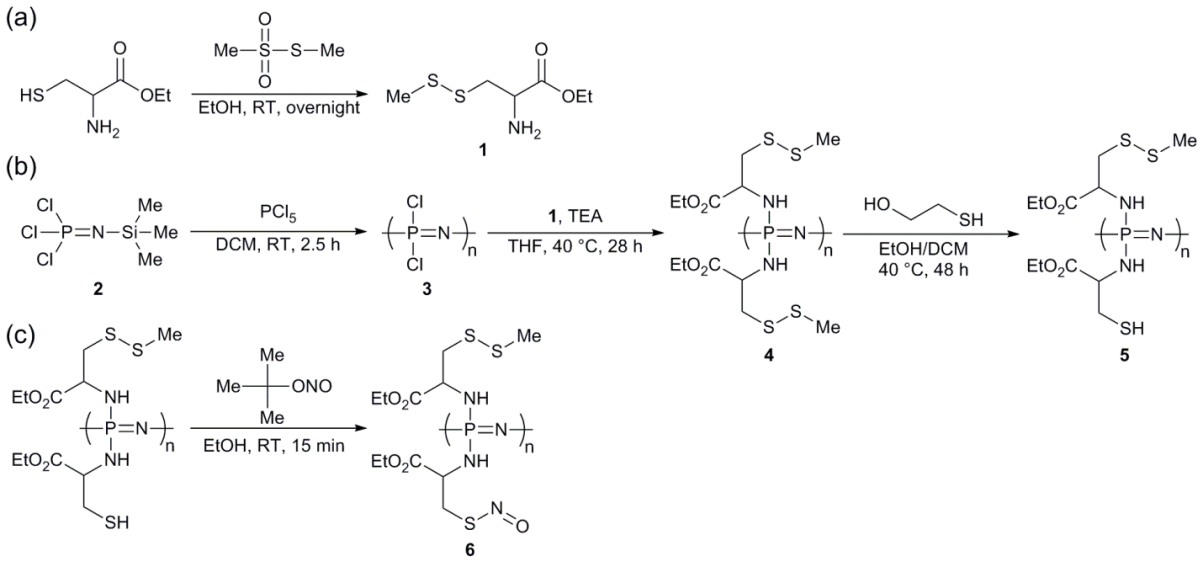

Figure 3.1 Synthesis of *S*-nitrosated poly(ethyl *S*-methylthiocysteinyl-co-ethyl cysteinyl phosphazene) and precursors. (a) Synthesis of ethyl *S*-methylthiocysteinate, (b) synthesis of poly(ethyl *S*-methylthiocysteinyl-*co*-ethyl cysteinyl phosphazene) (POP-EtCys-SH), (c) *S*-nitrosation of POP-EtCys-SH (POP-EtCys-NO). Reproduced by permission of The Royal Society of Chemistry.

flasks using trypsin-EDTA (0.25%) in order to perform viability, LIVE/DEAD, and morphological assays.

Extract preparation. HDF studies were performed following the general guidelines of ISO 10993.[46] Polymer samples (POP-EtCys-SH and POP-EtCys-NO) were suspended in cell media under physiological conditions (37 °C with 5% CO_2 in a humid environment) at a concentration of 10 mg/mL for 24 h prior to the cell experiments. Cell media was removed after the 24 h extraction period and used to perform subsequent cell experiments.

CellTiter-Blue viability assay. 25,000 cells per well (n = 9) were seeded in a 24-well plate (TC polystyrene) for 48 h under physiological conditions (37 °C with 5% CO_2 in a humid environment), and the cell medium was exchanged after 24 h. When the 48 h incubation period had elapsed, the medium was replaced with the respective material

extract (POP-EtCys-SH/POP-EtCys-NO) or pure cell growth medium as a positive control and cells were allowed to grow for an additional 24 h. The medium was subsequently removed and wells were washed once with PBS, then exposed to 400 μL CellTiter-Blue solution prepared from 20 μL of CellTiter-Blue reagent combined with 100 μL warmed HDF media. The plate was incubated at 37 °C for 4 h before 100 μL aliquots were transferred to a 96-well plate and the absorbance at 570 and 600 nm was obtained using a plate reader. Absorbance values were used to calculate cell viability by comparison to positive controls.

LIVE/DEAD assay. 25,000 cells per well (n = 6) were seeded in a 24-well plate for 48 h, with a medium change at 24 h. After 48 h, the medium was replaced with the material extract (POP-EtCys-NO) or pure medium as a positive control and cells were allowed to grow for an additional 24 h. For negative control, the medium was removed, the wells were washed once with sodium chloride solution, then methanol was added. The plate was incubated at RT for 45 min to allow the methanol to disrupt the cell membranes before proceeding with the assay. The cell medium (or methanol) was removed and wells were washed twice with sodium chloride before the two stains (PI and SYTO 9) were added to each well. Staining solution was prepared from 2 μL PI with 0.7 μL SYTO 9/1 mL NaCl solution. The plates were incubated for 1 h at RT before imaging by fluorescence microscope. The excitiation and emission wavelengths for PI and SYTO 9 were 533/617 nm and 485/498 nm, respectively.

Morphological assay. 50,000 cells per well (n = 6) were seeded in a 24-well plate for 48 h with a medium change at 24 h. After 48 h, the medium was replaced with the respective material extract or pure medium as a positive control and cells were allowed to grow for

an additional 24 h. The medium was subsequently removed and wells were washed twice with PBS. Formaldehyde solution (3.7% in PBS) was added to each well and allowed to sit at RT for 10 min. The solution was removed, wells were washed twice with PBS, and cold acetone was added to the wells for an additional 3 min. The acetone was removed, wells were washed twice with PBS, and the two stains (Alexa and DAPI) were added to each well. The staining solution was prepared from 25.5 μL Alexa and 1.4 μL DAPI/1 mL PBS. Wells were imaged by fluoresence microscope after sitting for an additional 20 min. The excitiation and emission wavelengths for Alexa and DAPI were 578/600 nm and 360/460 nm, respectively.

3.3. Results and discussion

3.3.1. Synthesis of poly(bis(ethyl *S*-methylthiocysteinyl)phosphazene) and deprotection

Polyphosphazene derivatives with organic pendant groups are commonly synthesized from the precursor PDCP, which is prepared from the thermal ring-opening polymerization of hexachlorocyclotriphosphazene (HCCP) or by PCl_5-initiated polymerization of trichloro(trimethylsilyl)phosphoranimine.[47,48] It was anticipated from previous reports and the established behavior of thiol-bearing polymers that disulfide-forming oxidative crosslinking might impair the solubility of high molecular weight thiol-substituted POPs, therefore trichloro(trimethylsilyl)phosphoranimine was utilized to prepare lower molecular weight PDCP for subsequent modification.[10,49] The phosphoranimine was synthesized following a protocol previously reported by Wang *et al.* and gave a 67% total recovery after distillation.[50] While the synthesis and purification of the highly-reactive phosphoranimine was carried out under anhydrous, oxygen-free conditions, it was observed that

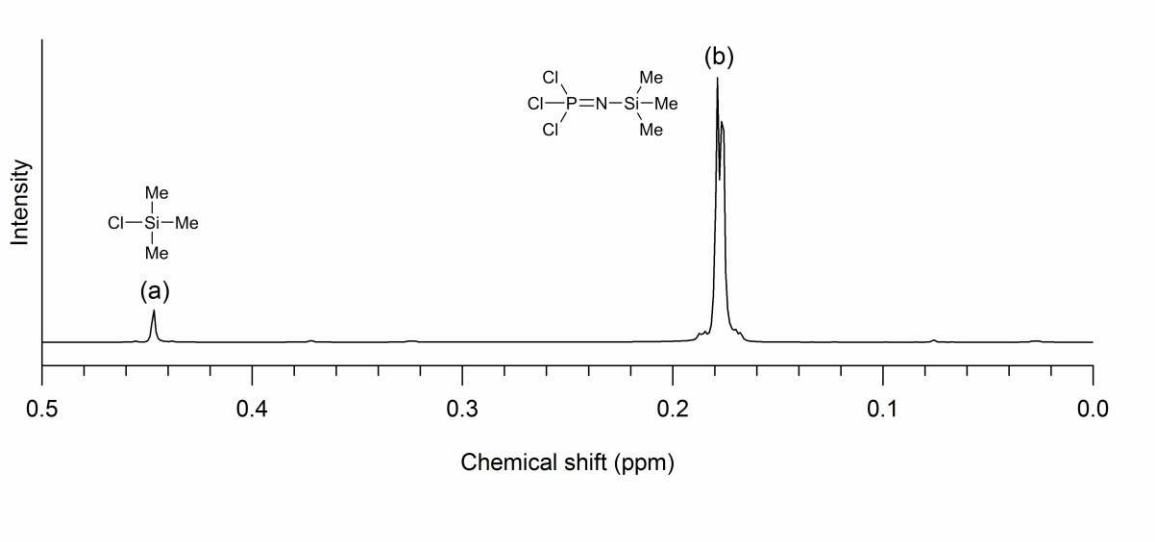

Figure 3.2 ^{1}H NMR of trichloro(trimethylsilyl)phosphoranimine. ^{1}H NMR δ_H/ppm (400 MHz, $CDCl_3$): (a) 0.45 (Me_3SiCl impurity, approx. 5%), (b) 0.18 (distorted doublet, $Cl_3P{=}NSiMe_3$). Reproduced by permission of The Royal Society of Chemistry.

the purified compound tolerated brief exposure to atmosphere at 20 °C (RH = 25%) without detectable changes in the ^{1}H or ^{31}P NMR spectra (Figure 3.2 and 3.3a). The phosphoranimine was subsequently polymerized in DCM using PCl_5 as initiator to give viscous PDCP as the product, which was characterized by ^{31}P NMR and found to be consistent with literature reports (Figure 3.3b).[51] The synthesis of the cysteine-substituted polyphosphazene was carried out using a procedure modified from one previously reported by Weikel *et al.*, where the thiol group of ethyl cysteinate was first protected as an asymmetric disulfide derivative prior to reaction with PDCP.[10] This strategy was employed to avoid chemoselectivity issues arising from nucleophilic competition of the thiol and amine groups of ethyl cysteinate during reaction with PDCP. While Weikel employed *S*-ethyl ethanethiosulfinate as the thiol protecting agent, we converted ethyl cysteinate hydrochloride to the methyl disulfide derivative by treatment with commercially available MMTS, a reagent commonly utilized to effect the reversible blockage of cysteine residues in proteins.[52,53] This gave ethyl *S*-

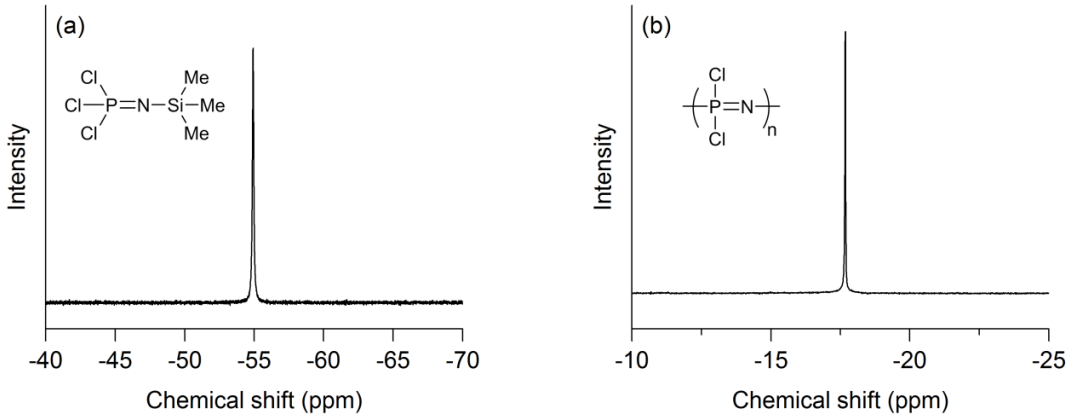

Figure 3.3 ^{31}P NMR of (a) trichloro(trimethylsilyl)phosphoranimine and (b) poly(dichlorophosphazene).^{31}P NMR δ_P/ppm (162 MHz, $CDCl_3$): (a) -55 ($Cl_3P{=}NSiMe_3$), (b) -18 ($-PCl_2{=}N-$). Spectra referenced to triphenylphosphine (-6 ppm, not shown). Reproduced by permission of The Royal Society of Chemistry.

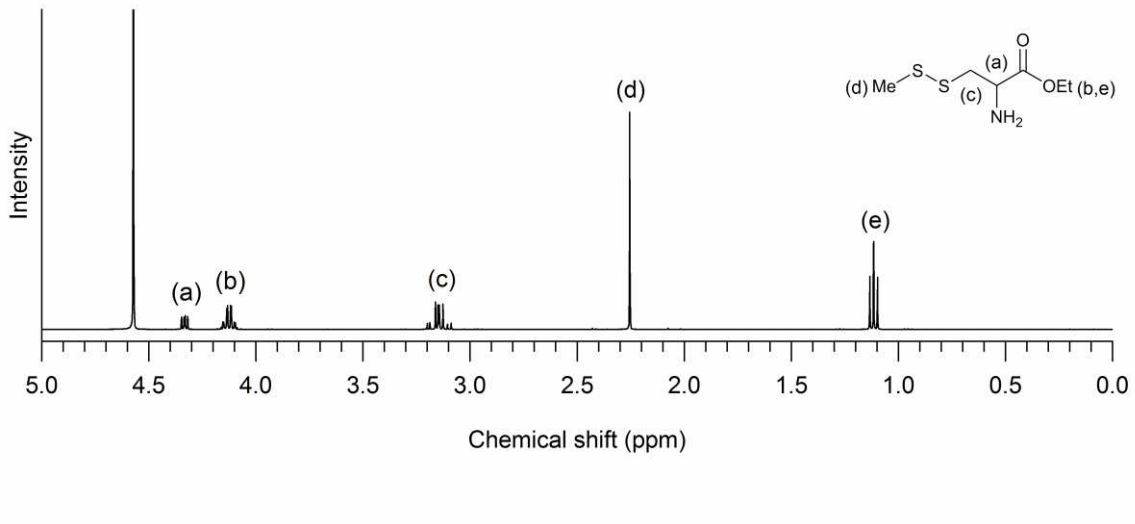

Figure 3.4 ^{1}H NMR of ethyl *S*-methylthiocysteinate. ^{1}H NMR δ_H/ppm (400 MHz, D_2O): (a) 4.34 (dd, -CH-), (b) 4.18 - 4.07 (m, $-OCH_2-$), (c) 3.20 - 3.09 (m, $-SSCH_2-$), (d) 2.25 (s, $-SSCH_3$), (e) 1.12 (t, $-CH_3$). Spectrum referenced to maleic acid (6.2 ppm, not shown). Reproduced by permission of The Royal Society of Chemistry.

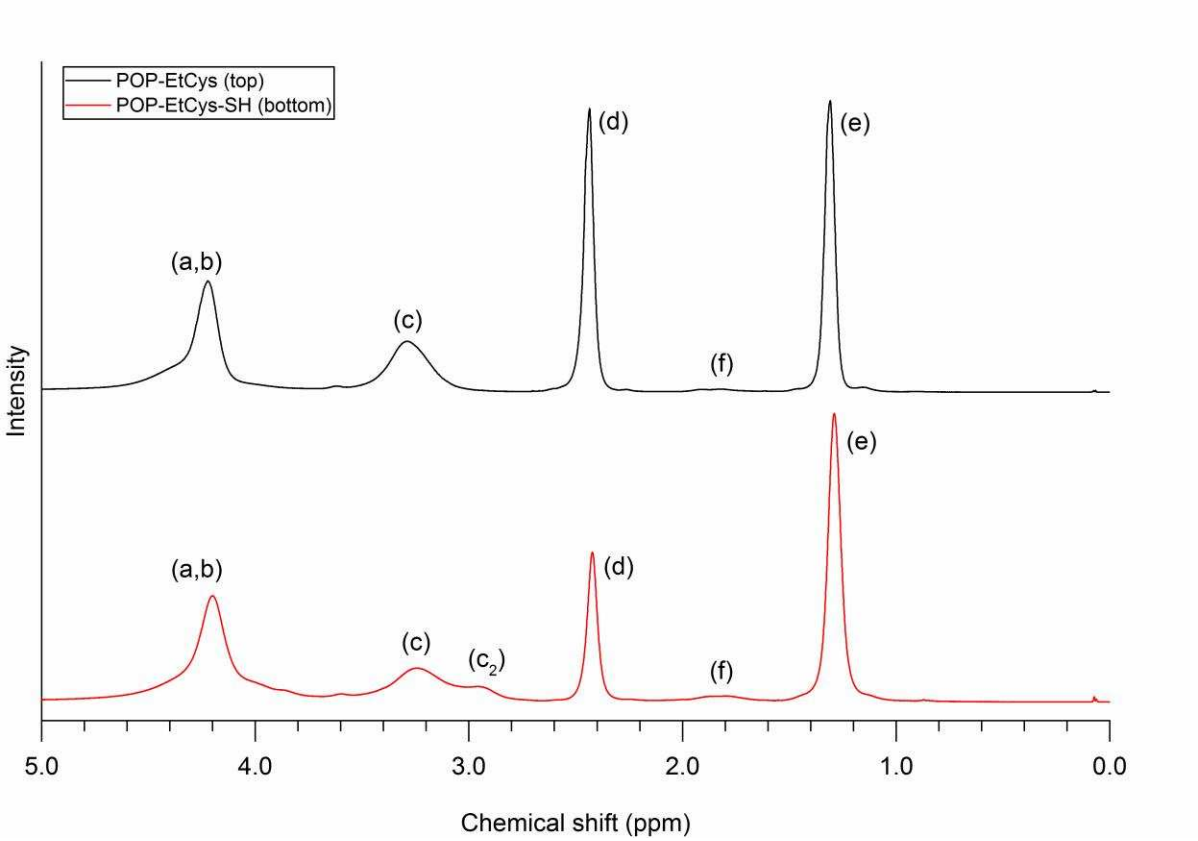

Figure 3.5 ^{1}H NMR of poly(bis(ethyl *S*-methylthiocysteinyl)phosphazene) (POP-EtCys) and poly(ethyl *S*-methylthiocysteinyl-*co*-ethyl cysteinyl phosphazene) (POP-EtCys-SH). ^{1}H NMR δ_H/ppm (400 MHz, $CDCl_3$): (a,b) 4.6 - 4.0 (-CH-, -OCH_2-), (c) 3.29 (-$SSCH_2$-), (c_2) 2.95 (-SCH_2-), (d) 2.43 (-$SSCH_3$), (e) 1.31 (-CH_3), (f) 1.83 (-SH). Concentration: 20 mg mL^{-1}. Reproduced by permission of The Royal Society of Chemistry.

methylthiocysteinate hydrochloride in 60% yield (Figure 3.4), which was subsequently reacted with PDCP in THF at 40 °C for 28 h to form the substituted POP-EtCys. The polymer was recovered by precipitation with hexanes and characterized by ^{1}H NMR before proceeding to the following step (Figure 3.5). ^{1}H NMR gave broad features, with peaks at 4.22 (-OCH_2-) and 1.31 ppm (-CH_3) corresponding to the ethyl ester of the ethyl *S*-methylthiocysteinyl substituents, and the resonance from the methyl group of the disulfide linkage is observed at 2.43 ppm. A peak associated with the methylene group of cysteine is present at 3.29 (-CH_2-) ppm, and a feature between 4.6 and 4.0 ppm is partially attributable to the methine proton (-CH-) and overlaps the

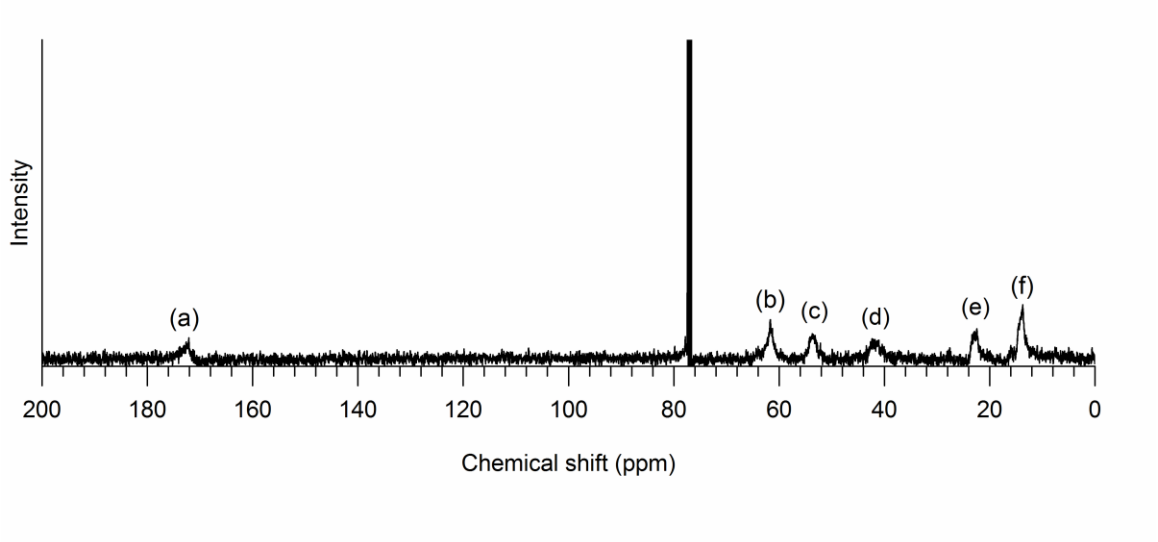

Figure 3.6 ^{13}C NMR of poly(ethyl *S*-methylthiocysteinyl-*co*-ethyl cysteinyl phosphazene) (POP-EtCys-SH). ^{13}C NMR δ_c/ppm (100 MHz, $CDCl_3$): (a) 173 (-CO_2-), (b) 61 (-OCH_2-), (c) 54 (-CH-), (d) 43 (-$SSCH_2$-), (e) 23 (-$SSCH_3$), (f) 14 (-CH_3). Concentration: 200 mg mL^{-1}. Reproduced by permission of The Royal Society of Chemistry.

methylene resonance from the ethyl group. The N-H resonance is not well-defined and may occur in a region of considerable overlap with more prominent features, while a broad, subtle feature corresponding to trace free thiol is present at 1.83 ppm. The polymer was suspended in a mixture of DCM/ethanol and thiol groups were partially deprotected using 2-mercaptoethanol at 40 °C for 48 h to form POP-EtCys-SH. After disulfide cleavage, ^1H NMR features were generally conserved from the spectrum of poly(bis(ethyl *S*-methylthiocysteinyl)phosphazene), with an expected reduction in the peak associated with the methyl disulfide and the appearance of a new resonance at 2.95 ppm arising from the partial upfield shift of the cysteine methylene protons adjacent to thiol. The ^{13}C NMR spectrum was consistent with the expected structure, with peaks at 173, 54, and 43 ppm corresponding to the carbonyl, methine, and methylene carbons of cysteine (Figure 3.6). The methylene and methyl carbons of the ethyl ester appear at 61 and 14 ppm, respectively, while the methyl group from the remaining disulfide produces a

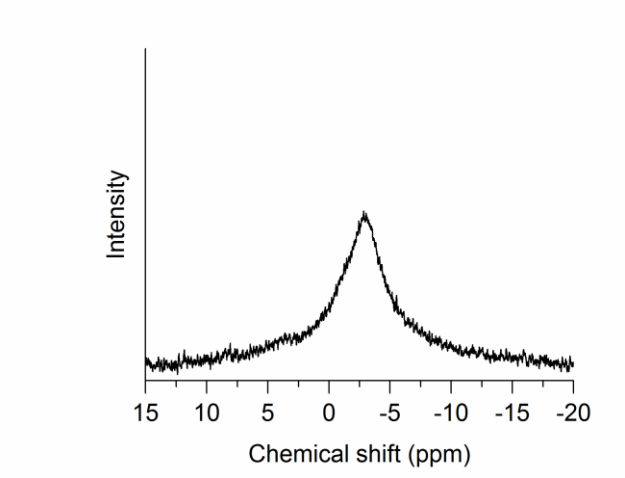

Figure 3.7 ^{31}P NMR of poly(ethyl *S*-methylthiocysteinyl-*co*-ethyl cysteinyl phosphazene) (POP-EtCys-SH). ^{31}P NMR δ_P/ppm (162 MHz, $CDCl_3$): -2.6. Spectrum referenced to triphenylphosphine (-6 ppm, not shown) to determine central value, then reacquired in the absence of a reference to avoid peak overlap. Concentration: 200 mg mL^{-1}. Reproduced by permission of The Royal Society of Chemistry.

resonance at 23 ppm. Partial cleavage of the disulfide bond results in the appearance of a weak, poorly-resolved feature at 16 ppm that corresponds to the methylene protons of cysteine. ^{31}P NMR gave a broad resonance centered at approximately -2.6 ppm, as depicted in Figure 3.7. Major IR bands provide additional structural confirmation and include the features characteristic of the cysteine-derived substituents at 3320 (N-H stretch), 2980, 2914 (C-H stretch), 1732 (C=O stretch), 1417, 1367 (C-H bend) 1180, and 1117, and 1026 (C-O stretch) (Figure 3.8). The bands appearing at 1295 and 853 cm^{-1} are associated with vibration of the polyphosphazene backbone, while the band at 950 cm^{-1} is most directly attributable to P-N vibrations resulting from substitution at the phosphorus atom.[54,55] The weak thiol S-H stretch was not clearly resolved in the IR spectrum, and S-S vibrations arising from disulfide linkages are typically expected to occur below 650 cm^{-1}.[56,57] However, the minor feature at 698 cm^{-1} was assigned to C-S stretching. As previously established by Weikel for the corresponding ethyl disulfide, the methyl disulfide scission is incomplete using 5 equivalents of 2-mercaptoethanol and increasing the

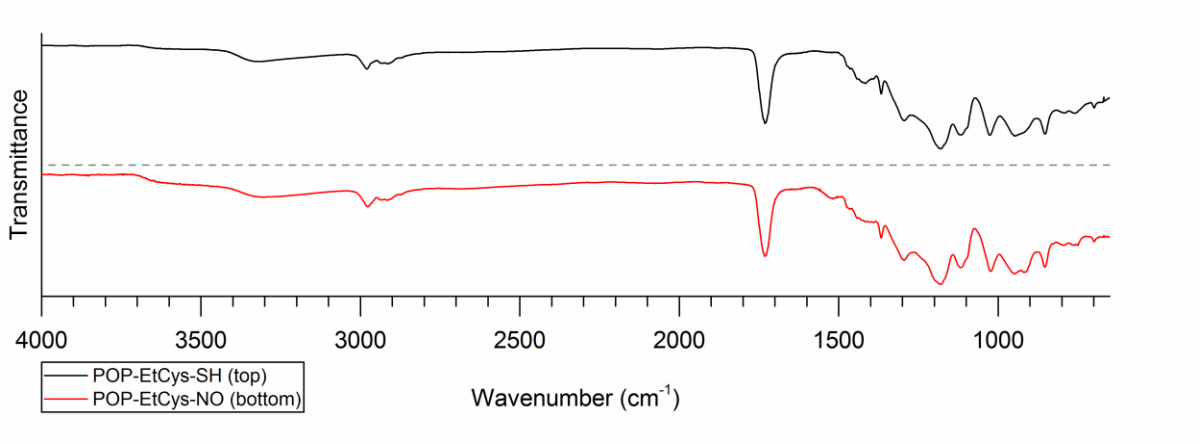

Figure 3.8. ATR-FTIR spectra of polymers. Poly(ethyl *S*-methylthiocysteinyl-*co*-ethyl cysteinyl phosphazene) (POP-EtCys-SH) (top), and its *S*-nitrosated derivative (POP-EtCys-NO) (bottom). POP-EtCys-SH: IR ν_{max}/cm^{-1}: 3320, 2980, 2914, 1732, 1417, 1367, 1295, 1180, 1117, 1026, 948, 853, 792, 760, 698. POP-EtCys-NO: IR ν_{max}/cm^{-1}: 3300, 2977, 2915, 1732, 1520, 1367, 1296, 1180, 1117, 1024, 950, 920, 853, 794, 763, 750, 699. Reproduced by permission of The Royal Society of Chemistry.

concentration of the reagent does not significantly improve the outcome of the reaction. The thiol content of the polymer subsequent to disulfide cleavage with 2-mercaptoethanol was estimated by both ^{1}H NMR spectroscopy and colorimetrically using a modification of Ellman's assay for thiol determination. For ^{1}H NMR, the ratio of the protons of the methyl disulfide group (2.43 ppm) to the methyl protons of the ester group (1.31 ppm) was used to estimate the relative extent of disulfide scission and therefore the thiol content. This method suggested that 50% of the methyl disulfide linkages were cleaved during the reaction, an outcome that is consistent with the values reported by Weikel for the ethyl disulfide. However, this method may not account for symmetrical disulfide resulting from either oxidation of free thiol or by disulfide exchange, which leads to features that may significantly overlap in the observed ^{1}H NMR spectrum of the polymer. As a further estimate of thiol content, polymer samples were evaluated using a modified Ellman's assay with bis(2,4-dinitrophenyl) disulfide in DMF, following a previously reported protocol.[58] The calculated thiol content was 1.45 ± 0.13 mmol g^{-1} (mean ± SD, n = 5),

corresponding to an estimated 20% deprotection (Table 3.1). This more conservative value was used in subsequent calculations, in the event that crosslinking from disulfide formation is a significant factor in the deprotection process. An alternative deprotection strategy utilizing tris(2-carboxyethyl)phosphine as the disulfide reducing agent resulted in the apparent total cleavage of the methyl disulfide, however the expense of this reagent and inefficient removal prohibits its use on larger scales. Harsher reducing conditions (Zn/HCl) were previously reported by Weikel to lead to concomitant decomposition of a similar polymer. The deprotected polymer was soluble in chloroform, DCM, DMF and THF, poorly soluble in acetone, ethanol, and methanol, and did not exhibit appreciable solubility in water or diethyl ether. GPC analysis (DMF) gave an average molecular weight of $M_n = 4.73 \times 10^3$ g mol^{-1} with a PDI of 1.25, while TGA indicated an onset decomposition temperature of 166 °C. DSC gave an initial T_g of 24 °C, however subsequent thermal cycles continuously increased the temperature of the transition, an observation which may arise from disulfide exchange between free sulfhydryl groups and the methyl disulfide linkage. This process potentially results in crosslinking that could account for the observed increase in T_g as a function of heating cycle.[59,60]

Table 3.1 Total thiol (POP-EtCys-SH) and nitric oxide (POP-EtCys-NO) content. Data reported as mean ± SD (n ≥ 3). [a]Value determined by modified Ellman's assay protocol. [b]Value determined by UV decomposition of *S*-nitrosothiol (100 W, 365 nm, 40 °C). [c]Calculated as mol NO/mol SH × 100%.

Thiol content (mmol g^{-1})[a]	NO content by UV-Vis decomposition (mmol g^{-1})[b]	Conversion to *S*-nitrosothiol (%)[c]
1.45 ± 0.13	0.55 ± 0.04	38 ± 4

3.3.2. Synthesis of *S*-nitrosated poly(ethyl *S*-methylthiocysteinyl-*co*-ethyl cysteinyl phosphazene)

S-Nitrosothiols are most commonly synthesized through the reaction of thiols with reagents such as nitrous acid or nitrosyl chloride (both typically formed *in situ* by the reaction of nitrite with aqueous hydrochloric acid) and by oxygen-to-sulfur transnitrosation reactions with alkyl nitrites.[61] In the case of *S*-nitrosothiols bound to hydrolytically-sensitive polymers, it can be anticipated that the presence of aqueous acid may result in concomitant hydrolysis of the polymer. Since polyphosphazenes may be expected to experience an increased rate of hydrolytic degradation under highly acidic conditions, the *S*-nitrosation was carried out under milder conditions using *t*-BuONO in organic solvent. Although the *S*-nitrosation slowly proceeded in both DCM and DMF, the use of DCM resulted in accelerated decomposition of the *S*-nitrosothiol and DMF prevented isolation of the polymer due to low volatility. Despite poor solubility in ethanol, a system consisting of 10% v/v *t*-BuONO/ethanol was found to effectively *S*-nitrosate the material while avoiding the complications found in other solvents, since this mixture did not greatly accelerate decomposition and was easily removed *in vacuo*. As noted in prior reports, the reaction of *t*-BuONO and ethanol may lead to the formation of an equilibrium concentration of ethyl nitrite that is also capable of acting as a nitrosating agent.[62] The successful *S*-nitrosation of the polymer was accompanied by the development of a distinct red/pink color and was confirmed by the appearance of bands in the UV-Vis spectrum at 337 and 547 nm, corresponding to what have been variably described as $\pi \rightarrow \pi^*$ or $n_O \rightarrow \pi^*$ (approximately 340 nm) and $n_N \rightarrow \pi^*$ (approximately 550 nm) transitions of the *S*-nitrosothiol functional group (Figure 3.9).[63,64] The removal of *t*-BuONO was confirmed by the absence of the prominent multiplet typically associated with alkyl nitrites near 400 nm, and no

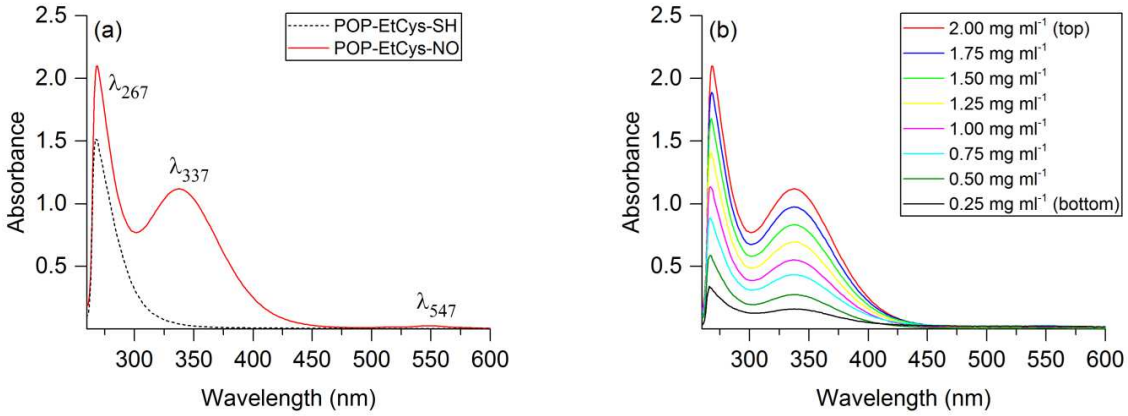

Figure 3.9 UV-Vis spectra of polymers. Poly(ethyl *S*-methylthiocysteinyl-*co*-ethyl cysteinyl phosphazene) (POP-EtCys-SH) and its *S*-nitrosated derivative (POP-EtCys-NO) in DMF. The characteristic absorbances associated with the successful formation of primary *S*-nitrosothiols are shown in (a), while (b) illustrates the relationship between polymer concentration and the prominent absorbance at 337 nm that is often attributed to a $\pi \rightarrow \pi^*$ transition. Reproduced by permission of The Royal Society of Chemistry.

features developed that indicated the formation of *N*-nitroso species.[65,66] As further confirmation, IR features at 1520 and 750 cm^{-1} appeared that were assigned to fundamental N=O and C-S stretching vibrations (Figure 3.8).[57,67,68] In 10% v/v *t*-BuONO/ethanol, the extent of *S*-nitrosation (monitored by UV-Vis) did not increase after 15 min at RT and began to decline thereafter, corresponding to the gradual decomposition of *S*-nitrosothiol. The *S*-nitrosated polymer generally retained the same solubility characteristics as the parent thiolated material and readily dissolved in chloroform, DCM, DMF, and THF at concentrations in excess of 150 mg mL^{-1}. Unlike the parent polymer, the *S*-nitrosated polyphosphazene exhibited diminishing solubility over time and was no longer appreciably soluble in DCM or DMF after storage for 24 h at 25 °C under ambient light. This behavior can be attributed to crosslinking arising from the formation of disulfide linkages during decomposition of the *S*-nitrosothiol. Storage of the *S*-nitrosated polymer at -20

°C greatly inhibited decomposition, with 103 ± 5% (mean ± SD, n = 3) of *S*-nitrosothiol (UV-Vis) remaining at the end of 7 weeks and no loss of solubility in DMF. Interestingly, when ethyl cysteinate hydrochloride was treated with *t*-BuONO under similar nitrosating conditions, the compound rapidly decomposed with vigorous evolution of gas and the formation of a transient red color that quickly faded. This observation may indicate that covalent attachment of ethyl cysteinate to the polyphosphazene backbone prevents reaction of the primary amine with nitrosating agents, and consequently inhibits diazotization-related decomposition pathways.[69] It is difficult to attribute the increased stability of the polymer-bound *S*-nitrosothiol to a single factor. However, the development of a hydrogen bond involving the N-H group of pendant ethyl cysteinyl moieties is indicated by the shift in vibrational frequency from 3320 to 3300 cm^{-1} subsequent to *S*-nitrosation. Hydrogen bonding interactions in computational models of *S*-nitrosocysteine and *S*-nitroso-*N*-acetylcysteine have been previously suggested to induce polarization of the N=O bond that may increase thermal stability.[70] Although this phenomenon may be operative in the case of POP-EtCys-NO, it is difficult to make direct comparisons with *S*-nitrosated ethyl cysteinate due to its rapid decomposition.

3.3.3. Nitric oxide release

Additional characterization was performed by evaluating the ability of POP-EtCys-NO to release gaseous NO under various conditions. NO measurements were carried out using commercial chemiluminesence-based NO-selective analyzers that rely on the gas-phase reaction of NO with ozone to produce nitrogen dioxide in the excited state ($NO + O_3 \rightarrow NO_2^* + O_2$).[71] The relaxation of excited-state NO_2 results in emission of light that is

detected by the instrument and used to quantify NO concentration as a function of time. In all cases, solvents were deoxygenated by nitrogen purge prior to use, and released NO was swept into the instrument with a constant nitrogen flow/purge following previously reported protocols. Since *S*-nitrosothiols are known to rapidly and quantitatively decompose to release NO through distinct photolytic and copper-catalyzed pathways, both methods were utilized to assess the NO content of the S-nitrosated polymer.[40,72] Photolytic decomposition with UV light (365 nm) at 40 °C in DMF resulted in a total NO content of 0.55 ± 0.04 mmol g^{-1} (mean ± SD, $n \geq 3$), corresponding to the conversion of 38 ± 4% of thiol groups (Ellman's assay) to *S*-nitrosothiol (Table 3.1). This value suggests that the efficacy of the *S*-nitrosation reaction is limited when considering the total quantity of available thiol, which may be a consequence of poor polymer solubility in ethanol or loss of nitrosating agent as ethyl nitrite, which exists as a gas below room temperature. Control samples consisting of non-nitrosated polymer exposed to UV light did not produce detectable NO. Decomposition with 5.0×10^{-4} M copper(II) chloride at ambient temperature in ethanol gave a total NO content of 0.46 ± 0.05 mmol g^{-1}. However, the poor solubility of the polymer in ethanol may have resulted in impaired catalyst access and incomplete decomposition of the *S*-nitrosothiol, since the majority of the NO release occurred comparatively slowly (2 h) and continuing low-level NO emission persisted. The reaction could not be carried out in DMF, since the activity of the copper catalyst was significantly reduced in that solvent, and other organic solvents exhibited impractically high volatility or did not effectively dissolve the polymer or catalyst. The values obtained from UV decomposition were therefore utilized in subsequent calculations. In addition, a molar extinction coefficient of 810 ± 20 M^{-1} cm^{-1} (mean ± SD, 337 nm, DMF) for the polymer-bound *S*-nitrosothiol was determined by relating the UV absorbance to molar NO content at varying polymer concentrations. This value was consistent

with prior studies reporting molar extinction coefficients of various *S*-nitrosothiols near 1000 M^{-1} cm^{-1} for the absorbance centered near 340 nm.[63]

S-nitrosothiols have been frequently invoked as useful sources of releasable NO due to their ability to decompose under physiological conditions through thermal or transition metal ion-mediated pathways to produce NO and disulfide. Moreover, *S*-nitrosothiols such as S-nitrosocysteine (commonly in the form of *S*-nitrosated protein residues as in S-nitrosoalbumin) have been established to exist endogenously as participants in various physiological processes. To evaluate the ability of the *S*-nitrosated polymer to release NO under physiological conditions, NO release profiles were collected at 37 °C in pH 7.4 PBS over 24 h (Figure 3.10). At the end of the 24 h period, cumulative NO release was 0.35 ± 0.02 mmol g^{-1} (mean ± SD, n = 3), corresponding to 64% of theoretical NO. The remaining theoretical NO was recovered by UV-induced photolytic decomposition at 40 °C, and suggested the potential for continuing NO release over an extended period.

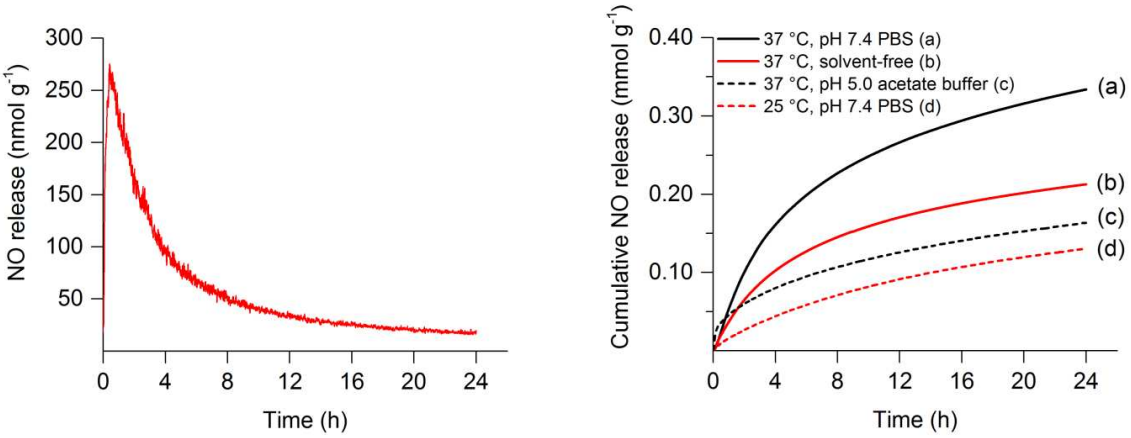

Figure 3.10 NO release profiles of *S*-nitrosated poly(ethyl S-methylthiocysteinyl-co-ethyl cysteinyl phosphazene). Left: Representative NO release profile of POP-EtCys-NO over 24 h (37 °C, pH 7.4 PBS, n = 3). Right: Cumulative NO release of POP-EtCys-NO under varying conditions (n = 3). Reproduced by permission of The Royal Society of Chemistry.

The physiological release profile was generally consistent with second-order exponential decay following initial equilibration, with the greater portion of this NO release occurring within approximately 4 h. This data indicates that POP-EtCys-NO exhibits a relatively high level of total NO content and serves as an effective source of releasable NO under physiological conditions. In comparison, our previously reported NO-releasing polyester consisting of *S*-nitrosated L-cysteine covalently attached to poly(lactic-*co*-glycolic-*co*-2,2-bis(hydroxymethyl)propionic acid) demonstrated a total NO content of 0.17 mmol g^{-1} and released 93% of available NO over 48 h at 37 °C in pH 7.4 PBS, while the citrate-based elastomer poly(citric-*co*-maleic acid-*co*-1,8-octanediol) modified to incorporate *S*-nitrosated ethyl cysteinyl pendant groups contained 0.16 mmol g^{-1} NO and released 41% over 4 days.[73,74] Frost reported another cysteine-based NO-releasing material consisting of fumed silica particles with covalently incorporated *S*-nitrosocysteine that exhibited total NO loading of 0.021 mmol g^{-1} and released a maximum of 40% of available NO in toluene in the presence of a copper initiator.[75] POP-EtCys-NO exhibits a greater extent of total NO loading than these prior cysteine-based systems and retains solubility in organic solvents, permitting subsequent processing.

Although the chemical behavior of *S*-nitrosothiols has been comprehensively elucidated in prior reports, change in the NO release properties of the *S*-nitrosated polyphosphazene in response to varying temperature and pH was briefly investigated. To this end, additional release profiles were acquired over the same 24 h interval at 25 °C in pH 7.4 PBS, 37 °C in pH 5.0 acetate buffer, and 37 °C under anhydrous, solvent-free conditions (Table 3.2, Figure 3.10, Figure 3.11). In PBS, the temperature dependence of NO-producing *S*-nitrosothiol decomposition was apparent in the slower NO release kinetics observed at 25 °C. This behavior resulted in a 58% reduction in cumulative NO release over 24 h, from 0.35 ± 0.02 to 0.15 ± 0.02 mmol g^{-1}, and

Table 3.2 Cumulative nitric oxide release from *S*-nitrosated poly(ethyl S-methylthiocysteinyl-co-ethyl cysteinyl phosphazene). Data reported as mean ± SD (*n* = 3) over 24 h of release. [a]0.2 mg mL^{-1}, 5 mL pH 7.4 PBS, 37 °C. [a]0.2 mg mL^{-1}, 5 mL pH 7.4 PBS, 25 °C. [c]0.2 mg mL^{-1}, 5 mL pH 5.0 acetate buffer, 37 °C. [d]1 mg, 37 °C.

	37 °C, pH 7.4 PBS[a]	**25 °C, pH 7.4 PBS[b]**	**37 °C, pH 5.0 acetate buffer[c]**	**37 °C, anhydrous, solvent-free[d]**
Cumulative NO release (mmol g^{-1})	0.35 ± 0.02	0.15 ± 0.02	0.13 ± 0.03	0.22 ± 0.02

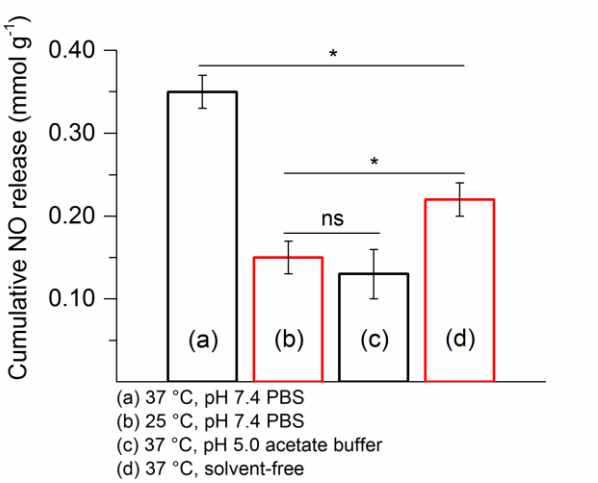

Figure 3.11 24 h cumulative NO release for *S*-nitrosated poly(ethyl S-methylthiocysteinyl-co-ethyl cysteinyl phosphazene). (mean ± SD , *n* = 3). Statistical differences evaluated by single-factor ANOVA analysis and Tukey's range test ($p < 0.05$). Reproduced by permission of The Royal Society of Chemistry.

may be attributable in part to increased stability of the S-N bond at lower temperature. In pH 5.0 acetate buffer, a similar 63% decline in cumulative NO release to 0.13 ± 0.03 mmol g^{-1} over 24 h was observed, an outcome that could be explained by previous studies that proposed increased stabilization of *S*-nitrosothiols under acidic conditions.[76,77] However, UV decomposition of the remaining *S*-nitrosothiol at 40 °C resulted in a total recovery of only 50 ± 10% of theoretical NO. This suggests that the apparent reduction in NO release may be a consequence of *S*-nitrosothiol decomposition in acetate buffer through a process that does not generate detectable NO. The

results for this system are therefore consistent with reports that indicate a significant *destabilization* and loss of *S*-nitrosothiol at acidic pH.[78] 24 h NO release from the polymer at 37 °C in the absence of solvent was reduced by 38% relative to pH 7.4 PBS at the same temperature, but remained marginally higher than the release observed in pH 7.4 PBS at 25 °C. These results suggest that decomposition of the polymer-bound *S*-nitrosothiol is not solely a function of temperature, but that the presence of PBS facilitates this process in a temperature-dependent manner.

3.3.4. Degradation study

To assess the degradation characteristics of both POP-EtCys-SH and the *S*-nitrosated derivative POP-EtCys-NO under physiological conditions, samples (n = 5) were immersed in pH 7.4 PBS at 37 °C for a total of 6 weeks (Figure 3.12). At intervals of 1 week, the buffer was removed and samples were washed thoroughly with Millipore water. The samples were subsequently lyophilized for 24 h to remove water and the mass of dry polymer was recorded. The thiolated polymer was found to undergo a 36% average mass loss over 6 weeks, with more rapid degradation occurring in the first three weeks of the study. The *S*-nitrosated derivative experienced 41% mass loss over the same period, with a gradual decrease in the rate of degradation that paralleled the properties of the thiolated material. The pH of the buffer solutions was generally not observed to vary significantly relative to PBS controls, except in the case of the *S*-nitrosated derivative, where the release of NO during the first week decreased the pH to 6-7. This may have resulted from the formation of low concentrations of HNO_2 or HNO_3 produced from the reaction of NO with water and atmospheric oxygen, and was an anticipated outcome of *S*-nitrosothiol decomposition.[79] For the *S*-nitrosated polymer, this initial increase in

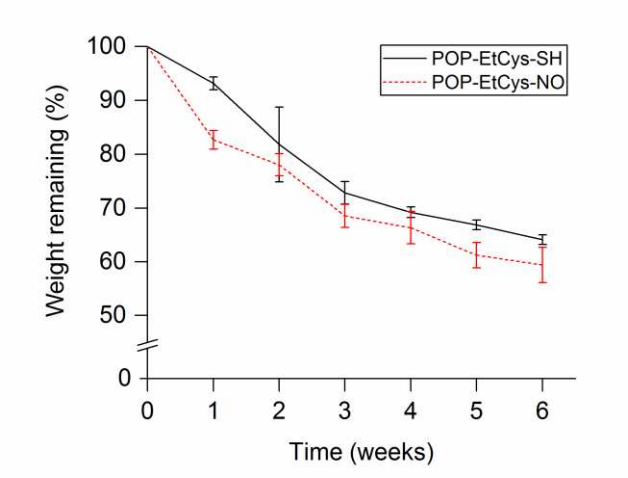

Figure 3.12 Degradation of polymers over 6 weeks (37 °C, PBS, mean ± SD, n = 5). Reproduced by permission of The Royal Society of Chemistry.

the rate of hydrolysis is most directly responsible for the greater degree of degradation observed at the end of the study. The declining rate of degradation for both polymers was attributed to crosslinking arising from disulfide formation, which may be attributed to thiol oxidation under mildly basic, oxygenated conditions or to *S*-nitrosothiol decomposition.[80] After the end of the 6 week degradation period, the IR spectra of both the thiolated and *S*-nitrosated materials were consistent with those initially obtained for the thiolated polymer, indicating that no significant compositional changes occurred. Furthermore, the polymers no longer exhibited any appreciable solubility in DCM, DMF, or other common organic solvents, which may provide further indication of crosslinking.

3.3.5. Cell studies

Preliminary assessment of the cytotoxicity of both the thiolated (POP-EtCys-SH) and *S*-nitrosated materials (POP-EtCys-NO) was carried out through exposure of HDF to polymer extracts obtained following the general method described in ISO 10993.[46] This method provides insight into the toxicity of leachables that may be removed or formed from the polymer samples

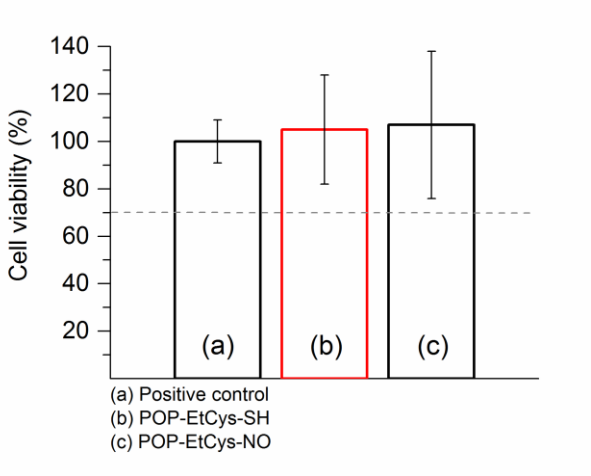

Figure 3.13. CellTiter-Blue viability assay results for HDF (mean ± SD , *n* = 9) exposed to polymer extracts. Dashed line indicates the 70% cell viability threshold. Reproduced by permission of The Royal Society of Chemistry.

over the 24 h extraction period and has been previously utilized to evaluate the potential toxicity of biomaterials.[74,81] The CellTiter-Blue assay was used to evaluate HDF viability after exposure to polymer extracts (*n* = 9), a method that exploits the reductive conversion of resazurin to resorufin as a consequence of cellular metabolic activity. For both POP-EtCys-SH and POP-EtCys-NO, the percentage of viable cells (normalized to the positive control) remained above the 70% cell viability threshold, indicating low relative cytotoxicity for extracts obtained over 24 h (Figure 3.13). In the case of POP-EtCys-SH, leachables were anticipated to primarily take the form of trace ethanol liberated from hydrolysis of the ethyl ester, cysteine and cysteine derivatives, and the phosphate and ammonia products typically produced from the degradation of polyphosphazenes.[11] Since the majority of such leachables have been previously established to possess relatively low toxicity, it is perhaps more significant to note that the methyl disulfide group introduced by reaction of ethyl cysteinate with MMTS did not induce significant leaching-related toxicity at the tested extraction concentration. POP-EtCys-NO introduces the additional possibility of NO release that may lead to the formation of various byproducts under aerobic

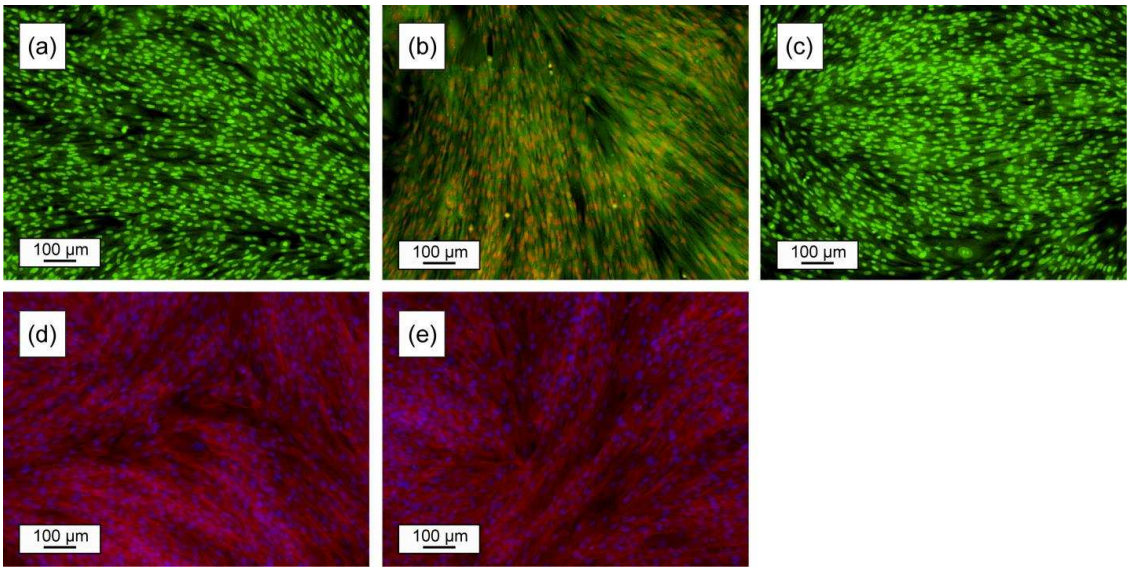

Figure 3.14 LIVE/DEAD and cell morphology images after 24 h polymer extract exposure. Fluorescence microscope images for LIVE/DEAD assay are (a) positive control consisting of HDF cultured in cell medium, (b) negative control (methanol exposure), and (c) HDF after exposure to extracts from POP-EtCys-NO. Morphological images are (d) positive control, and (e) HDF after exposure to extracts from POP-EtCys-NO. For LIVE/DEAD and cell morphology experiments, n = 6. Reproduced by permission of The Royal Society of Chemistry.

conditions, but this was not observed to produce any significant decrease in cell viability relative to the thiolated material. For this reason, only POP-EtCys-NO was subjected to further assessment.

In addition to the CellTiter-Blue cell viability assay, fluorescence microscopy was utilized to evaluate both the qualitative viability (LIVE/DEAD assay) of HDF exposed to extracts from POP-EtCys-NO and to ensure that cell morphology was preserved. Figure 3.14a-c depicts the results of the LIVE/DEAD assay, where all cells exhibit the characteristic green color of the SYTO 9 fluorescent stain, while only non-viable cells with disrupted membranes exhibit the red color associated with PI. Figure 3.14a depicts the positive control, with the majority of cells exhibiting intact membranes, while the negative control in Figure 3.14b shows the development of the red color associated with disruption of cell membranes after exposure to methanol. Figure

3.14c shows the outcome of HDF exposure to extracts from POP-EtCys-NO (n = 6), which results in cells that exhibit similar staining to those seen in the positive control. In order to examine cellular morphology after exposure to the material extracts, the stains Alexa and DAPI were added to the HDF. Alexa has the ability to stain the cell actin cytoskeletons and appears red, while DAPI stains only the cell nuclei and appears blue. Figure 3.14d shows the results of the morphological assay for the positive TC control and Figure 3.14e shows cells exposed to extracts from POP-EtCys-NO (n = 6). Both the control and sample show the predicted cellular morphology of HDF, indicating that there is no distortion or alteration in morphology after 24 h exposure to the *S*-nitrosated polymer extract.

3.4. Conclusions

We have synthesized and characterized the biodegradable cysteine-based polyphosphazene poly(ethyl *S*-methylthiocysteinyl-*co*-ethyl cysteinyl phosphazene) (POP-EtCys-SH) and demonstrated NO release capability from an *S*-nitrosated derivative of this material (POP-EtCys-NO) under physiological conditions. The total average NO content of POP-EtCys-NO was found to be 0.55 ± 0.04 mmol g^{-1}, corresponding to a conversion of 38 ± 4% of thiol groups to *S*-nitrosothiol. Over the course of 24 h, 0.35 ± 0.02 mmol g^{-1} NO (64% of theoretical) was released under physiological conditions (37 °C, pH 7.4 PBS), with NO emission continuing at a low level thereafter. Slower NO release was observed over the same interval at physiological temperature under solvent-free conditions (0.22 ± 0.02 mmol g^{-1}), and both reduced temperature (25 °C, pH 7.4) and pH (37 °C, pH 5) produced decreased 24 h release of 0.15 ± 0.02 and 0.13 ± 0.03 mmol g^{-1} NO, respectively. Both POP-EtCys-SH and POP-EtCys-NO were found to degrade in PBS at physiological temperature, experiencing 36 and 41% mass loss over 6 weeks. The relative

cytotoxicity of extracts obtained from POP-EtCys-NO was evaluated by CellTiter-Blue assay, where HDF viability was found to remain above the 70% cytotoxicity threshold at the tested extract concentration. In addition, LIVE/DEAD assay and fluorescence microscopy imaging after staining with Alexa Fluor 568/SYTO 9 indicated that extracts did not produce significant disruption of cell membranes or alteration of cell morphology. Since polyphosphazenes have been extensively investigated for various biomedical purposes, these results suggest that POP-EtCys-NO may serve as an effective candidate material for such applications where the therapeutic properties of NO release are desirable.

Individual contributions and funding sources

Cytotoxicity studies performed by B. H. Neufeld, who was the primary author of section 3.3.5. M. J. Neufeld assisted during preparation of the manuscript. All other work carried out by A. Lutzke. Funding for this research was provided by the Department of Defense Congressionally Directed Medical Research Program (W81XWH-11-2-0113). Dr. Ketul Popat and Rachael Simon-Walker of Colorado State University contributed human dermal fibroblasts (HDF) for use in evaluating the cytotoxicity of extracts obtained from the polymers described in this work, and the lab of Dr. Eugene Chen of Colorado State University provided access to GPC instrumentation and assistance with data processing.

REFERENCES

1. Nair, L. S.; Laurencin, C. T. *Prog. Polym. Sci*. **2007**, *32*, 762-798.
2. Ulery, B. D.; Nair, L. S.; Laurencin, C. T. *J. Polym. Sci. B Polym. Phys*. **2011**, *49*, 832-864.
3. Basu, A.; Kunduru, K. R.; Abtew, E.; Domb, A. J. *Bioconjug. Chem*. **2015**, *26*, 1396-1412.
4. Wang, Y. C.; Yuan, Y. Y.; Du, J. Z.; Yang, X. Z.; Wang, J. *Macromol. Biosci*. **2009**, *9*, 1154-1164.
5. Middleton, J. C.; Tipton, A. J. *Biomaterials* **2000**, *21*, 2335-2346.
6. Gleria, M.; De Jaeger, R. *Top. Curr. Chem.* **2005**, *250*, 165-251.
7. Allcock, H. R. *Appl. Organometal. Chem*. **1998**, *12*, 659-666.
8. Deng, M.; Kumbar, S. G.; Wan, Y.; Toti, U. S.; Allcock, H. R.; Laurencin, C. T. *Soft Matter* **2010**, *6*, 3119-3132.
9. Allcock, H. R.; Pucher, S. R. *Macromolecules* **1994**, *27*, 1071-1075.
10. Weikel, A. L.; Owens, S. G.; Fushimi, T.; Allcock, H. R. *Macromolecules* **2010**, *43*, 5205-5210.
11. Allcock, H. R.; Fuller, T. J.; Mack, D. P.; Matsumura, K.; Smeltz, K. M. *Macromolecules* **1977**, *10*, 824-830.
12. Lakshmi, S.; Katti, D. S.; Laurencin, C. T. *Adv. Drug Deliv. Rev.* **2003**, *55*, 467-482.
13. Anderson, J. M. *Annu. Rev. Mater. Sci*. **2001**, *31*, 81-110.
14. Anderson, J. M.; Rodriguez, A.; Chang, D. T. *Semin. Immunol.* **2008**, *20*, 86-100.
15. Gorbet, M. B.; Sefton, M. V. *Biomaterials* **2004**, *25*, 5681-5703.
16. Kohane, D. S.; Langer, R. *Chem. Sci*. **2010**, *1*, 441-446.

17. Puranik, A. S.; Dawson, E. R.; Peppas, N. A. *Int. J. Pharm*. **2013**, *441*, 665-679.

18. Bridges, A. W.; Garcia, A. J. *J. Diabetes Sci. Technol*. **2008**, *2*, 984-994.

19. Liang, Y.; Kiick, K. L. *Acta Biomater*. **2014**, *10*, 1588-1600.

20. Seabra, A. B.; Durán, N. *J. Mater. Chem*. **2010**, *20*, 1624-1637.

21. Bogdan, C. *Nat. Immunol*. **2001**, *2*, 907-916.

22. Toledo, J. C., Jr.; Augusto, O. *Chem. Res. Toxicol*. **2012**, *25*, 975-989.

23. Butler, A. R.; Williams, D. L. H. *Chem Soc. Rev*. **1993**, *22*, 233-241.

24. Ignarro, L. J.; Buga, G. M.; Wood, K. S.; Byrns, R. E.; Chaudhuri, G. *Proc. Natl. Acad. Sci. U. S. A*. **1987**, *84*, 9265-9269.

25. Ignarro, L. J., Ed. *Nitric Oxide: Biology and Pathobiology*, 2nd ed; Elsevier: Amsterdam, 2010; p 12.

26. Wang, G. R.; Zhu, Y.; Halushka, P. V.; Lincoln, T. M.; Mendelsohn, M. E. *Proc. Natl. Acad. Sci. U. S. A.* **1998**, *95*, 4888-4893.

27. Lüscher, T. F.; Steffel, J.; Eberli, F. R.; Joner, M.; Nakazawa, G.; Tanner, F. C.; Virmani, R. *Circulation* **2007**, *115*, 1051-1058.

28. Carpenter, A. W.; Schoenfisch, M. H. *Chem. Soc. Rev*. **2012**, *41*, 3742-3752.

29. Schairer, D. O.; Chouake, J. S.; Nosanchuk, J. D.; Friedman, A. J. *Virulence* **2012**, *3*, 271-279.

30. Regev-Shoshani, G.; Ko, M.; Miller, C.; Av-Gay, Y. *Antimicrob. Agents Chemother*. **2010**, *54*, 273-279.

31. Isenberg, J. S.; Ridnour, L. A.; Espey, M. G.; Wink, D. A.; Roberts, D. A. *Microsurgery* **2005**, *25*, 442-451.

32. Witte, M. B.; Barbul, A.; *Am. J. Surg*. **2002**, *183*, 406-412.

33. Lowe, A.; Bills, J.; Verma, R.; Lavery, L.; Davis, K.; Balkus, K. J., Jr. *Acta Biomater*. **2015**, *13*, 121-130.

34. Nichols, S. P.; Storm, W. L.; Koh, A.; Schoenfisch, M. H. *Adv. Drug. Deliv. Rev*. **2012**, *64*, 1177-1188.

35. Diwan, A. D.; Wang, M. X.; Jang, D.; Zhu, W.; Murrell, G. A. *J. Bone Miner. Res.* **2000**, *15*, 342-351.

36. Ichinose, F.; Roberts, J. D., Jr.; Zapol, W. M. *Circulation* **2004**, *109*, 3106-3111.

37. Thomas, D. D.; Liu, X.; Kantrow, S. P. Lancaster, J. R., Jr. *Proc. Natl. Acad. Sci. U. S. A.* **2001**, *98*, 355-360.

38. Miller, M. R.; Megson, I. L. *Br. J. Pharmacol*. **2007**, *151*, 305-321.

39. Ignarro, L. J.; Napoli, C.; Loscalzo, J. *Circ. Res.* **2002**, *90*, 21-28.

40. Williams, D. L. H. *Chem. Commun*. **1996**, 1085-1091.

41. Keefer, L. K. *ACS Chem. Biol*. **2011**, *6*, 1147-1155.

42. Broniowska, K. A.; Diers, A. R.; Hogg, N. *Biochim. Biophys. Acta* **2013**, *1830*, 3173-3181.

43. Stamler, J. S.; Jaraki, O.; Osborne, J.; Simon, D. I.; Keaney, J.; Vita, J.; Singel, D.; Valeri, C. R.; Loscalzo, J. *Proc. Natl. Acad. Sci. U. S. A.* **1992**, *89*, 7674-7677.

44. Massy, Z. A.; Fumeron, C.; Borderie, D.; Tuppin, P.; Nguyen-Khoa, T.; Benoit, M. O. Jacquot, C.; Buisson, C.; Drüeke, T. B.; Enkindjian, O. G.; Lacour, B.; Iliuo, M. C. *J. Am. Soc. Nephrol*. **2004**, *15*, 470-476.

45. Tsikas, D.; Schmidt, M.; Böhmer, A.; Zoerner, A. A.; Gutzki, F. M.; Jordan, J. *J. Chromatogr. B*. **2013**, *927*, 147-157.

46. International Organization for Standardization, Biological evaluation of medical devices - Part 5: Test for *in vitro* cytotoxicity. ISO 10993-5, Geneva, Switzerland, 2009, pp. 1-34.

47. Allen, G.; Lewis, C. J.; Todd, S. M. *Polymer* **1970**, *11*, 31-43.

48. Honeyman, C. H.; Manners, I. Morrissey, C. T.; Allcock, H. R. *J. Am. Chem. Soc*. **1995**, *117*, 7035-7036.

49. Marschütz, M. K.; Bernkop-Schnürch, A. *Eur. J. Pharm. Sci.* **2002**, *15*, 387-394.

50. Wang, B.; Rivard, E.; Manners, I. *Inorg. Chem*. **2002**, *41*, 1690-1691.

51. Henke, H.; Wilfert, S.; Iturmendi, A.; Brüggemann, O.; Teasdale, I. *J. Polym. Sci. A Polym. Chem.* **2013**, *51*, 4467-4473.

52. Smith, D. J.; Miggio, E. T.; Kenyon, G. L. *Biochemistry* **1975**, *14*, 766-771.

53. Roberts, D. D.; Lewis, S. D.; Ballou, D. P.; Olson, S. T.; Shafer, J. A. *Biochemistry*, **1986**, *25*, 5595-5601.

54. Matyjaszewski, K.; Lindenberg, M. S.; Moore, M. K.; White, M. L. *J. Polym. Sci. A Polym. Chem*. **1994**, *32*, 465-473.

55. Singler, R. E.; Schneider, N. S.; Hagnauer, G. L. *Polym. Eng. Sci.* **1975**, *15*, 321-338.

56. Coates, J. Interpretation of Infrared Spectra, A Practical Approach. In *Encyclopedia of Analytical Chemistry*; R. A. Meyers, Ed.; John Wiley & Sons, Ltd.: Chichester, 2000; pp. 10815-10837.

57. Lin-Vien, D.; Colthup, N. B.; Fateley, W. G.; Grasselli, J. G. *The Handbook of Infrared and Raman Characteristic Frequencies of Organic Molecules*; Academic Press: San Diego, 1991; p 226.

58. Gabor, G.; Vincze, A. *Anal. Chim. Acta* **1977**, *92*, 429-431.

59. Fox, T. G.; Flory, P. J. *J. Polym. Sci*. **1954**, *14*, 315-319.

60. Shefer, A.; Gottlieb, M. *Macromolecules* **1992**, *25*, 4036-4042.

61. Williams, D. L. H. *Nitrosation Reactions and the Chemistry of Nitric Oxide*; Elsevier: Amsterdam, 2004; p 118.

62. Doyle, M. P.; Terpstra, J. W.; Pickering, R. A.; LePoire, D. M. *J. Org. Chem.* **1983**, *48*, 3379-3382.

63. Williams, D. L. H. *Acc. Chem. Res.* **1999**, *32*, 869-876.

64. M. D. Bartberger, M. D.; Houk, K. N.; Powell, S. C.; Mannion, J. D.; Lo, K. Y.; Stamler, J. S.; Toone, E. J. *J. Am. Chem Soc.* **2000**, *122*, 5889-5890.

65. Ungnade, H. E.; Smiley, R. A. *J. Org. Chem*. **1956**, *21*, 993-996.

66. Wang, P. G.; Xian, M.; Tang, X.; Wu, X.; Wen, Z.; Cai, T.; Janczuk, A. J. *Chem. Rev.* **2002**, *102*, 1091-1134.

67. Philippe, R. J. *J. Mol. Spectrosc*. **1961**, *6*, 492-496.

68. Socrates, G. *Infrared and Raman characteristic group frequencies: tables and charts*; John Wiley & Sons, Ltd: Chichester, 2004; p 194.

69. Friedman, L.; Bayless, J. H. *J. Am. Chem. Soc.* **1969**, *91*, 1790-1794.

70. de Oliveira, M. G.; Shishido, S. M.; Seabra, A. B.; Morgon, N. H. *J. Phys. Chem. A* **2002**, *106*, 8963-8970.

71. Fontijn, A.; Sabadell, A. J.; Ronco, R. J. *Anal. Chem*. **1970**, *42*, 575-579.

72. Singh, R. J.; Hogg, N.; Joseph, J.; Kalyanaraman, B. *J. Biol. Chem.* **1996**, *271*, 18596-18603.

73. Damodaran, V. B.; Joslin, J. M.; Wold, K. A.; Lantvit, S. M.; Reynolds, M. M. *J. Mater. Chem.* **2012**, *22*, 5990-6001.

74. Yapor, J. P.; Lutzke, A.; Pegalajar-Jurado, A.; Neufeld, B. H.; Damodaran, V. B.; Reynolds, M. M. *J. Mater. Chem. B* **2015**, *3*, 9233-9241.

75. Frost, M. C.; Meyerhoff, M. E. *J. Biomed. Mater. Res. A* **2005**, *72*, 409-419.

76. Adam, C.; García-Río, L.; Leis, J. R.; Ribeiro, L. *J. Org. Chem*. **2005**, *70*, 6353-6361.

77. Smith, J. N.; Dasgupta, T. P. *Nitric Oxide* **2000**, *4*, 57-66.

78. Hornyák, I.; Marosi, K.; Kiss, L.; Gróf, P.; Lacza, Z. *Free Radical Res*., 2012, **46**, 214-225.

79. Aga, R. G.; Hughes, M. N. *Methods Enzymol*., 2008, **436**, 35-48.

80. Smith, M. B.; March, J. *March's Advanced Organic Chemistry: Reactions, Mechanisms, and Structure*, 5th ed.; John Wiley & Sons, Ltd: New York, 2001; pp. 1543-1544.

81. Lutzke, A.; Pegalajar-Jurado, A.; Neufeld, B. H.; Reynolds, M. M. *J. Mater. Chem. B*, 2014, **2**, 7449-7458.

CHAPTER 4

SUSTAINED NITRIC OXIDE RELEASE FROM A TERTIARY *S*-NITROSOTHIOL-BASED POLYPHOSPHAZENE COATING

4.1. Introduction

Nitric oxide (NO) is a naturally-occurring bioactive molecule with well-established physiological functions in the cardiovascular and immune systems.[1,2] Endogenous NO is primarily formed by the action of NO synthase (NOS) enzymes on L-arginine or through the NOS-independent nitrate-nitrite-nitric oxide pathway.[3,4] NO produced by endothelial cells serves as a regulator of vascular tone and inhibitor of platelet adhesion and aggregation, while phagocytes utilize NO as an antimicrobial agent as part of the immune response.[5,6] Supplemental NO gas has been employed in medicine as a vasodilator and as an FDA-approved treatment for pulmonary hypertension.[7,8] Furthermore, the ability of NO to exert antithrombotic, wound-healing, and broad-spectrum antimicrobial effects has led to continued interest in the development of NO-based therapies for a variety of biointerfacial applications.[9] However, the fact that NO is rapidly consumed by reaction with biomolecules (*e.g.* oxyhemoglobin) or molecular oxygen complicates its physiological delivery and necessitates the synthesis of materials capable of localized NO release.[10] Because NO exhibits pronounced antiplatelet effects, NO-releasing polymers form an important class of therapeutic materials that have been frequently proposed for use in the fabrication of thromboresistant, blood-contacting medical

Reprinted with permission from:

Lutzke, A.; Tapia, J. B.; Neufeld, M. J.; Reynolds, M. M. Sustained Nitric Oxide Release from a Tertiary *S*-Nitrosothiol-based Polyphosphazene Coating. *ACS Appl. Mater. Interfaces* **2017**, *9*, 2104-2113.

devices such as stents and catheters.[11] Other NO-releasing polymers have been found to exhibit promising antimicrobial activity as both solution-phase sources of NO and in the form of bactericidal wound dressings for treatment of injuries.[12,13] NO-releasing materials are most commonly prepared by incorporation of species such as *N*-diazeniumdiolates and *S*-nitrosothiols (RSNOs), which form NO under physiological conditions or when triggered by environmental stimuli.[14,15] RSNOs including *S*-nitrosoglutathione (GSNO) and macromolecular *S*-nitrosoalbumin are present in blood and decompose as part of their natural biochemical function to form benign disulfides (2 RSNO → 2 NO + RSSR), and it has been argued that this category of NO donor possesses certain advantages over wholly synthetic NO-forming species.[16] For example, *N*-diazeniumdiolates have occasionally been shown to form potentially carcinogenic *N*-nitrosamines as a byproduct of their decomposition, and alternative NO donors like sydnonimines, furoxans, and metal nitrosyls are frequently complex to synthesize, toxicologically unsuitable, or lacking the versatility required for biomaterials applications.[17] As the therapeutically-relevant component of many NO-releasing polymer systems, RSNOs have been widely utilized in biomaterials. Brisbois *et al.* reported that polyurethane-based catheters doped with *S*-nitroso-*N*-acetylpenicillamine (SNAP) were capable of extended NO release, resulting in reduced thrombus formation and bacterial adhesion in sheep.[18] Li and Lee demonstrated that conjugates of GSNO or *S*-nitrosated phytochelatins and poly(vinyl methyl ether-*co*-maleic anhydride) could be complexed with poly(vinyl pyrrolidone) to produce NO-releasing materials capable of accelerating wound healing in diabetic mice.[19] Moreover, Vogt *et al.* reported the development of a gelatin-based, light-triggered material derivatized with SNAP that exhibited antibacterial effects against *Staphylococcus aureus* (*S. aureus*), while Riccio *et al.*

demonstrated that *S*-nitrosated polysiloxane-derived xerogels exhibited promising antibacterial effects against *Pseudomonas aeruginosa* (*P. aeruginosa*).[20,21]

More recently, we reported on the use of *S*-nitrosated biodegradable poly(organophosphazenes) (POPs) as potential platforms for therapeutic NO release.[22] POPs possess a polymeric inorganic backbone consisting of alternating nitrogen and phosphorus atoms, and are frequently synthesized by substitution of poly(dichlorophosphazene) (PDCP) with amines or alkoxides.[23] Inclusion of organic substituents results in variable physical and chemical characteristics that have permitted the development of POPs that range from specialty elastomers for industrial use to materials intended for biomedical applications.[24] In an example of their potential for medical device fabrication, a study conducted by Huang *et al.* found that coronary stents coated with poly(bis(trifluoroethoxy)phosphazene) (PTFEP) exhibited long-term biocompatibility after implantation in pigs.[25] Similarly, Henn *et al.* showed that PTFEP-coated stents inhibited thrombus formation and reduced in-stent stenosis and inflammation in a porcine model.[26] The use of amino acid-based substituents has led to the development of a wide variety of bioerodible POPs incorporating esters of glycine, alanine, phenylalanine, and others.[27] Such polymers are understood to degrade hydrolytically through liberation of the amino acid and decomposition of the polyphosphazene backbone into low-toxicity and self-neutralizing phosphate and ammonia.[28] Biodegradable POPs of this type have been proposed as materials suitable for bone tissue engineering, drug delivery, and the development of coatings for medical devices.[29-31] In these roles, polyphosphazenes substituted with amino acid derivatives or similar naturally-occurring, non-toxic compounds represent a potential alternative to widely-used polyesters and other biodegradable polymers in biomedical applications.

We previously demonstrated that cysteine-based poly(ethyl *S*-methylthiocysteinyl-*co*-ethyl cysteinyl phosphazene) could be effectively *S*-nitrosated to form a biodegradable, NO-releasing material. However, the stability of the polymer-bound primary *S*-nitrosothiol was found to be limited under physiological conditions, resulting in the release of 64% (0.35 mmol g^{-1}) of available NO over 24 h in pH 7.4 phosphate buffered saline (PBS) at 37 °C. The greater reported stability of tertiary RSNOs (such as SNAP) has led to their frequent use as longer-term NO donors.[32] For this reason, it was anticipated that prolonged NO release could be achieved *via* development of a polyphosphazene bearing tertiary RSNO substituents. Herein, we present the development of *S*-nitrosated poly(bis(3-mercapto-3-methylbut-1-yl glycinyl)phosphazene) (POP-Gly-MMB), the first NO-releasing POP based on a tertiary RSNO architecture. The organic pendant group was derived from glycine and 3-mercapto-3-methylbutan-1-ol (MMB), a food-grade tertiary thiol identified in wine produced from *Vitis rotundifolia* and both commercial lagers and coffee.[33-35] To evaluate the ability of the polymer to function as an NO-releasing surface, the thiolated material (POP-Gly-MMB-SH) was adhered to glass test substrates and subsequently converted to the *S*-nitrosated derivative POP-Gly-MMB-NO. The NO release properties of this coating were evaluated at physiological pH and temperature (pH 7.4 PBS, 37 °C), where it was determined to maintain a physiologically-relevant NO flux (6.5-0.09 nmol min^{-1} cm^{-2}) over a 2 week period by chemiluminescence-based NO detection. The hydrolytic degradation properties of both POP-Gly-MMB-SH and POP-Gly-MMB-NO were assessed over 6 weeks (pH 7.4 PBS, 37 °C), and their primary hydrolytic degradation products were identified by time-of-flight mass spectrometry (TOF-MS). Results indicate that POP-Gly-MMB-NO coatings function as comparatively long-term macromolecular reservoirs of NO, exhibiting continuous two week NO release in a range suitable for antiplatelet applications. Furthermore,

the greater stability and correspondingly slower NO release from POP-bound tertiary RSNOs represents significant progress toward the development of biodegradable polymers capable of sustained NO release.

4.2. Materials and methods

4.2.1. Materials

4-(Dimethylamino)pyridine (DMAP, 99%), chloroacetic acid (99%), *N*,*N*′-dicyclohexylcarbodiimide (DCC, 99%), lithium bis(trimethylsilyl)amide (LiHMDS, 99%), sulfuryl chloride (97%), and triphenylphosphine (99%) were purchased from Alfa Aesar (Ward Hill, MA, USA). Disodium ethylenediaminetetraacetate dihydrate (EDTA-Na_2, 99%), food-grade 3-mercapto-3-methylbutan-1-ol (MMB, 98%), sodium azide (99.5%), and *tert*-butyl nitrite (*t*-BuONO, 90%) were purchased from Sigma-Aldrich (St. Louis, MO, USA). Phosphorus pentachloride (98%) and phosphorus trichloride (98%) were obtained from Strem Chemicals, Inc. (Newburyport, MA, USA). Phosphate buffered saline (PBS) tablets and triethylamine (TEA, 99%) were purchased from EMD Chemicals (Gibbstown, NJ, USA). A Millipore Direct-Q water purification system was used to produce deionized water for general use and the preparation of PBS (EMD Millipore, Billerica, MA, USA). Phosphorus trichloride and sulfuryl chloride were distilled prior to use. Triethylamine was distilled from calcium hydride. *tert*-Butyl nitrite was treated with 10% w/v EDTA-Na_2 to remove trace metal impurities. All other chemicals were used as received.

4.2.2. Characterization methods

General characterization techniques. NMR spectra were obtained using an Agilent (Varian) Inova 400 MHz FT-NMR spectrometer (Agilent Technologies, Inc., Santa Clara, CA, USA). ^{1}H NMR and ^{13}C NMR spectra were referenced relative to the solvent ($CDCl_3$), and ^{31}P NMR spectra were referenced relative to triphenylphosphine (-6 ppm) or triphenylphosphine oxide (29 ppm) standards. ATR-FTIR spectra were collected between 650-4000 cm^{-1} using a Nicolet 6700 FTIR spectrometer (Thermo Electron Corporation, Madison, WI, USA) fitted with a Smart iTR ATR sampling accessory and ZnSe crystal plate. UV-Vis measurements were carried out using a Nicolet Evolution 300 spectrophotometer (Thermo Electron Corporation). Gel permeation chromatography (GPC) utilized a Waters 515 HPLC pump, a Waters 717 autosampler, and a Waters 2414 refractive index (RI) detector. Separation was performed with a PLgel guard column (Polymer Labs) and three PLgel mixed-C columns (7.5 × 300 mm, 5 μm; Polymer Labs) using HPLC grade DMF at 30 °C with a flow rate of 1.0 mL/min. The instrument was calibrated with poly(methyl methacrylate) standards, and the chromatograms were processed with Waters Empower software (version 2002).

Contact angle measurements. To evaluate wettability of polymer coatings, water contact angle (WCA) measurements (n = 8) were performed by sessile drop technique under ambient lab conditions using a Krüss DSA10 contact angle goniometer (Hamburg, Germany). All samples were dosed with 2 μL of deionized water and still images were immediately acquired. The contact angle was then determined by manually selecting the baseline and using Tangent Method 1 from the Drop Shape Analysis 1.5 software provided with the instrument.

Nitric oxide release measurements. NO release measurements were obtained using Sievers chemiluminescence-based NO analyzers (NOA 280i) (GE Analytical Instruments, Boulder, CO, USA). The instruments were calibrated with UHP nitrogen and 45 ppm NO/nitrogen. To collect 24 h NO release profiles, polymer-coated substrates (n = 3) were placed in custom gas-flow cells connected to the NO analyzers and immersed in 5 mL of deoxygenated 10 mM pH 7.4 PBS maintained at 37 °C and protected from exposure to ambient light. The buffer solution and headspace were purged with a constant flow of nitrogen to sweep NO into the analyzer, and the NO concentration (ppb/ppm) was recorded as a function of time. NO concentration was converted to NO release (mol) using a calibration constant (mol NO ppb^{-1} s^{-1}) obtained from the reduction of sodium nitrite and verified by copper-catalyzed decomposition of GSNO. To obtain NO flux measurements over 14 d, the NO release from polymer-coated substrates (n = 3) was measured at regular intervals following immersion in 5 mL of deoxygenated 10 mM pH 7.4 PBS at 37 °C. The initial NO release measurement (t = 0) corresponds to the maximum mean NO release observed after immersion in PBS, while subsequent measurements (t = 1-14 d) correspond to mean NO release. Between measurements, samples were incubated in 5 mL of 10 mM pH 7.4 PBS at 37 °C under ambient atmosphere and protected from exposure to light. NO release (ppb) was converted to NO flux (nmol min^{-1} cm^{-2}) using the NO analyzer calibration constant and the surface area of the sample. To determine total NO content, polymer-coated substrates (n = 3) were irradiated with UV light in PBS at 40 °C using a 100 W Blak-Ray B-100AP UV lamp (UVP, Upland, CA, USA) to photolytically decompose RSNO. The resulting NO release was used to calculate the quantity of releasable NO present in the material. The sum of NO released over 24 h (10 mM pH 7.4 PBS, 37 °C) and the residual NO obtained from UV decomposition was used to determine the total NO content of the

material (mmol g^{-1}). An identical process was used to quantify remaining NO after incubation of polymer-coated substrates in 5 mL of 10 mM pH 7.4 PBS at 37 °C for 3, 7, and 14 d. In all cases, glassware used for NO release measurements was washed with saturated EDTA-Na_2 followed by deionized water (18.2 MΩ·cm) prior to use.

Molar extinction coefficient determination. The RSNO molar extinction coefficient for POP-Gly-MMB-NO was determined by correlation of UV-Vis absorbance with NO release. The absorbance (341 nm) of dissolved POP-Gly-MMB-NO in DMF was obtained by UV-Vis spectroscopy at 5 different concentrations (n = 3) within the linear range, and an aliquot of each solution was injected into an NO analyzer gas-flow cell. Decomposition of the RSNO was induced by exposure to UV light as described previously, and the resulting NO release was used to establish a linear relationship between absorbance and NO content.

Degradation study. POP-Gly-MMB-SH samples (20 mg, n = 5) were weighed out and immersed in 5 mL of 10 mM PBS 7.4 PBS. Additional POP-Gly-MMB-SH samples (20 mg, n = 5) were weighed out, converted to the *S*-nitrosated derivative POP-Gly-MMB-NO by reaction with *t*-BuONO, and similarly immersed in 5 mL of 10 mM PBS 7.4 PBS. The samples were incubated at 37 °C under ambient atmosphere while protected from light for a total of six weeks. PBS was replaced on a weekly basis through the removal and addition of buffer by pipette under ambient laboratory conditions, with care taken to avoid the unwanted transfer of non-degraded polymer. At the end of each week, the material was removed from the buffer solution, washed twice with 1 mL Millipore water, and lyophilized for 24 h to remove residual water. For each sample, the dry mass of the material and the pH of the buffer solution was recorded after removal of the sample.

Mass spectrometry. To identify potential hydrolytic degradation products, samples of POP-Gly-MMB-SH and POP-Gly-MMB-NO were hydrolyzed in deionized water at 37 °C under ambient atmosphere for two weeks. The media were subsequently analyzed using time-of-flight mass spectrometry (TOF-MS) to characterize the polymer degradation products. All mass spectrometry analyses were performed using an Agilent 6224 LC-MS. The instrument was equipped with an Agilent multimode ionization (MMI) source capable of electrospray ionization (ESI) and atmospheric pressure chemical ionization (APCI). For all experiments, mixed mode ionization in both positive and negative polarity was employed with the range of mass analysis set at 70 - 3200 m/z. The sample solutions were introduced into the ion source using flow injection at a flow-rate of 2.2 µL/min *via* the ESI nebulizer using methanol as the mobile phase ($n \geq 3$). The ion source conditions were as follows: capillary voltage, 2500 V; fragmentor voltage, 120 V; skimmer voltage, 60 V; charge voltage, 2000 V; drying gas temperature, 310 °C; drying gas flow-rate (nitrogen gas), 10 L/min; and nebulizer pressure, 45 psi. All data was processed using Agilent MassHunter Qualitative Analysis B.07.00.

Statistical analysis. Data reported as mean ± standard deviation of ≥ 3 replicate measurements, unless otherwise noted.

4.2.3. Synthetic methods

3-Mercapto-3-methylbut-1-yl chloroacetate (1). MMB (30 mmol) was dissolved in 30 mL dry THF and cooled to 0 °C. Chloroacetic acid (30 mmol), DMAP (1.5 mmol), and DCC (30 mmol) were added and the solution was stirred for 1 h at 0 °C, followed by 2 h at RT. The solvent was evaporated and the mixture was taken up in 45 mL DCM and washed twice with both 0.5 M hydrochloric acid (30 mL) and saturated $NaHCO_3$ solution (30 mL), then once with 10% NaCl

(30 mL). The solution was dried over anhydrous $MgSO_4$, filtered, and the solvent was evaporated to give a cloudy oil. The oil was stored at -20 °C overnight to precipitate residual dicyclohexylurea, and then filtered to isolate the crude product as a clear, colorless oil (5.01 ± 0.19 g, 85 ± 3%): ^{1}H NMR (400 MHz, $CDCl_3$) δ 4.42 (t, *J* = 7.2 Hz, 2H), 4.06 (s, 2H), 1.98 (t, *J* = 7.2, 2H), 1.76 (s, 1H), 1.44 ppm (s, 6H). ^{13}C NMR (100 MHz, $CDCl_3$) δ 167.23, 63.84, 44.13, 42.78, 40.85, 33.10 ppm.

3-Mercapto-3-methylbut-1-yl azidoacetate (2). **1** (5 mmol) was dissolved in 30 mL DMF without further purification and cooled to 0 °C. Sodium azide (1 eq. by crude mass) was added and the mixture was stirred for 30 min at 0 °C, then 1.5 h at RT. The solution was decanted into ice-cold water (60 mL) and the product was extracted twice with diethyl ether (60 mL), then washed 4 times with water (15 mL) and dried with anhydrous $MgSO_4$. After filtration, the ether was evaporated to yield the crude product as a clear, pale yellow oil (4.42 ± 0.06 g, 89 ± 3%): ^{1}H NMR (400 MHz, $CDCl_3$) δ 4.43 (t, *J* = 7.2 Hz, 2H), 3.88 (s, 2H), 1.99 (t, *J* = 7.2, 2H), 1.76 (s, 1H), 1.44 ppm (s, 6H). ^{13}C NMR (100 MHz, $CDCl_3$) δ 168.23, 63.44, 50.41, 44.15, 42.74, 33.08 ppm.

3-Mercapto-3-methylbut-1-yl glycinate hydrochloride (3). 2 (5 mmol) was dissolved in dry THF (10 mL) and cooled to 0 °C. Triphenylphosphine (1 eq.) was added and the mixture was stirred for 15 min at 0 °C, then 1.5 h at RT. Deionized water (0.5 mL) was added and the mixture was stirred for 1 h, followed by removal of solvent under vacuum. The amine was extracted 3 times from DCM (5 mL) with ice-cold 0.5 M hydrochloric acid (5 mL), and the combined aqueous layers were washed 3 times with DCM (5 mL). The aqueous hydrochloride salt was subsequently filtered and lyophilized to isolate the crude product as a white solid (est. by ^{1}H NMR, 0.49 ± 0.02 g, 65 ± 1%): ^{1}H NMR (400 MHz, $CDCl_3$) δ 8.53 (s, 3H), 4.42 (t, *J* = 7.2 Hz,

2H), 4.03 (q, J = 6.0, 2H), 1.97 (t, J = 7.2, 2H), 1.86 (s, 1H), 1.41 ppm (s, 6H). ^{13}C NMR (100 MHz, $CDCl_3$) δ 167.77, 64.12, 43.98, 42.80, 40.76, 33.09 ppm.

Trichloro(trimethylsilyl)phosphoranimine (4). LiHMDS (100 mmol) was suspended in dry diethyl ether (200 mL) and cooled under nitrogen to 0 °C. PCl_3 (100 mmol) was slowly added over 30 min, then the resulting suspension was allowed to warm to RT and stirred for 1 h. The mixture was again cooled to 0 °C and SO_2Cl_2 (100 mmol) was added over 30 min. After this addition, the mixture was warmed and stirred for 1 h, filtered, and the solvent was removed under vacuum. The product was distilled twice under vacuum (1 Torr, 21 °C) and was recovered as a clear, colorless liquid (8.78 g, 39%): ^{1}H NMR (400 MHz, $CDCl_3$) δ 0.18 ppm (d, $^4J_{HP}$ = 1.2 Hz, 9H). ^{31}P NMR (162 MHz, $CDCl_3$) δ -55 ppm (s).

Poly(dichlorophosphazene) (PDCP) (5). In a typical procedure, 0.50 g of **4** was stirred in a solution of 5 × 10^{-3} M PCl_5 in DCM (5 mL) for 18 h under nitrogen at RT. The solvent was removed under vacuum to yield a viscous polymer (quantitative): ^{31}P NMR (162 MHz, $CDCl_3$) δ -18 ppm.

Poly(bis(3-mercapto-3-methylbut-1-yl glycinyl)phosphazene) (POP-Gly-MMB-SH). In a typical procedure, **3** (1.15 g, 5.39 mmol) was dissolved in THF (25 mL) and TEA (1.80 mL) was added. The mixture was stirred at RT for 1 h, then filtered into a solution of **5** (0.25 g) in 5 mL THF. The reaction was stirred under nitrogen for 48 h at 25 °C. The solvent was subsequently removed under vacuum and the residue was redissolved in THF (10 mL) and precipitated with 100 mL hexanes. The precipitated solid was allowed to settle, then the supernatant was decanted and the polymer washed three times with hexanes (25 mL). The polymer was redissolved in 10 mL toluene and washed twice with deionized water (5 mL) and once with 10% sodium chloride (5 mL). The organic layer was dried over anhydrous $MgSO_4$, filtered, and the solvent was

removed under vacuum. The polymer was taken up in THF (10 mL) and precipitated with 100 mL hexanes, then the supernatant was decanted and the polymer was again washed three times with hexanes (25 mL). Evaporation of residual solvent under vacuum yielded a yellow-white powder (0.745 ± 0.014 g, 87 ± 2%): ^{1}H NMR (400 MHz, $CDCl_3$) δ 4.28, 3.90, 3.73, 1.95, 1.83, 1.42 ppm. ^{13}C NMR (100 MHz, $CDCl_3$) δ 172.76, 62.22, 44.29, 43.14, 42.87, 33.17 ppm. ^{31}P NMR (162 MHz, $CDCl_3$) δ -0.41 ppm. IR *v* 3349, 2961, 2923, 2865, 2563, 1737, 1455, 1416, 1388, 1367, 1190, 1122, 1008, 975, 865, 707 cm^{-1}

Preparation of S-nitrosated poly(bis(3-mercapto-3-methylbut-1-yl glycinyl)phosphazene) films. POP-Gly-MMB-SH was dissolved in THF at a concentration of 75 mg mL^{-1} and cast onto 12 mm diameter glass circles to form a single-sided 5 mg coating. After evaporation of THF, the coated substrates were individually immersed in 1 mL 10% *t*-BuONO/pentane and agitated at ambient temperature (20 °C) for 60 min. Following this reaction, the liquid was removed and the coated substrates were washed with 2 × 1 mL pentane and placed under vacuum to remove residual *t*-BuONO/pentane, yielding a faintly green film (POP-Gly-MMB-NO): IR *v* 3323, 2965, 2928, 2867, 1737, 1492, 1455, 1418, 1389, 1367, 1194, 1128, 1006, 971, 879, 780, 709, 665 cm^{-1}. UV-Vis λ 341 (915 ± 9 M^{-1} cm^{-1}), 600 nm.

4.3. Results and discussion

4.3.1. Synthesis of poly(bis(3-mercapto-3-methylbut-1-yl glycinyl)phosphazene)

NO-donating RSNOs are generally prepared from the reaction of thiols with nitrous acid or similar nitrosating reagents. It has been established that tertiary RSNOs (obtained directly from tertiary thiols) frequently exhibit significantly greater thermal stability than primary equivalents. This concept is most clearly illustrated by the fact that SNAP may be isolated as a stable solid,

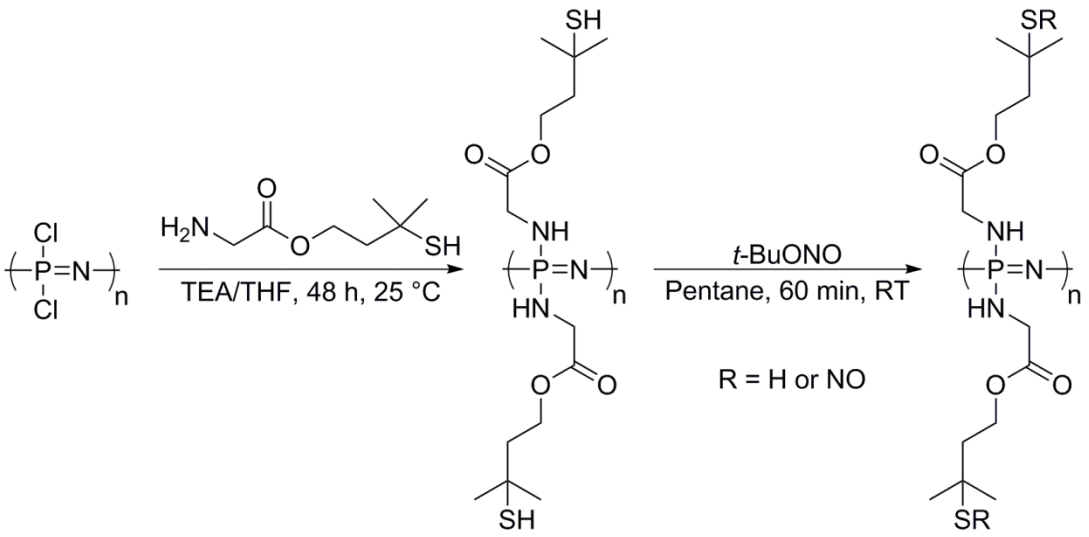

Figure 4.1 Synthesis of *S*-nitrosated poly(bis(3-mercapto-3-methylbut-1-yl glycinyl)phosphazene) from poly(dichlorophosphazene). Copyright 2017 American Chemical Society.

while its primary analog *S*-nitroso-*N*-acetylcysteine rapidly decomposes when concentrated.[36] For this reason, the use of tertiary RSNOs (or unusually stable primary species such as GSNO) represents an obvious method of delaying decomposition and thereby extending the effective NO release period. To exploit this difference in stability, POP-Gly-MMB-SH was prepared from the substitution of PDCP with the tertiary thiol 3-mercapto-3-methylbut-1-yl glycinate, an ester derived from MMB and glycine (Figure 4.1). MMB is a naturally-occurring bifunctional tertiary thiol found in a variety of food sources and utilized commercially as a flavoring/odor agent.[33-35] MMB is also present in the biochemistry of certain felines as a metabolite of the amino acid felinine.[37] Because PDCP is easily substituted by amino acids, it was reasoned that a glycine-MMB ester would permit straightforward conjugation of the tertiary thiol to the polyphosphazene. Toward this end, 3-mercapto-3-methylbut-1-yl glycinate hydrochloride was synthesized from the Steglich esterification of monochloroacetic acid with MMB, followed by substitution with sodium azide and reduction of this intermediate with triphenylphosphine. After

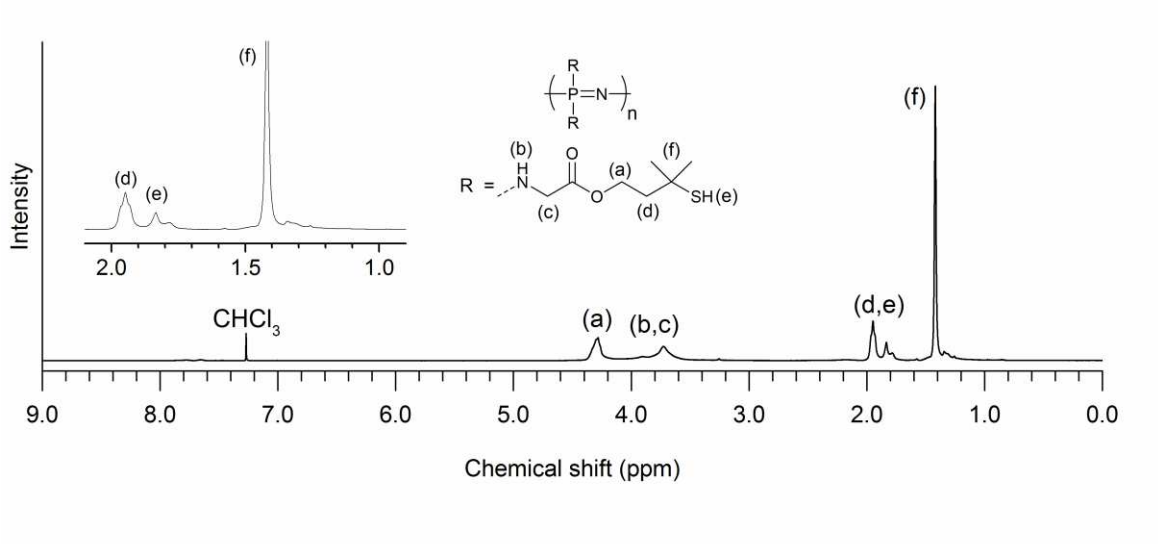

Figure 4.2 ^{1}H NMR spectrum of poly(bis(3-mercapto-3-methylbut-1-yl glycinyl)phosphazene). ^{1}H NMR (400 MHz, $CDCl_3$) δ 4.28, 3.90, 3.73, 1.95, 1.83, 1.42 ppm. Copyright 2017 American Chemical Society.

acidic work-up and isolation by lyophilization, the hydrochloride salt was obtained in crude form (approximately 92% by ^{1}H NMR). Although the corresponding thioester was also a potential product of the carbodiimide-mediated esterification of MMB, it was not recovered in any detectable quantity (^{1}H NMR) from the reaction. Instead, the major product was the ester 3-mercapto-3-methylbut-1-yl chloroacetate. The amino acid ester was reacted with PDCP in the presence of triethylamine to form the thiolated polymer POP-Gly-MMB-SH, which was isolated in 87% yield. The ^{1}H NMR spectrum of POP-Gly-MMB-SH was largely consistent with that of 3-mercapto-3-methylbut-1-yl glycinate, with broadened features appearing at 4.28 and 1.95 ppm corresponding to the methylene protons of MMB, and a prominent peak at 1.42 ppm originating from the *gem* dimethyl group (Figure 4.2). The thiol proton appeared at 1.83 ppm, while features at 3.90 and 3.73 ppm were assigned to the PN-H proton and the methylene group of the glycinyl residue, respectively. ^{13}C NMR peaks (assigned by HSQC) at 173.8 and 43.1 ppm originated from the carbonyl and methylene carbons of the glycinyl moiety, while the remaining peaks at 62.2 (-OCH_2-), 44.3 (-CH_2-), 42.9 (CSH), and 33.2 (-CH_3) were attributable to the 3-

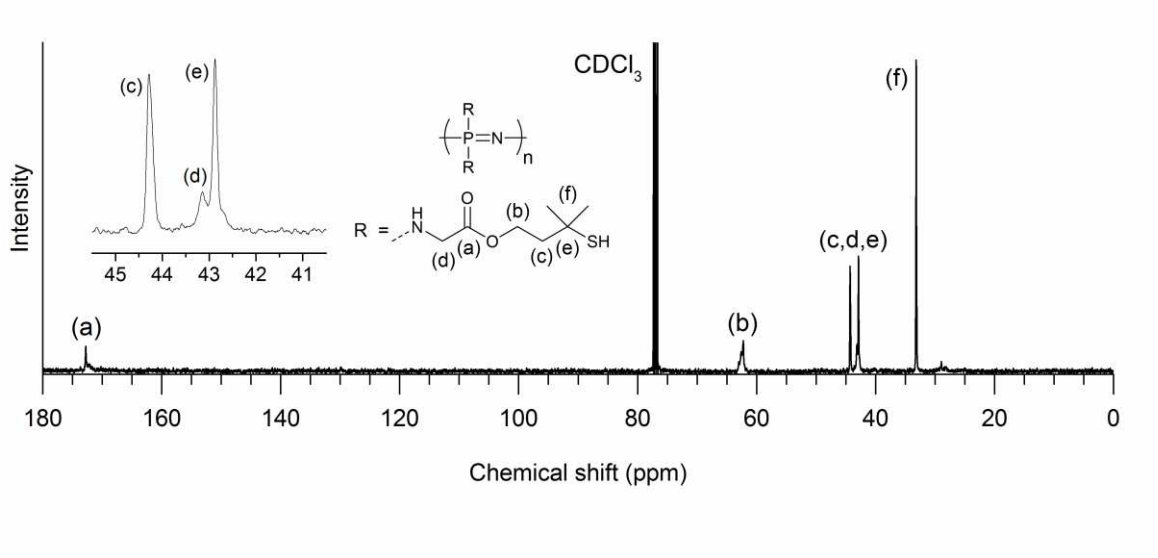

Figure 4.3 ^{13}C NMR spectrum of poly(bis(3-mercapto-3-methylbut-1-yl glycinyl)phosphazene). ^{13}C NMR (100 MHz, $CDCl_3$) δ 172.76, 62.22, 44.29, 43.14, 42.87, 33.17 ppm. Copyright 2017 American Chemical Society.

methyl-3-mercaptobut-1-yl ester (Figure 4.3). In the case of ^{31}P NMR, a relatively broad feature centered at -0.41 ppm was consistent with previous reports of amine-substituted polyphosphazenes, with a feature at 18 ppm potentially attributable to minor hydrolysis of the backbone during aqueous work-up (Figure 4.4).[22] ATR-FTIR was used to further characterize the polymer and the spectrum was found to be consistent with the anticipated structure, with key vibrational bands originating from the pendant group at 3349 (PN-H stretch), 2961, 2923, 2865 (C-H stretch), 2563 (S-H stretch), 1737 (ester C=O), 1190, and 1122 cm^{-1} (ester) (Figure 4.5). Amine-substitution at phosphorus (P-N) is likely to produce the band observed at 975 cm^{-1}, while additional vibrations from the polyphosphazene backbone itself appear at 1367 and 865 cm^{-1}.[38,39] The presence of the thiol S-H stretch and the absence of the distinct asymmetric/symmetric N-H stretching pattern of primary amines supports P-N bond formation as the primary mode of substitution. POP-Gly-MMB-SH exhibited solubility in many common organic solvents, including toluene, DCM, and DMF. Solubility was minimal in diethyl ether, and the polymer was insoluble in aliphatic hydrocarbons such as hexane and pentane. GPC

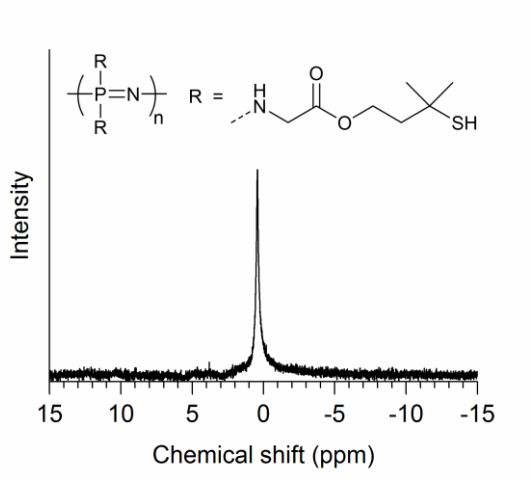

Figure 4.4 ^{31}P NMR spectrum of poly(bis(3-mercapto-3-methylbut-1-yl glycinyl)phosphazene). ^{31}P NMR (162 MHz, $CDCl_3$) δ -0.41 ppm. Minor additional peaks at 29 (triphenylphosphine oxide reference) and 18 ppm not depicted. Copyright 2017 American Chemical Society.

analysis indicated a molecular weight (M_n) of 616 kDa with a polydispersity of 1.29, resulting in a calculated degree of polymerization (M_n/M_0) of 1550 using a presumed monomeric unit mass of 397.5 Da.

Thiolated polymers have attracted significant interest due to their ability to participate in both reversible (disulfide formation) and irreversible (thiol-ene) crosslinking, permitting inducible changes to their physical and mechanical properties. Furthermore, conversion of polymer-bound thiol to the corresponding RSNO derivative has been widely utilized to prepare NO-releasing materials for biomedical applications. Despite the wide interest in the development of thiolated polymers, few thiolated poly(organophosphazenes) have been reported to date. Potta *et al.* described the development of a crosslinkable poly(organophosphazene) prepared from the substitution of PDCP with α-amino-ω-methoxy-poly(ethylene glycol), isoleucine ethyl ester, and cystamine, followed by reduction of the disulfide linkages with dithiothreitol.[40] Weikel et al. synthesized a thiolated polymer from deprotection of poly(bis(cysteine ethyl disulfide ethyl ester)phosphazene) with dithiothreitol or 2-mercaptoethanol.[41] In both reports, the precursor

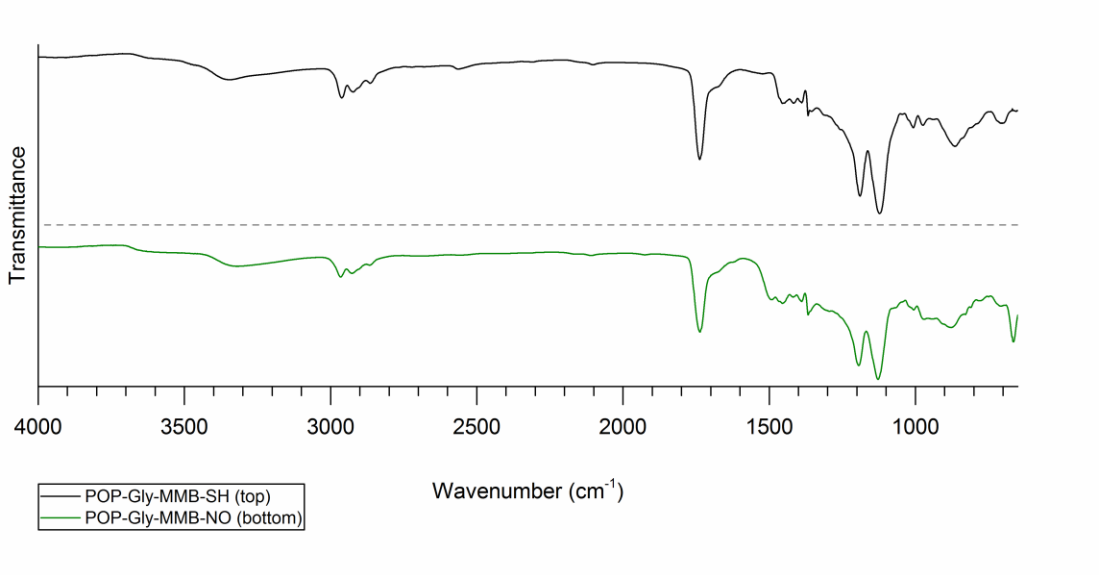

Figure 4.5 ATR-FTIR spectra of polymers. Top: ATR-FTIR spectrum of poly(bis(3-mercapto-3-methylbut-1-yl glycinyl)phosphazene) (POP-Gly-MMB-SH). IR: 3349, 2961, 2923, 2865, 2563, 1737, 1455, 1416, 1388, 1367, 1190, 1122, 1008, 975, 865, 707 cm^{-1}. Bottom: ATR-FTIR spectrum of *S*-nitrosated poly(bis(3-mercapto-3-methylbut-1-yl glycinyl)phosphazene) (POP-Gly-MMB-NO). IR: 3323, 2965, 2928, 2867, 1737, 1492, 1455, 1418, 1389, 1367, 1194, 1128, 1006, 971, 879, 780, 709, 665 cm^{-1}. Copyright 2017 American Chemical Society.

PDCP was substituted with amine-bearing disulfides which were subsequently cleaved to liberate free thiol using common disulfide reducing agents. Weikel *et al.* observed that the direct introduction of thiol in the form of cysteine ethyl ester resulted in competitive substitution at phosphorus by both the amine and thiol groups, necessitating the use of a disulfide-based protection/deprotection strategy to avoid chemoselectivity issues. In contrast, we observe that 3-mercapto-3-methylbut-1-yl glycinate preferentially substitutes PDCP through the amine group without protection of the thiol, potentially indicating that a significant level of chemoselectivity is attained through simple hindrance of the tertiary thiol. This may represent a useful method of preparing future thiolated polyphosphazenes, since it does not require the formation of asymmetric disulfide linkages that are often incompletely cleaved and retained in the final polymer, or the use of potentially toxic disulfide scission reagents (e.g. 2-mercaptoethanol).

4.3.2. *S*-Nitrosation of poly(bis(3-mercapto-3-methylbut-1-yl glycinyl)phosphazene) coatings

S-Nitrosation of POP-Gly-MMB-SH was achieved using *t*-BuONO, an alkyl nitrite that functions as a mild nitrosating agent in the presence of free sulfhydryl groups. While *S*-nitrosation of the polymer proceeds under both heterogeneous and homogeneous conditions, it was found that dissolution in organic solvents leads to comparatively rapid decomposition of the RSNO. Furthermore, the solubility of POP-Gly-MMB-NO is significantly impaired relative to the thiolated precursor and results in limited access to solution-phase coating techniques or other processing methods based on dissolution. For this reason, POP-Gly-MMB-SH was first applied as a single-sided coating to glass substrates, followed by immersion in 10% *t*-BuONO/pentane. POP-Gly-MMB-SH was also found to adhere to (and blend with) medically-relevant, biodegradable polymers such as polycaprolactone and poly(lactic acid) (PLA). However, the need for a comparatively inert substrate for *S*-nitrosation and subsequent NO release experiments dictated the use of glass over polymer surfaces. Using this approach, the insoluble polymer remained attached to the substrate during the *S*-nitrosation process, while the volatility of *t*-BuONO/pentane permitted their straightforward removal under vacuum following the reaction. Since the non-nitrosated precursor POP-Gly-MMB-SH exhibits excellent solubility in a diverse range of organic solvents, this method demonstrates that it can be applied as a coating or otherwise processed into a usable form prior to conversion to the *S*-nitrosated derivative. As previously noted, the *S*-nitrosated polymer exhibits poor solubility that is most directly explainable by crosslinking arising from disulfide formation. Such an outcome is predicted by the classical RSNO decomposition pathway, wherein the NO-forming homolytic cleavage of the

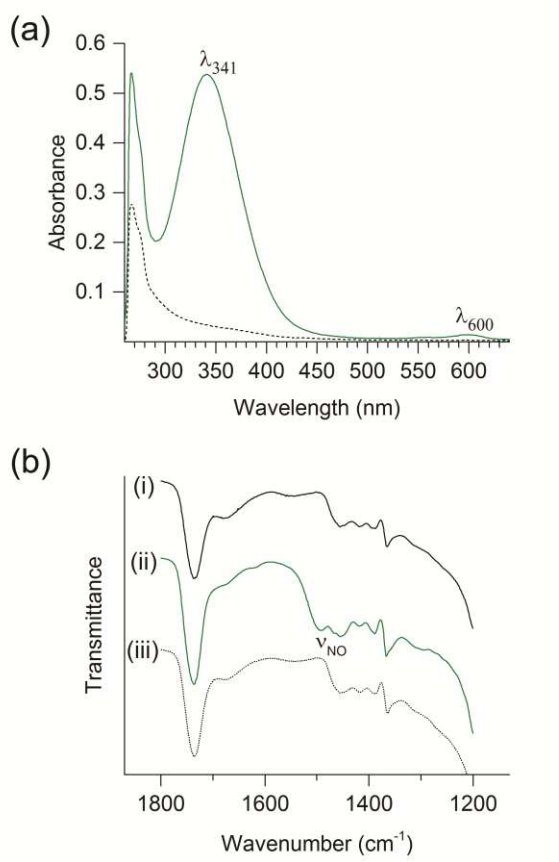

Figure 4.6 UV-Vis spectra of polymers. (a) UV-Vis spectra of POP-Gly-MMB-SH (dotted line) and POP-Gly-MMB-NO (solid line) in DMF at arbitrary concentration. Characteristic absorptions arising from the RSNO functional group are identified on the plot and occur at 341 ($\pi \rightarrow \pi^*$) and 600 nm ($n_N \rightarrow \pi^*$). (b) ATR-FTIR spectra of (i) POP-Gly-MMB-SH, (ii) POP-Gly-MMB-NO immediately following *S*-nitrosation, and (iii) POP-Gly-MMB-NO after six weeks of immersion in pH 7.4 PBS at 37 °C. The diagnostic N=O vibrational band is identified at 1492 cm^{-1}. Copyright 2017 American Chemical Society.

S-N bond is accompanied by the subsequent formation of disulfide according to the equation 2 RSNO → 2 NO + RSSR.[41] This limited solubility and the continuous thermal decomposition of the RSNO hindered the use of NMR and GPC as reliable characterization techniques. However, RSNOs are routinely characterized by UV-Vis spectroscopy and exhibit distinctive absorption features at approximately 340 (variably described as $\pi \rightarrow \pi^*$ or $n_O \rightarrow \pi^*$ transitions) and 550 ($n_N \rightarrow \pi^*$) nm.[32,42] Further discrimination between primary/secondary and tertiary

substitution patterns is possible due to a bathochromic shift in the $n_N \rightarrow \pi^*$ transition toward 600 nm in the case of tertiary RSNOs. In the case of POP-Gly-MMB-NO, solubility was sufficient to acquire UV-Vis spectra of the polymer in DMF, and the successful formation of RSNO was confirmed by the appearance of diagnostic absorptions at 341 and 600 nm in the UV-Vis spectrum (Figure 4.6a). UV-Vis absorptions attributable to alkyl nitrites (*e.g. t*-BuONO) or *N*-nitroso species were not observed.[43,44] The molar extinction coefficient of 915 ± 9 M^{-1} cm^{-1} (DMF) determined for the absorbance feature at 341 nm was consistent with the approximate value of 1000 M^{-1} cm^{-1} typically found for RSNOs.[15] While the non-nitrosated polymer has a colorless or faintly yellow appearance, POP-Gly-MMB-NO the non-nitrosated precursor, although *S*-nitrosation resulted in the disappearance of the thiol S-H stretch and the appearance of new bands at 1492 and 665 cm^{-1} that were attributable to N=O and N-S vibrational modes, respectively (Figure 4.5 and 4.6b).[45] As shown in Figure 4.6b, the diagnostic N=O stretch develops following *S*-nitrosation and is no longer detectable after extended immersion in PBS at physiological temperature and pH. Furthermore, the PN-H stretch (centered at 3323 cm^{-1} in the ATR-FTIR spectrum of POP-Gly-MMB-NO) is retained, indicating that reaction with *t*-BuONO does not produce *N*-nitrosation under the given reaction conditions.

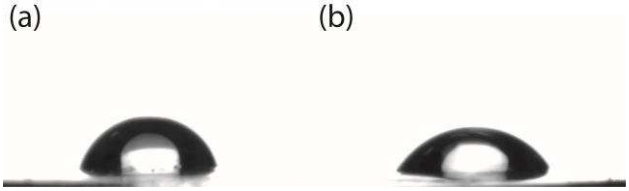

Figure 4.7 Water contact angle images. Representative images of water droplets on (a) POP-Gly-MMB-SH and (b) POP-Gly-MMB-NO surfaces, displaying the decrease in WCA following *S*-nitrosation. Copyright 2017 American Chemical Society.

Contact angle goniometry demonstrated an increase in wettability subsequent to *S*-nitrosation, with the measured WCA decreasing by 16° with the conversion of POP-Gly-MMB-SH (70 ± 7°) to POP-Gly-MMB-NO (54 ± 4°) (Figure 4.7). This outcome may be rationalized by introduction of the polar, hydrogen bond accepting NO moiety or an alteration of surface roughness following exposure to *t*-BuONO during the *S*-nitrosation.

4.3.3. Nitric oxide release measurements

NO release measurements were obtained using commercial Sievers chemiluminescence-based NO analyzers. The function of these instruments relies on the chemiluminescent reaction of NO with ozone ($NO + O_3 \rightarrow NO_2 + O_2$), which results in the formation of excited-state NO_2.[46] The relaxation of excited-state NO_2 is accompanied by the release of light, which is quantified by the instrument to determine gas-phase NO concentration (ppb/ppm). NO concentration is subsequently converted to NO release (mol) using a calibration constant obtained from the reduction of sodium nitrite and verified by decomposition of GSNO. This method is highly selective for NO and is widely utilized in the quantification of NO release from NO donors such as RSNOs. The NO-forming thermal or photolytic decomposition of RSNOs is generally theorized to proceed through homolytic cleavage of the S-N bond, followed by either non-productive recombination or the irreversible generation of NO and disulfide according to the equation $2\ RSNO \rightarrow 2\ NO + RSSR$.[15,47] It has also been demonstrated that transition metals such as copper are capable of catalytically initiating the NO-forming decomposition of RSNOs through more complex mechanisms that are not fully elucidated.[48] To assess the ability of POP-Gly-MMB-NO to release NO at physiological pH and temperature, samples were immersed in deoxygenated pH 7.4 PBS maintained at 37 °C (and protected from exposure to ambient light)

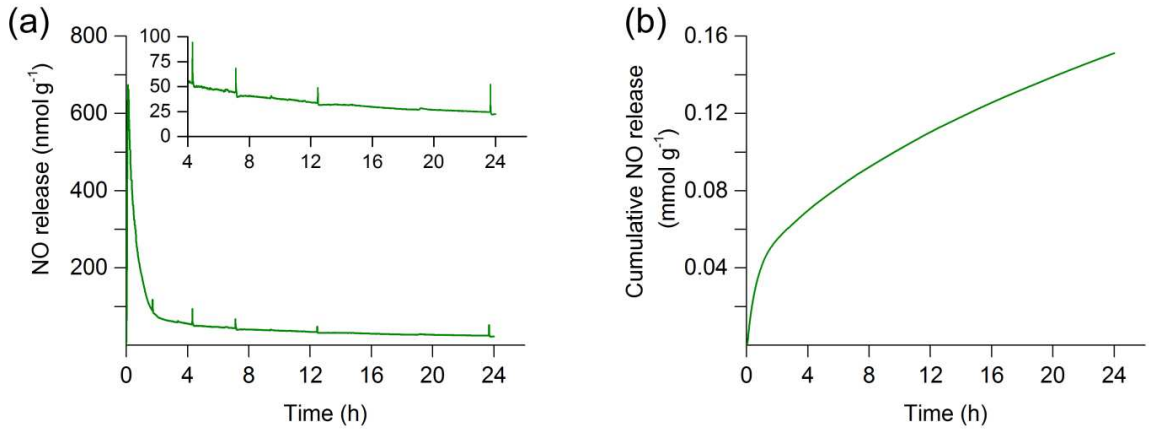

Figure 4.8 24 h NO release profiles of *S*-nitrosated poly(bis(3-mercapto-3-methylbut-1-yl glycinyl)phosphazene) coatings. (a) Mean NO flux profile obtained over 24 h from 12 mm diameter POP-Gly-MMB-NO coated substrate suspended in pH 7.4 PBS at 37 °C (n = 3). Inset: Interval between 4 - 24 h, after the initial burst of NO release. Recurrent spikes in NO release may be attributable to the release of trapped gaseous NO within the polymer coating. (b) Mean cumulative NO release from POP-Gly-MMB-NO films over 24 h at pH 7.4 PBS at 37 °C (n = 3). Reported data obtained from three discrete polymer syntheses. Copyright 2017 American Chemical Society.

and the resulting NO release was recorded. To permit calculation of NO content (mmol g^{-1}) and NO flux (nmol min^{-1} cm^{-2}), all release measurements were obtained from 12 mm diameter glass circles coated with a single-sided layer of POP-Gly-MMB-NO of known mass derived from triplicate syntheses. Since NO release profiles arising from the decomposition of RSNOs frequently display exponential decay, NO release was monitored continuously over the initial 24 h release period to illustrate the relatively rapid change in NO release over this period (Figure 4.8a and 4.8b). To avoid the influence of dissolved copper on the observed decomposition profiles, glassware used in NO analysis experiments was treated with a saturated solution of EDTA-Na_2, then washed with Millipore water before use. Furthermore, PBS was analyzed by ICP-AES and not found to contain detectable levels of dissolved copper. Over 24 h of immersion, 0.15 ± 0.01 mmol NO g^{-1} was released, corresponding to 17 ± 2% of total available NO. This indicates a significantly slower rate of RSNO decomposition relative to the previously

reported *S*-nitrosated polyphosphazene derived from poly(*S*-methylthiocysteinyl-*co*-ethyl cysteinyl phosphazene), where 64% of available NO was released over 24 h under identical conditions. The formation of NO from the tertiary RSNO groups of POP-Gly-MMB-NO was anticipated to follow the general thermal decomposition pathway established for small-molecule RSNOs, wherein the S-N bond undergoes homolytic scission to form NO and the corresponding thiyl radical. As mentioned previously, these species may recombine non-productively, or thiyl radicals may combine to form disulfide with the concomitant release of NO. When compared to the previous cysteine-based NO-releasing POP, the reduction in the rate of NO release observed for POP-Gly-MMB-NO may largely result from the greater stability of the tertiary RSNO groups present in this polymer. Computationally, this difference in stability has been attributed to considerable steric congestion during dimerization of tertiary thiyl radicals, which favors recombination with NO.[36] Following each 24 h experiment, remaining NO was recovered by exposure of the coated substrates to UV light at 40 °C to obtain a total releasable NO content of 0.89 ± 0.09 mmol g^{-1}, or 4.3 ± 0.6 μmol cm^{-2}. Exposure to UV light was not found to produce any detectable NO release from POP-Gly-MMB-SH controls immersed in an identical medium. Comparison of the NO content of POP-Gly-MMB-NO with other materials based on tertiary RSNOs indicates a relatively large NO storage capacity. For example, Riccio *et al.* reported NO storage in the range of 0.87-1.78 μmol cm^{-2} for an NO-releasing xerogel incorporating a tertiary RSNO derived from *N*-acetylpenicillamine.[21] The ability of POP-Gly-MMB-NO to produce a prolonged NO flux was examined by measuring NO release from the coated substrates at regular intervals over a period of 14 d (Figure 4.9a). To represent the exponential decay observed for the NO release profile, the value of the initial flux (t = 0) was obtained from the maximum mean NO release immediately following immersion in PBS. All other flux calculations were based on the

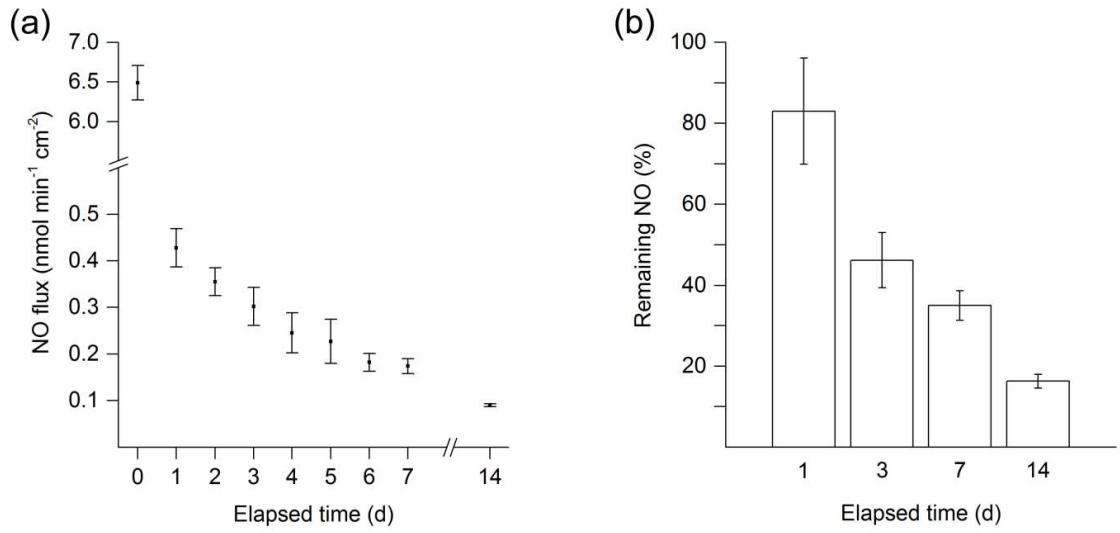

Figure 4.9 14 d NO flux from *S*-nitrosated poly(bis(3-mercapto-3-methylbut-1-yl glycinyl)phosphazene) coatings and residual NO content. (a) Mean NO flux over 14 d from glass substrates coated with POP-Gly-MMB-NO and suspended in pH 7.4 PBS at 37 °C. (b) Remaining NO at 1, 3, 7, and 14 d as determined by thermal/photolytic decomposition of polymer-coated substrates. Data points/bar height represent mean values and error bars represent standard deviation (n = 3). Reported data obtained from three discrete polymer syntheses. Copyright 2017 American Chemical Society.

mean NO release recorded at subsequent measurement points, where rapid changes in the rate of NO release no longer occurred. Between measurements, samples were incubated in pH 7.4 PBS at 37 °C under ambient atmosphere. The maximum initial NO flux of 6.5 ± 0.2 nmol min^{-1} cm^{-2} was followed by rapid decay to 0.43 ± 0.04 nmol min^{-1} cm^{-2} at the end of 24 h, followed by further decline to 0.090 ± 0.003 nmol min^{-1} cm^{-2} at the end of 14 d. To evaluate the stability of POP-Gly-MMB-NO under physiological conditions, substrates coated with the polymer were incubated in 5 mL of pH 7.4 PBS at 37 °C for 3, 7, and 14 days and their residual NO content was quantified by UV decomposition as previously described (Figure 4.9b). After 3 days, 46 ± 7% of the original NO content remained, with this value declining over 7 and 14 days of incubation to 35 ± 4% and 10 ± 1%, respectively.

Interpretation of the NO release properties of POP-Gly-MMB-NO requires reference to the body of literature concerning the effect of NO release with respect to various biological applications. It was reported by Ramamurthi and Lewis that platelet inhibition was largely complete at an NO surface flux between 0.3 and 0.6 fmol s^{-1} cm^{-2} (2×10^{-5}-4×10^{-5} nmol min^{-1} cm^{-2}) .[49] In the case of NO-releasing sol-gel microarrays, Robbins *et al.* found that an NO flux of 0.4 pmol s^{-1} cm^{-2} (0.02 nmol min^{-1} cm^{-2}) was sufficient to reduce platelet adhesion under certain conditions.[50] Furthermore, cultured bovine endothelial cells were found to exhibit an NO flux as low as 0.05 nmol min^{-1} cm^{-2}, while the endothelium has been mathematically estimated to produce an NO flux as high as 6.8×10^{-14} μmol s^{-1} μm^{-2} (0.41 nmol min^{-1} cm^{-2}).[51,52] This range has previously been used for comparative purposes to assess the potential utility of NO-releasing materials.[53,54] Substrates coated with POP-Gly-MMB-NO demonstrated an NO flux that remained within this broad endothelial range for the entirety of the two week measurement period. Moreover, the measured NO flux was significantly greater than the minimum level observed to exert antiplatelet effects, suggesting potential use as a source of antithrombotic NO in the case of bioresorbable stents or similar devices. Nablo and Schoenfisch reported that a sustained NO flux greater than 20 pmol s^{-1} cm^{-2} (1.2 nmol min^{-1} cm^{-2}) was required to prevent 75% of *P. aeruginosa* adhesion to a PVC-coated sol-gel, with the maximum antibacterial effect attributed to NO fluxes greater than 35 pmol s^{-1} cm^{-2} (2.1 nmol min^{-1} cm^{-2}).[55] Furthermore, Hetrick and Schoenfisch found that NO-releasing xerogels producing an NO flux of ~21 pmol s^{-1} cm^{-2} (1.3 nmol min^{-1} cm^{-2}) reduced *P. aeruginosa* adhesion by ~65%, with effective reduction in bacteria coverage also observed at significant lower NO fluxes.[56] Substrates coated with POP-Gly-MMB-NO exhibited a maximal NO flux at least 3 times greater than that required for the most effective reduction of *P. aeruginosa* adhesion in the case of prior, unrelated materials.

However, this NO flux is maintained for significantly less than 24 h, and thereafter the flux is limited to a range without significant antibacterial effects. While increased NO flux may theoretically be obtained from the deposition of a greater quantity of *S*-nitrosated polymer, doubling the mass of the coating did not produce any corresponding elevation in NO release. This observation was a probable consequence of the inability of the nitrosating agent *t*-BuONO to access the bulk polymer. Assessment of the swelling characteristics of POP-Gly-MMB-SH in *t*-BuONO/pentane using a gravimetric approach indicates no appreciable uptake of solvent over the course of the nitrosation. This lack of solvent diffusion suggests that *S*-nitrosation is largely confined to the surface of the polymer coating. NO has also been shown to influence wound healing under a variety of circumstances, which has led to the development of NO-releasing materials for the treatment of injuries.[9] For example, Diwan *et al.* observed that suppression of endogenous NO production impaired bone fracture healing, and that delivery of supplemental NO directly to the site of injury using a polymer-bound *N*-diazeniumdiolate ameliorated this impairment.[57] Because biodegradable polyphosphazenes have frequently been proposed as useful materials in bone tissue engineering, this may suggest a potential role for POP-Gly-MMB-NO beyond the development of NO-releasing coatings.[28]

4.3.4. Degradation study

Biodegradation of amine-substituted polyphosphazenes has been previously established to occur through gradual hydrolysis that liberates the organic substituents and ultimately converts the phosphorus-nitrogen backbone into self-neutralizing phosphate and ammonia.[28] For this reason, biodegradable POPs substituted with amino acids may be less likely to produce the local pH depression often associated with polyester degradation *in vivo*.[24,58] In the case of amino acid

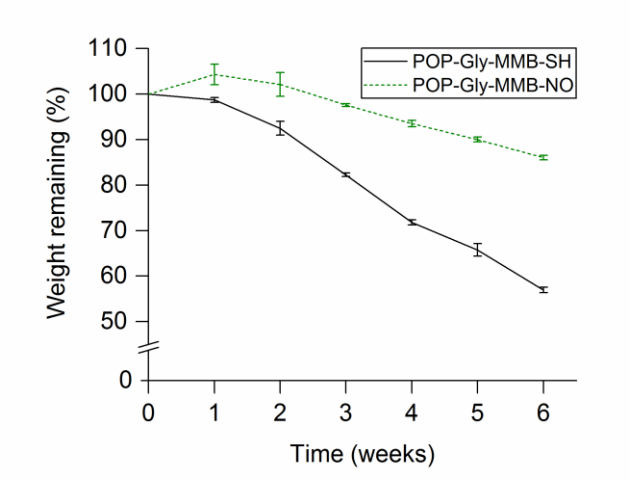

Figure 4.10 Degradation of polymers over six weeks. Conditions: pH 7.4 PBS at 37 °C. Data points represent mean values and error bars represent standard deviation (n = 5). Copyright 2017 American Chemical Society.

esters, POP degradation is accompanied by hydrolytic cleavage of the ester linkage to regenerate the parent alcohol. The specific degradation characteristics of POP-Gly-MMB-SH and POP-Gly-MMB-NO were assessed by immersion in pH 7.4 PBS at 37 °C for a total of six weeks (Figure 4.10).

To permit direct comparison with POP-Gly-MMB-SH, the initial mass of POP-Gly-MMB-NO was recorded in the form of the non-nitrosated precursor. This results in a subsequent mass increase from the conversion of thiol groups to RSNO. The buffer solution was replaced at the end of each week and found to maintain a constant pH. In the case of POP-Gly-MMB-SH, continuous degradation was observed during immersion in PBS, with 56.9 ± 0.6% of the initial mass remaining after the six week incubation period. POP-Gly-MMB-NO experienced a significantly slower rate of degradation when compared to the thiolated precursor, and 86.1 ± 0.5% of the initial mass remained at the end of the study. As noted previously, decomposition of the RSNO functional groups of POP-Gly-MMB-NO is accompanied by disulfide formation, a process that decreases the rate of degradation through crosslinking. This curing phenomenon

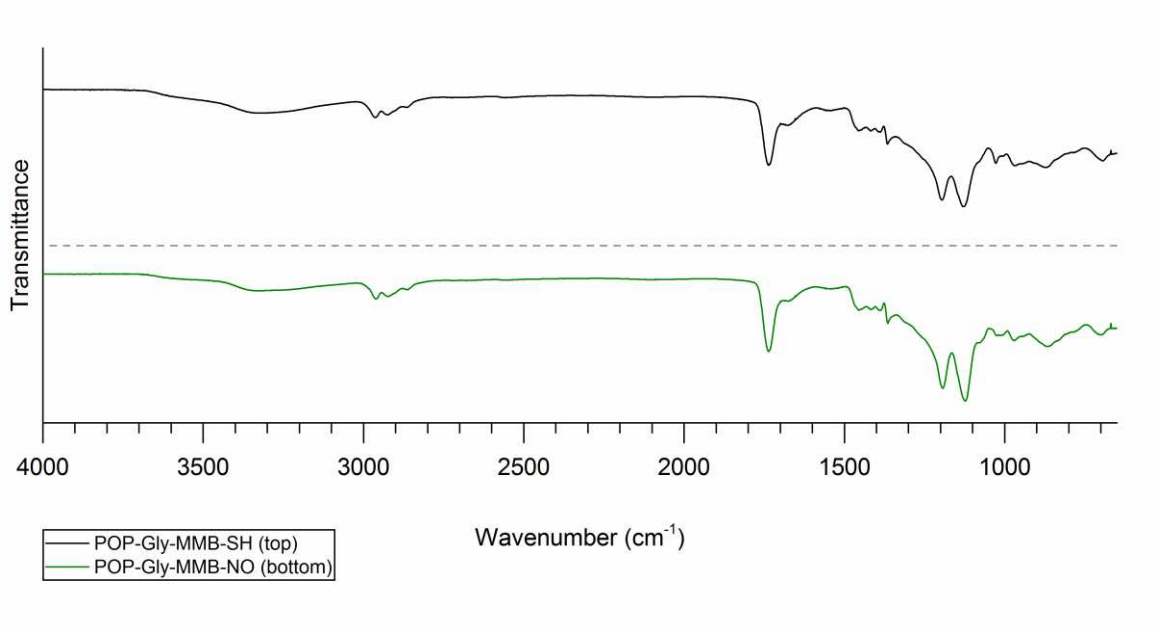

Figure 4.11 Top: ATR-FTIR spectrum of poly(bis(3-mercapto-3-methylbut-1-yl glycinyl)phosphazene) (POP-Gly-MMB-SH), following a 6-week degradation study. IR: 3326, 2963, 2926, 2866, 1737, 1682, 1542, 1456, 1418, 1388, 1365, 1196, 1128, 1028, 967, 873, 695 cm^{-1}. Bottom: ATR-FTIR spectrum of *S*-nitrosated poly(bis(3-mercapto-3-methylbut-1-yl glycinyl)phosphazene) (POP-Gly-MMB-NO), following a 6-week degradation study. IR: 3326, 2961, 2924, 2865, 1736, 1676, 1541, 1456, 1418, 1388, 1364, 1193, 1123, 1025, 971, 867, 701 cm^{-1}. Copyright 2017 American Chemical Society.

confers greater resistance to hydrolytic decomposition and improves the durability of POP-Gly-MMB-NO relative to the non-nitrosated material. After the six week degradation study had concluded, neither polymer exhibited any appreciable solubility. ATR-IR spectra of both POP-Gly-MMB-SH and POP-Gly-MMB-NO were generally consistent with that of the original non-nitrosated material (Figure 4.11). POP-Gly-MMB-NO no longer exhibited IR absorbance bands at 1492 (N=O) and 665 cm^{-1} (N-S) or the green color of tertiary RSNOs, supporting the expected decomposition of the NO donor moieties. In separate experiments, additional samples of the nitrosated and non-nitrosated polymer were suspended in deionized water for three weeks at 37 °C to evaluate the result of their degradation without buffering. POP-Gly-MMB-SH produced a minor pH elevation to 7.4, an outcome that was generally consistent with the anticipated near-neutrality of POP decomposition and lack of substantial acidic product formation.[28] In contrast,

Table 4.1 Mass spectrometry data.

Name	Formula	Exact Mass (m/z)	Measured Mass (m/z)	Mass Error (ppm)	Polarity
Glycine	$C_2H_5NO_2$	76.0393 $[M+H]^+$	76.0398	6.24	(+)
3-Mercapto-3-methylbutyl glycinate	$C_7H_{15}NO_2S$	178.0896 $[M+H]^+$	178.0893	2.1	(+)
3-Mercapto-3-methylbutanol	$C_5H_{12}OS$	119.0536 $[M-H]^-$	119.0545	6.96	(-)
3-((4-Hydroxy-2-methylbutan-2-yl)disulfanyl)-3-methylbutyl glycinate*****	$C_{12}H_{25}NO_3S_2$	296.1349 $[M+H]^+$	296.1348	0.47	(+)
3-((4-(Glycyloxy)-2-methylbutan-2-yl)disulfanyl)-3-methylbutyl 2-hydroxyacetate*	$C_{14}H_{27}NO_5S_2$	354.1403 $[M+H]^+$	354.1405	0.25	(+)

degradation of POP-Gly-MMB-NO produced a pH decline to the range of 3-4, which likely arises from the oxidation of NO to HNO_2 or HNO_3 in the presence of water and atmospheric oxygen and was an anticipated consequence of NO release under unbuffered conditions.[59]

To identify organic hydrolysis products of the polymers, samples were incubated in water for two weeks and the resulting media were analyzed by TOF-MS. The primary identifiable degradation products common to both polymers were glycine ($C_2H_5NO_2$), MMB ($C_5H_{12}OS$), and 3-mercapto-3-methylbut-1-yl glycinate ($C_7H_{15}NO_2S$), as shown in Table 4.1. This outcome is consistent with the anticipated degradation pattern of amine-substituted POPs, and suggests that glycine and MMB are the ultimate products of hydrolysis of the polymer and the liberated glycine-MMB ester. In the case of the *S*-nitrosated POP-Gly-MMB-NO, several additional ions

consistent with the disulfides 3-((4-hydroxy-2-methylbutan-2-yl)disulfanyl)-3-methylbut-1-yl glycinate ($C_{12}H_{25}NO_3S_2$) and 3-((4-(glycyloxy)-2-methylbutan-2-yl)disulfanyl)-3-methylbut-1-yl 2-hydroxyacetate ($C_{14}H_{27}NO_5S_2$) were found. Both molecules are likely to represent products of the disulfide-forming decomposition of RSNO. In the former case, the mass is consistent with a disulfide dimer of the glycine-MMB ester after the hydrolytic removal of a single glycine unit. In the latter case, the mass is attributable to a similar dimer with the substitution of a single glycine unit with glycolic acid. This apparent substitution is likely to arise from *N*-nitrosation of the glycine unit *via* nitrosating agents formed *in situ* by oxidation of released NO, such as nitrous acid or N_2O_3. This *N*-nitrosated intermediate is expected to lead to the diazotization of the amine group, followed by displacement of nitrogen gas and the formation of a glycolate derivative through reaction with water.[60]

4.4. Conclusions

This work presents the first use of a tertiary RSNO to achieve NO release from a biodegradable polyphosphazene. Previously, the synthesis of thiol-bearing polyphosphazenes from PDCP has been complicated by thiol protection schemes required to achieve selective substitution by amine groups. Unlike prior examples, it was found that no thiol protection/deprotection steps were necessary to achieve amine-selective substitution of PDCP during the synthesis of POP-Gly-MMB-SH, an outcome that was attributable to the use of a tertiary thiol. Substrates coated with POP-Gly-MMB-NO maintain a physiologically-relevant NO flux in the range of 6.5-0.090 nmol min^{-1} cm^{-2} for at least two weeks when compared to a reported natural endothelial flux of 0.05-0.4 nmol min^{-1} cm^{-2}. In addition, the overall NO content (0.89 ± 0.09 mmol g^{-1}, 4.3 ± 0.6 μmol cm^{-2}) indicated the presence of a significant reservoir of

releasable NO. 86.1 ± 0.5% of the original mass of POP-Gly-MMB-NO was found to remain after six weeks of immersion in pH 7.4 PBS at 37 °C, with the formation of degradation products that are consistent with the hydrolysis of amino ester-substituted polyphosphazenes in the presence of NO. This hydrolytic degradation largely resulted in the production of glycine and various esters derived from the naturally-occurring thiol MMB. Collectively, the data suggest that polyphosphazenes incorporating tertiary RSNOs are capable of physiologically-relevant NO release for an extended duration, and may be adaptable for use in biomaterials applications.

Individual contributions and funding sources

J. B. Tapia performed mass spectrometry studies. M. J. Neufeld acquired water contact angle measurements. All other work carried out by A. Lutzke. Funding for this work originated from the Department of Defense Congressionally Directed Medical Research Program (W81XWH-11-2-0113). The lab of Dr. Eugene Chen at Colorado State University provided access to GPC instrumentation and assistance with data processing.

Nuclear magnetic resonance spectra

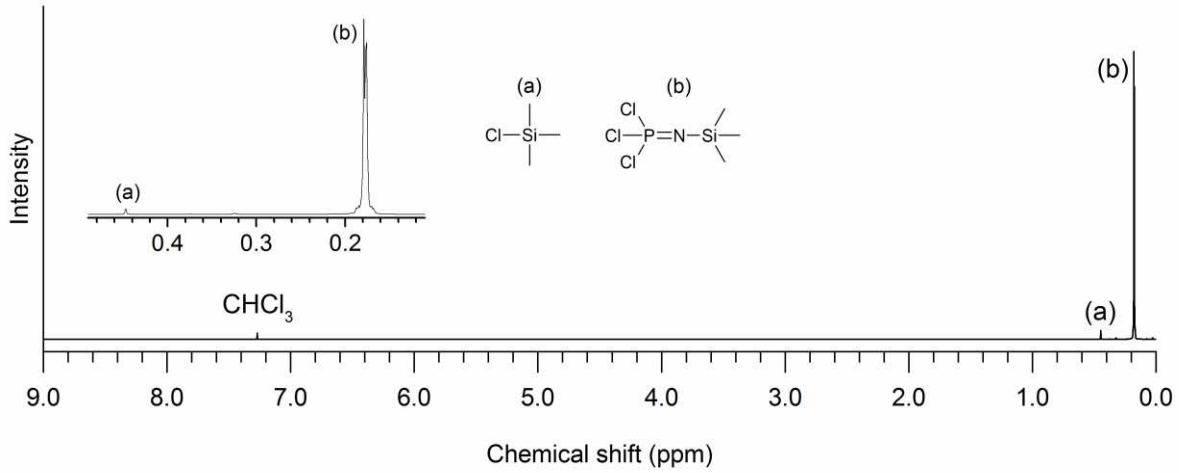

Figure 4.12 ^{1}H NMR spectrum of trichloro(trimethylsilyl)phosphoranimine. ^{1}H NMR (400 MHz, $CDCl_3$) δ 0.18 ppm (d, 9H). Chlorotrimethylsilane impurity at 0.45 ppm. Copyright 2017 American Chemical Society.

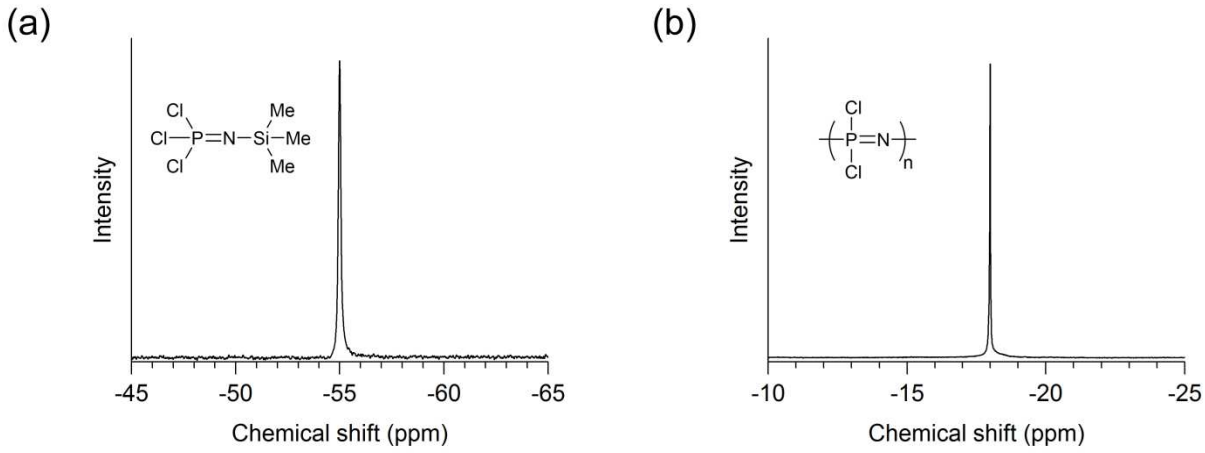

Figure 4.13 ^{31}P NMR spectra of trichloro(trimethylsilyl)phosphoranimine and poly(dichlorophosphazene). (a) Trichloro(trimethylsilyl)phosphoranimine ^{31}P NMR (162 MHz, $CDCl_3$) δ -55 ppm. (b) Poly(dichlorophosphazene). ^{31}P NMR (162 MHz, $CDCl_3$) δ -18 ppm. Copyright 2017 American Chemical Society.

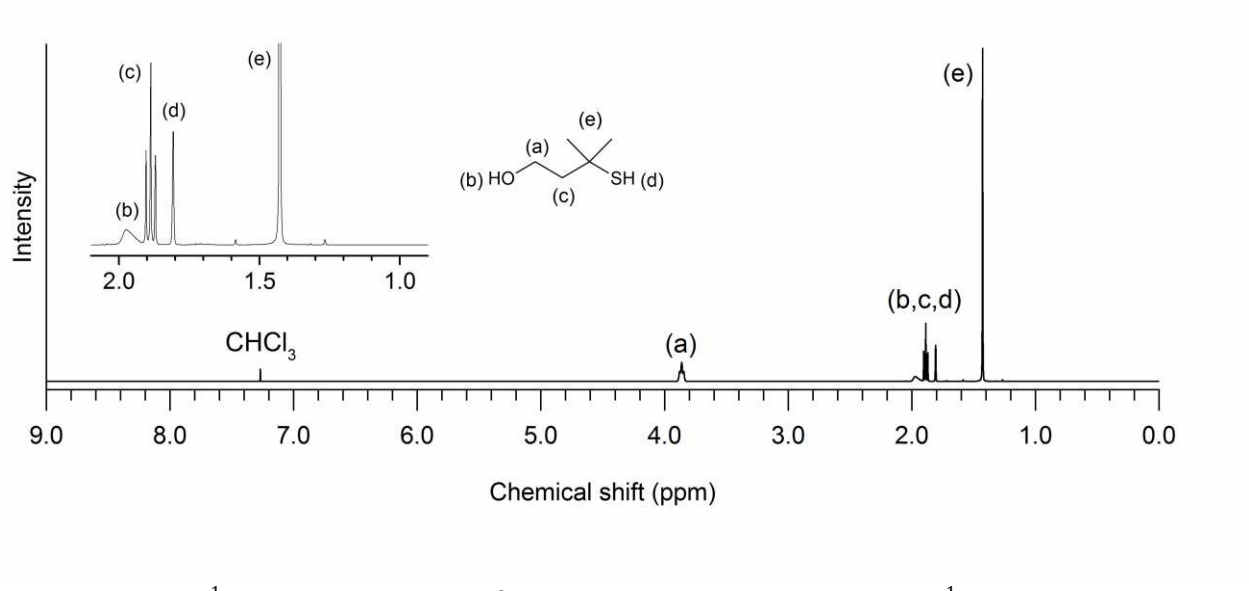

Figure 4.14 ^{1}H NMR spectrum of 3-mercapto-3-methylbutan-1-ol. ^{1}H NMR (400 MHz, $CDCl_3$) δ 3.86 (t, *J* = 6.8 Hz, 2H), 1.97 (s, 1H), 1.89 (t, *J* = 6.8, 2H), 1.81 (s, 1H), 1.43 ppm (s, 6H). Copyright 2017 American Chemical Society.

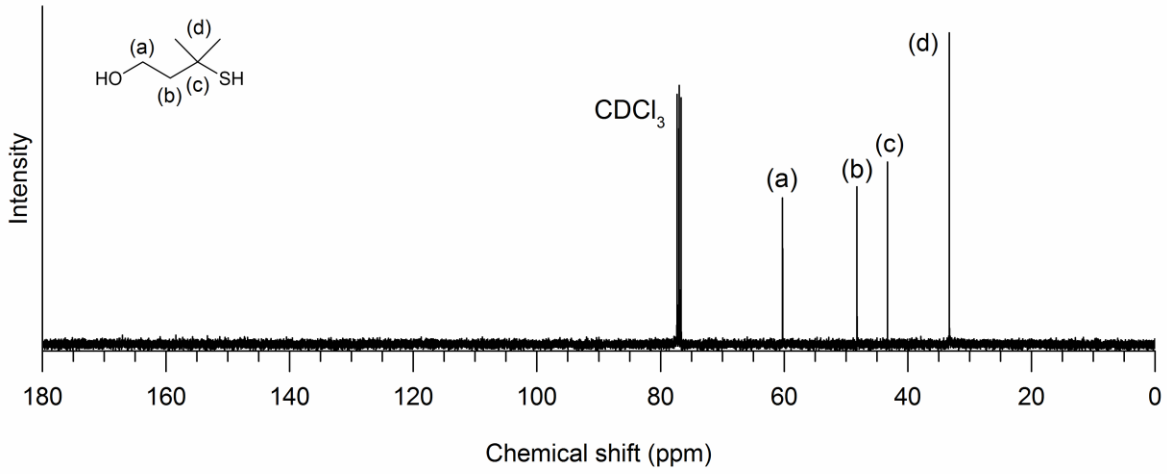

Figure 4.15 ^{13}C NMR spectrum of 3-mercapto-3-methylbutan-1-ol. ^{13}C NMR (100 MHz, $CDCl_3$) δ 60.26, 48.23, 43.28, 33.29 ppm. Copyright 2017 American Chemical Society.

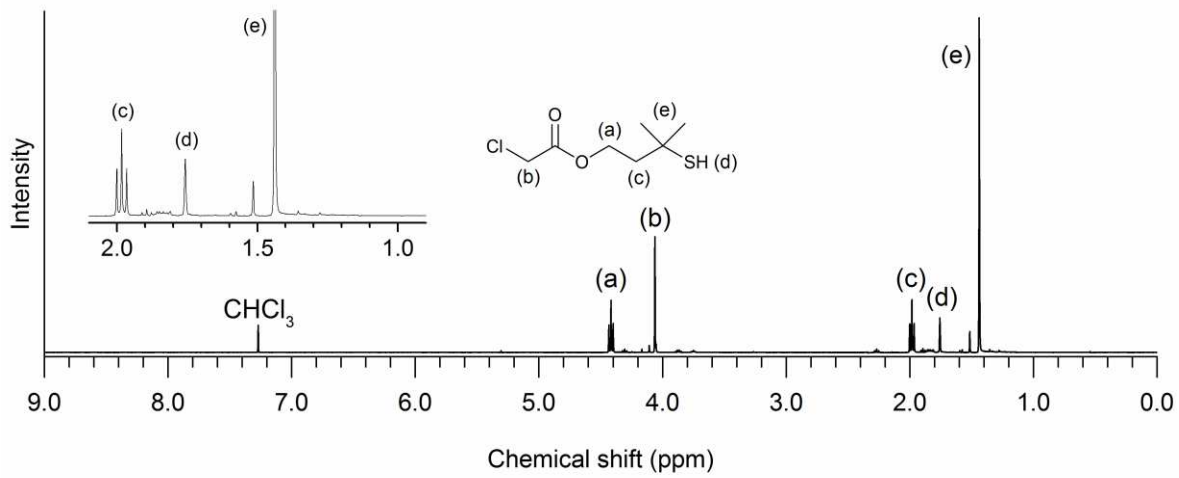

Figure 4.16 ^{1}H NMR spectrum of 3-mercapto-3-methylbut-1-yl chloroacetate. ^{1}H NMR (400 MHz, $CDCl_3$) δ 4.42 (t, *J* = 7.2 Hz, 2H), 4.06 (s, 2H), 1.98 (t, *J* = 7.2, 2H), 1.76 (s, 1H), 1.44 ppm (s, 6H). Copyright 2017 American Chemical Society.

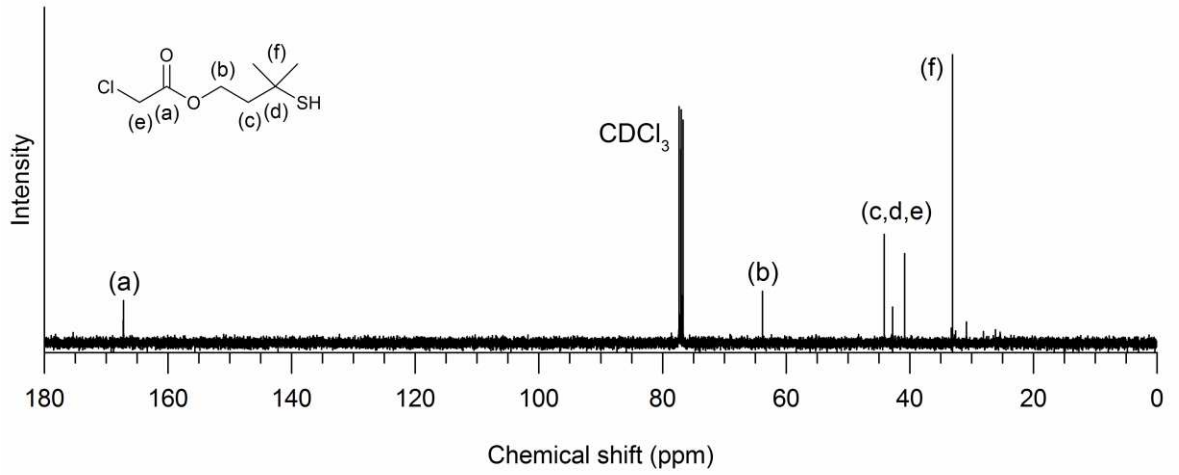

Figure 4.17 ^{13}C NMR spectrum of 3-mercapto-3-methylbut-1-yl chloroacetate. ^{13}C NMR (100 MHz, $CDCl_3$) δ 167.23, 63.84, 44.13, 42.78, 40.85, 33.10 ppm. Copyright 2017 American Chemical Society.

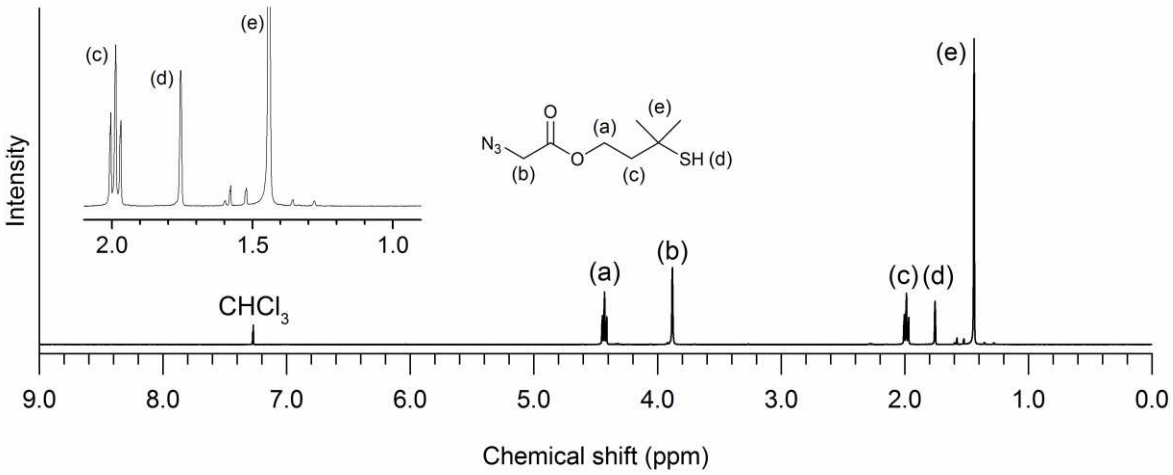

Figure 4.18. ^{1}H NMR spectrum of 3-mercapto-3-methylbut-1-yl azidoacetate. ^{1}H NMR (400 MHz, $CDCl_3$) δ 4.43 (t, *J* = 7.2 Hz, 2H), 3.88 (s, 2H), 1.99 (t, *J* = 7.2, 2H), 1.76 (s, 1H), 1.44 ppm (s, 6H). Copyright 2017 American Chemical Society.

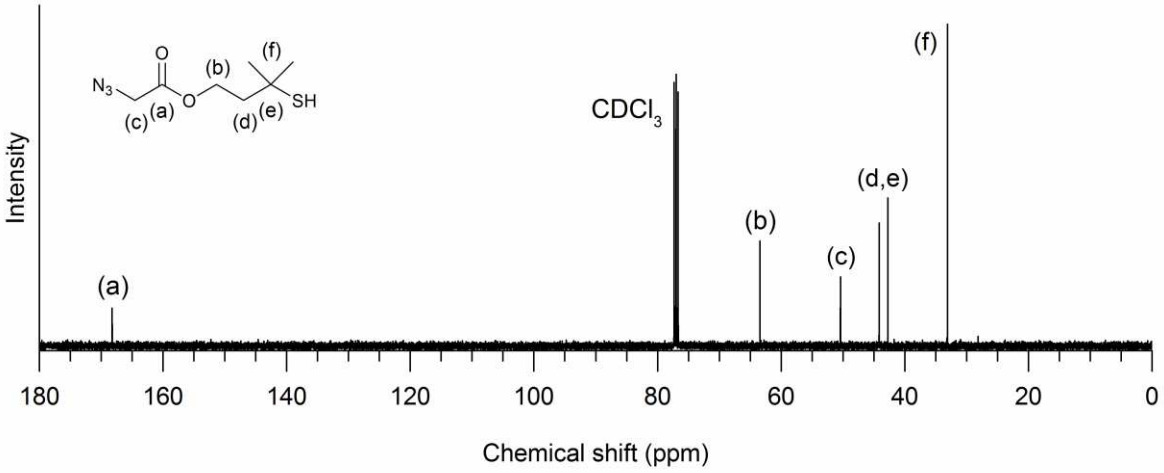

Figure 4.19 ^{13}C NMR spectrum of 3-mercapto-3-methylbut-1-yl azidoacetate. ^{13}C NMR (100 MHz, $CDCl_3$) δ 168.23, 63.44, 50.41, 44.15, 42.74, 33.08 ppm. Copyright 2017 American Chemical Society.

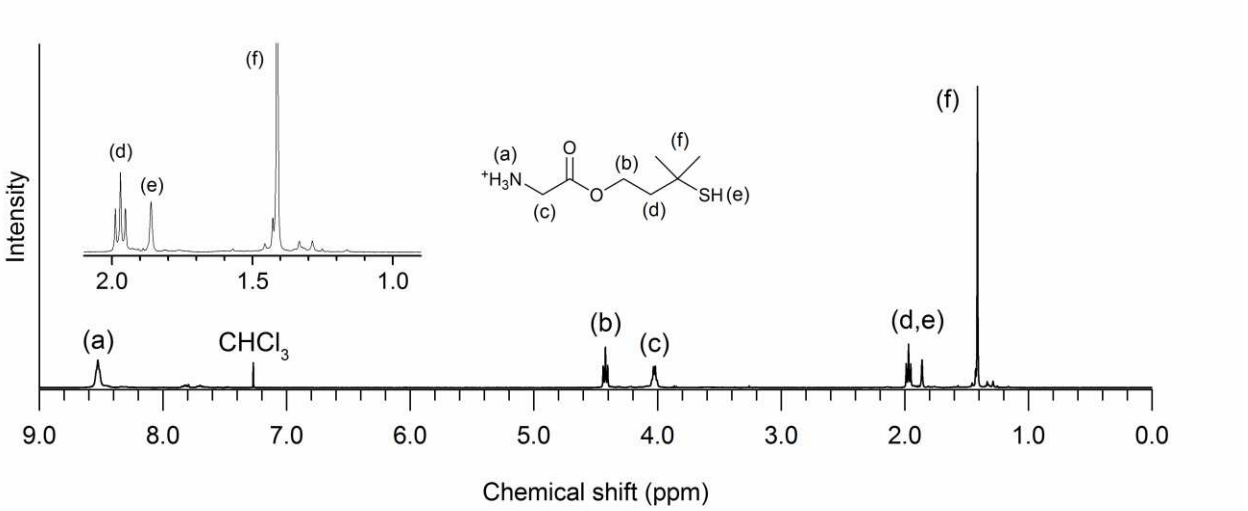

Figure 4.20 ^{1}H NMR spectrum of 3-mercapto-3-methylbut-1-yl glycinate hydrochloride. ^{1}H NMR (400 MHz, $CDCl_3$) δ 8.53 (s, 3H), 4.42 (t, *J* = 7.2 Hz, 2H), 4.03 (q, *J* = 6.0, 2H), 1.97 (t, *J* = 7.2, 2H), 1.86 (s, 1H), 1.41 ppm (s, 6H). Copyright 2017 American Chemical Society.

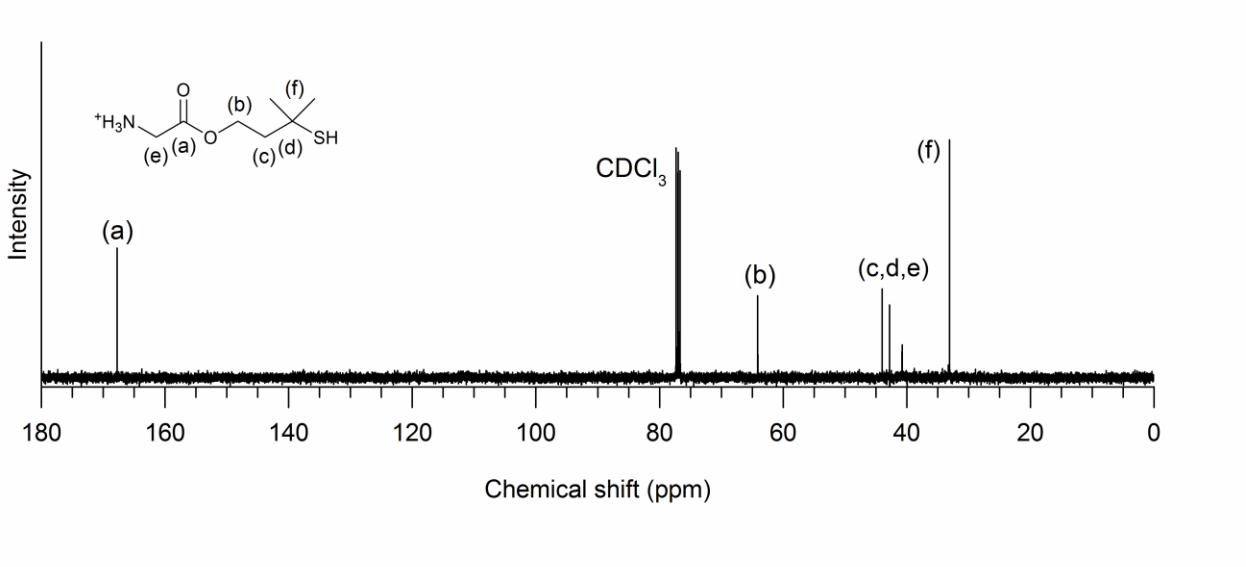

Figure 4.21 ^{13}C NMR spectrum of 3-mercapto-3-methylbut-1-yl glycinate hydrochloride. ^{13}C NMR (100 MHz, $CDCl_3$) δ 167.77, 64.12, 43.98, 42.80, 40.76, 33.09 ppm. Copyright 2017 American Chemical Society.

REFERENCES

1. Ignarro, L. J.; Buga, G. M.; Wood, K. S.; Byrns, R. E. Chaudhuri, G. *Proc. Natl. Acad. Sci. U.S.A.* **1987**, *84*, 9265-9269.
2. Bogdan, C. *Nat. Immunol.* **2001**, *2*, 907-916.
3. Andrew, P. J.; Mayer, B. *Cardiovasc. Res.* **1998**, *43*, 521-531.
4. Weitzberg, E.; Hezel, M.; Lundberg, J. O.. *Anesthesiology* **2010**, *113*, 1460-1475.
5. Moncada, S.; Higgs, E. A. *Br. J. Pharmacol.* **2006**, *147*, S193-S201.
6. Weinberg, J. B. *Mol. Med*. **1998**, *4*, 557-591.
7. Griffiths, M. J. D.; Evans, T. W. *N. Engl. J. Med.* **2005**, *353*, 2683-2695.
8. Carriedo, H.; Rhine, W. *J. Perinatol.* **2003**, *23*, 556-558.
9. Carpenter, A. W.; Schoenfisch, M. H. *Chem. Soc. Rev.* **2012**, *41*, 3742-3752.
10. Toledo, J. C., Jr.; Augusto, O. *Chem. Res. Toxicol*. **2012**, *25*, 975-989.
11. Reynolds, M. M.; Frost, M. C.; Meyerhoff, M. E. *Free Radic. Biol. Med*. **2004**, *37*, 926-936.
12. Lu, Y.; Slomberg, D. L.; Schoenfisch, M. H. *Biomaterials* **2014**, *35*, 1716-1724.
13. Schairer, D. O.; Chouake, J. S.; Nosanchuk, J. D.; Friedman, A. J. *Virulence* **2012**, *3*, 271-279.
14. Miller, M. R.; Megson, I. L. *Br. J. Pharmacol.* **2007**, *151*, 305-321.
15. Williams, D. L. H. *Chem. Commun*. **1996**, 1085-1091.
16. Tsikas, D.; Schmidt, M.; Böhmer, A.; Zoerner, A. A.; Gutzki, F-M.; Jordan, J. *J. Chromatogr. B.* **2013**, *927*, 147-157.
17. Keefer, L. K. *ACS Chem. Biol.* **2011**, *6*, 1147-1155.

18. Brisbois, E. J.; Davis, R. P.; Jones, A. M.; Major, T. C.; Bartlett, R. H.; Meyerhoff, M. E.; Handa, H. *J. Mater. Chem. B* **2015**, *3*, 1639-1645.

19. Li, Y.; Lee, P. I. *Mol. Pharmaceutics* **2010**, *7*, 254-266.

20. Vogt, C.; Xing, Q.; He, W.; Li, B.; Frost, M. C.; Zhao, F. *Biomacromolecules* **2013**, *14*, 2521-2530.

21. Riccio, D. A.; Coneski, P. N.; Nichols, S. P.; Broadnax, A. D.; Schoenfisch.. *ACS Appl. Mater. Interfaces* **2012**, *4*, 796-804.

22. Lutzke, A.; Neufeld, B. H.; Neufeld, M. J.; Reynolds, M. M. *J. Mater. Chem. B.* **2016**, *4*, 1987-1998.

23. Allcock, H. R. *Appl. Organometal. Chem*. **1998**, *12*, 659-666.

24. Rothemund, S.; Teasdale, I. *Chem. Soc. Rev*. **2016**, *45*, 5200-5215.

25. Huang, Y.; Liu, X.; Wang, L.; Li, S.; Verbeken, E.; De Scheerder, I. *Coron. Artery Dis*. **2003**, *14*, 401-408.

26. Henn, C.; Satzl, S.; Christoph, P.; Kurz, P.; Radeleff, B.; Stampfl, U.; Stampfl, S.; Berger, I.; Richter, G. M. *J. Vasc. Interv. Radiol.* **2008**, *19*, 427-437.

27. Allcock, H. R.; Pucher, S. R.; Scopelianos, A. G. *Macromolecules* **1994**, *27*, 1071-1075.

28. Deng, M.; Kumbar, S. G.; Wan, Y.; Toti, U. S.; Allcock, H. R.; Laurencin, C. T. *Soft Matter* **2010**, *6*, 3119-3132.

29. Deng, M.; Nair, L. S.; Nukavarapu, S. P.; Jiang, T.; Kanner, W. A.; Li, X.; Kumbar, S. G.; Weikel, A. L.; Krogman, N. R.; Allcock, H. R.; Laurencin, C. T. *Biomaterials* **2010**, *31*, 4898-4908.

30. Lakshmi, S.; Katti, D. S.; Laurencin, C. T. *Adv. Drug Delivery Rev.* **2003**, *55*, 467-482.

31. Scheerder, I. K.; Wilczek, K. L.; Verbeken, E. V.; Vandorpe, J.; Lan, P. N.; Schacht, E.; De Geest, H.; Piessens, J. *Atherosclerosis* **1995**, *7*, 105-114.

32. Bartberger, M. D.; Houk, K. N.; Powell, S. C.; Mannion, J. D.; Lo, K. Y.; Stamler, J. S.; Toone, E. J. *J. Am. Chem. Soc*. **2000**, *122*, 5889-5890.

33. Gürbüz, O.; Rouseff, J.; Talcott, S. T.; Rouseff, R. *J. Agric. Food Chem*. **2013**, *61*, 532-539.

34. Vermeulen, C.; Lejeune, I. Tran, T. T. H.; Collin, S. *J. Agric. Food Chem*. **2006**, *54*, 5061-5068.

35. Kumazawa, K.; Masuda, H. *J. Agric. Food Chem.* **2003**, *51*, 3079-3082.

36. Bainbrigge, N.; Butler, A. R.; Görbitz, C. H. *J. Chem. Soc., Perkin Trans. 2* **1997**, 351-354.

37. Miyazaki, M.; Yamashita, T.; Suzuki, Y.; Saito, Y.; Soeta, S.; Taira, H.; Suzuki, A. *Chem. Biol*. **2006**, *13*, 1071-1079.

38. Matyjaszewski, K.; Lindenberg, M. S.; Moore, M. K.; White, M. L. *J. Polym. Sci., Part A: Polym. Chem*. **1994**, *32*, 465-473.

39. Singler, R. E.; Schneider, N. S.; Hagnauer, G. L. *Polym. Eng. Sci.* **1975**, *15*, 321-338.

40. Potta, T.; Chun, C.; Song., S-C. *Biomaterials* **2009**, *30*, 6178-6192.

41. Weikel, A. L.; Owens, S. G.; Fushimi, T.; Allcock, H. R. *Macromolecules* **2010**, *43*, 5205-5210.

42. Williams, D. L. H. *Acc. Chem. Res.* **1999**, *32*, 869-876.

43. Ungnade, H. E.; Smiley, R. A. *J. Org. Chem.* **1956**, *21*, 993-996.

44. Wang, P. G.; Xian, M.; Tang, X.; Wu, X.; Wen, Z.; Cai, T.; Janczuk, A. J. *Chem. Rev.* **2002**, *102*, 1091-1134.

45. Arulsamy, N.; Bohle, D. S.; Butt, J. A.; Irvine, G. J.; Jordan, P. A.; Sagan, E. *J. Am. Chem. Soc.* **1999**, *121*, 7115-7123.

46. Fontijn, A.; Sabadell, A. J.; Ronco, R. J. *Anal. Chem.* **1970**, *42*, 575-579.

47. de Oliveira, M. G.; Shishido, S. M.; Seabra, A. B.; Morgon, N. H. *J. Phys. Chem. A* **2002**, *106*, 8963-8970.

48. Williams, D. L. H. *Methods Enzymol.* **1996**, *268*, 299-308.

49. Ramamurthi, A.; Lewis, R. S. *Biomed. Sci. Instrum.* **1999**, *35*, 333-338.

50. Robbins, M. E.; Hopper, E. D.; Schoenfisch, M. H. *Langmuir* **2004**, *20*, 10296-10302.

51. Radomski, M. W.; Palmer, R. M. J., Moncada, S. *Biochem. Biophy. Res. Commun.* **1987**, *148*, 1482-1489.

52. Vaughn, M. W.; Kuo, L.; Liao, J. C. *Am. J. Physiol.: Heart Circ. Physiol.* **1998**, *274*, H2163-H2176.

53. Pegalajar-Jurado, A.; Joslin, J. M.; Hawker, M. J.; Reynolds, M. M.; Fisher, E. R. *ACS Appl. Mater. Interfaces* **2014**, *6*, 12307-12320.

54. Skrzypchak, A. M.; Lafayette, N. G.; Bartlett, R. H.; Zhou, Z.; Frost, M. C.; Meyerhoff, M. E.; Reynolds, M. M. Annich, G. M. *Perfusion* **2007**, *22*, 193-200.

55. Nablo, B. J.; Schoenfisch, M. H. *Biomacromolecules* **2004**, *5*, 2034-2041.

56. Hetrick, E. M.; Schoenfisch, M. H.. *Biomaterials* **2007**, *28*, 1948-1956.

57. Diwan, A. D.; Wang, M. X.; Jang, D.; Zhu, W.; Murrell, G. A. C. *J. Bone Miner. Res.* **2000**, *15*, 342-351.

58. Liu, H.; Slamovich, E. B.; Webster, T. J. *Int. J. Nanomedicine* **2006**, *1*, 541-545.

59. Aga, R. G.; Hughes, M. N. *Methods Enzymol.* **2008**, *436*, 35-48.

60. Kirmse, W. *Angew. Chem. Int. Ed. Engl.* **1976**, *15*, 251-320.

CHAPTER 5

FUTURE DIRECTIONS AND PRACTICAL CONSIDERATIONS

5.1. *S*-Nitrosothiols as useful sources of therapeutic nitric oxide

The frequent use of RSNOs as NO donor molecules over the last two decades demonstrates continued interest in their unique NO-forming properties. However, it must be recognized that several notable shortcomings currently restrict the practical implementation of RSNOs in a medical context. The inability to control the fundamental instability of the RSNO functional group is arguably the most crucial limitation, and represents a significant barrier to long-term use within a biological setting. Exposure to heat and light accelerate the NO-forming decomposition of the RSNO functional group, which imposes the requirement that suitable storage conditions be maintained until use.[1] Although this is not a unique concern and applies to many pharmaceuticals, the comparatively rapid decomposition of RSNOs presents a challenge with respect to routine clinical use. As a partial consequence of the known susceptibility of RSNOs to temperature and light, the kinetics of the NO-forming decomposition of RSNOs depends upon prevailing conditions, which may complicate the controlled *in vivo* delivery of specific NO dosages. While *N*-diazeniumdiolates show clean first-order decomposition kinetics leading to the release of NO, RSNOs frequently exhibit much more complex behavior, including fractional kinetic orders.[2,3] This variation in kinetics may be attributable to the sensitivity of RSNOs to pH conditions, the presence of certain transition metal ions, thiols, and even dissolved gases, among other species known to influence the rate of RSNO decomposition.[1,4,5] Nevertheless, certain RSNOs exhibit great stability at room or physiological temperature, particularly when isolated

within polymers. For example, Brisbois *et al.* observed that the incorporation of SNAP within a polyurethane matrix permitted the retention of 82% of the initial quantity of RSNO after storage for 2 months at 37 °C.[6] This outcome is not representative of the more rapid decomposition typically observed for polymer-RSNO conjugates (where useful release periods are frequently limited to hours or days), and is most directly attributable to isolation of SNAP within a polymeric matrix. In general, it can be stated that finer control over the kinetics of decomposition and extension of the useful NO release period are desirable goals in the development of future RSNO-based biomaterials. This may be achieved on a fundamental level through the use of RSNOs that exhibit greater inherent stability, or through the engineering of materials that modulate exposure to environmental decomposition triggers.

For the purposes of this discussion, it should be understood that the most common method of preparing RSNO-based biodegradable materials is through the polymeric incorporation of a small molecule thiol, which is subsequently converted to the RSNO derivative. This thiol may be directly included as a monomer during polymerization,or may be conjugated to the backbone of a structurally-unrelated polymer after its synthesis.[7,8] The latter (and most common) approach produces numerous pendant groups that may exhibit chemical behavior that is quite distinct from that of the original polymer chain. As such, it is often useful to consider the RSNO moiety as a discrete (and potentially modular) component rather than an integral element of the polymer. In the past, many NO-releasing biomaterials have incorporated primary RSNO groups, often derived from naturally-occurring thiols such as L-cysteine.[9] With the exception of GSNO, the majority of primary RSNOs are remarkably unstable and generally do not permit extended (*i.e.* multi-day or multi-week) NO release when bound to polymers. While GSNO remains an appealing candidate due to its stability and natural occurrence in human biochemistry, its high

molecular weight and the chemical properties of its tripeptide structure may limit the versatility of materials that include it as an NO donor moiety. In general, the greater stability of tertiary RSNOs (in comparison to primary or secondary examples) suggests that future RSNO-based biomaterials should preferentially target these structures.[10] Unfortunately, the library of synthetically-useful, commercially-available tertiary thiols is limited and many entries have uncertain toxicological behavior. Moreover, even commonly used tertiary RSNOs such as racemic SNAP may warrant toxicity concerns. In the absence of definitive biological data, the formation of racemic SNAP *in vivo* during biodegradation of a polymer can be anticipated to produce health concerns related to the potential regeneration of the toxic pyridoxine inhibitor and metal chelator, L-penicillamine.[11] Chapter 4 of this dissertation utilized the food-grade tertiary thiol 3-mercapto-3-methylbutanol as an alternative to penicillamine-based compounds, but does not evaluate the toxicity of this compound with respect to mammalian cell lines.

Overall, the synthesis of biodegradable RSNO-based polymers would greatly benefit from the thorough chemical and toxicological characterization of new tertiary thiols/RSNOs that can be effectively incorporated within polymer structures. Because the major utility of the RSNO functional group is as an instrument of *useful* NO release, access to a larger library of well-characterized, stable RSNOs will encourage the thoughtful development of future NO-releasing materials. This groundwork is crucial in a field that has haphazardly paired RSNOs with various polymer architectures without clear alignment between their respective properties. This concern is not limited to NO release duration, and extends to fundamental incompatibilities between the RSNO unit and practical use of the polymer. In cases where hydrophobicity is desirable, it may be inappropriate to utilize amino acid-based RSNOs (particularly those with remaining amine or carboxylic acid groups) as NO donors. This similarly applies in cases where the presence of

acidic or basic functional groups are likely to influence the rate of polymer hydrolysis. Toxic thiols and their derivative RSNOs should not be utilized in any capacity if the polymer is intended to degrade in a biological environment. The mechanical properties of a polymer are also likely to be affected by disulfide-forming RSNO decomposition, since this process may facilitate crosslinking. It is therefore sensible to advise that future work should carefully consider whether the local structure of the incorporated RSNO supports the intended application of the polymer. In summary, while the usefulness of RSNOs as polymer-bound NO donors remains clear, additional work is needed at a fundamental level to ensure that chemically-compatible donors are utilized with controlled, biologically-relevant NO release.

5.2. The use of chitin and chitosan as nitric oxide release platforms

Although chitin has been investigated for select biomedical applications, it is not easily processed from solution into useful forms.[12] The most effective solvents are concentrated solutions of lithium chloride/dimethylacetamide or calcium chloride/methanol.[13,14] Furthermore, the useful antibacterial and hemostatic properties of chitin are largely attributable to the presence of glucosamine units, leading to the natural conclusion that the more fully deacetylated derivative chitosan represents a more useful material. For this reason, the development of NO-releasing chitin derivatives is likely to remain limited and of little practical consideration. In contrast, recent interest in NO-releasing chitosan derivatives (often in the oligosaccharide form) has been persistent and well-represented among multiple publications.[15-17] As a hemostatic agent, bulk chitosan is inherently unsuitable for development into an NO-releasing *antithrombotic* material.[12] Consequently, NO-releasing chitosan derivatives are restricted to antibacterial or wound-treatment applications. Much of the appeal of utilizing non-toxic, biodegradable chitosan

as an NO-release platform originates from the retention of its therapeutic characteristics. However, both RSNO formation and NO release from chitosan is not necessarily chemically innocuous with respect to the polysaccharide, and may produce undesirable structural changes that influence the ultimate behavior of the material. For example, the exposure of chitosan to nitrosating agents typically used in the preparation of RSNOs may result in the formation of alkyl nitrites (RONO) from the C3/C6 hydroxyl groups or deamination through diazotization and the subsequent displacement of nitrogen by opportunistic nucleophiles (or potentially by ring-contraction, as in the case of heparin).[18,19] In Chapter 2, ATR-FTIR was used to characterize the NO-releasing chitosan derivatives and the loss of either the hydroxyl groups or the primary amine was not evident. This was achieved through acidification of the reaction solution, which is likely to suppress *N*-nitrosation by protonation of primary amine groups.[20] Furthermore, the addition of methanol may produce an equilibrium that favors the formation of gaseous methyl nitrite over nitrosation of the polysaccharide hydroxyl groups.[21] It has also been demonstrated that HNO_2 (either used deliberately as a nitrosating agent or formed as a product of NO release) may effect the depolymerization of certain polysaccharides.[18] Regardless of the specific mode of interactivity, it is clear that chitosan cannot be expected to function as an inert NO release platform. Instead, chitosan should be treated as a reactive substrate that may be actively modified by NO chemistry. It is therefore the case that future NO-releasing chitosan derivatives must be carefully evaluated for evidence of deleterious chemical changes after NO release (particularly under biologically relevant conditions) or exposure to nitrosating agents. A greater degree of rigor in the general characterization protocols used for NO-releasing chitosan materials may permit the elimination of unwanted side reactions and facilitate their development into products suitable for *in vivo* use.

A second area of refinement concerns the synthetic methods used during incorporation of the RSNO donor group. The most direct approach to thiolation of chitosan involves the conjugation of a thiol-bearing carboxylic acid to the C2 primary amine *via* amide formation, an outcome that may be achieved through the use of carbodiimide chemistry.[22] Carbodiimide-based protocols have been utilized with varying degrees of success, and may be inhibited by the interception of reactive intermediates by sulfhydryl groups or other competitive nucleophiles.[23] Notably, Kurita *et al.* were unable to effectively acetylate chitosan using 1-ethyl-3-(3-dimethylaminopropyl)carbodiimide, even in the absence of a thiol group. The possibility of interference from thiol groups has previously led to the use of *S*-protection strategies that complicate the otherwise straightforward synthesis.[24] Moreover, the use of an amide-forming strategy requires the permanent functionalization of the C2 primary amine, which is likely to impair both the aqueous solubility and critical antibacterial and hemostatic properties of chitosan as the degree of derivatization increases. For these reasons, Chapter 2 discusses the use of an alternative approach involving modification of hydroxyl groups. This strategy begins with protection of the primary amine groups as the *N*-phthaloyl derivative, followed by *O*-tosylation, the thioether-forming introduction of the sulfhydryl group as the free end of a symmetrical dithiol, and deprotection by hydrazine. The resulting materials *qualitatively* retain the primary amine group, but exhibit impaired solubility that may be attributable to disulfide formation. Consequently, this comparatively chemistry-intensive synthesis can be described as altering the fundamental properties of chitosan — a non-ideal outcome from both preparative and applicative perspectives. Furthermore, the overall complexity of this synthesis increases the likelihood that side reactions or contaminants remain present that are not detected by ATR-FTIR. Future development in this area should ideally attempt to confer NO release function without any

significant alteration of the relevant physicochemical properties of chitosan itself, using the minimum number of synthetic steps. Furthermore, elimination of the dithiol reagents used to introduce the sulfhydryl functionality may reduce the likelihood of toxicity. While incorporation of RSNO by substitution of the hydroxyl groups is a useful protocol from a purely synthetic perspective, practical applications (*e.g.* processable chitosan derivatives for the preparation of bandages) will likely require less dramatic structural alteration. Since the water solubility of chitosan is maintained even at relative high degrees of acetylation, it is probable that the most chemically-benign strategy remains the functionalization of the C2 amine group *via* carbodiimide chemistry. The use of a carboxylic acid bearing a tertiary thiol may eliminate (through steric hindrance) certain concerns related to the reactivity of the sulfhydryl group, although this outcome cannot be assured. The implementation of *S*-protection chemistry has experimental utility as a method of screening for thiol-mediated side reactions, but may not be desirable as a component of a finalized protocol. As a general direction, the selection of an appropriate thiol for the modification of chitosan and the methodical evaluation of various coupling conditions is a sensible approach to the development of next-generation NO-releasing derivatives. In this context, the methodology described in Chapter 2 is complementary to direct, amine-targeted strategies that are less synthetically complex and more likely to produce polymers suited to biomedical applications.

5.3. The use of polyphosphazenes as nitric oxide release platforms

Although *S*-nitrosated polyesters have been widely employed as biodegradable NO release platforms, demonstrations of polyphosphazenes in this role are currently constrained to the two examples provided in Chapters 3 and 4 of this dissertation. As described elsewhere in this work,

the inorganic phosphorus-nitrogen polyphosphazene backbone permits the attachment of various organic substituents at the phosphorus atom, including thiols that may be subsequently converted to RSNOs. While the use of polyphosphazenes as NO-releasing polymers may be justified by their widespread investigation as biomaterials (primarily for tissue engineering or device coatings), much of their appeal is derived from synthetic considerations. Poly(dichlorophosphazene) (PDCP) can be accessed by multiple techniques, including the *conceptually* straightforward ring-opening reaction of hexachlorocyclotriphosphazene or the polymerization of phosphoranimines.[25,26] In the latter case, molecular weights generally exhibit relatively narrow polydispersities.[27] As demonstrated in Chapter 3 and 4, replacement of the geminal chlorine atoms by substitution with suitable thiol-containing nucleophiles occurs under mild conditions (as low as 25 °C), with good reproducibility. Although the nitrogen atom of the phosphazene unit exhibits some degree of basicity, *S*-nitrosation occurs without any apparent reaction of the polyphosphazene backbone when characterized by IR spectroscopy.[28] In both evaluated cases, the release of NO from *S*-nitrosated polyphosphazenes does not result in any apparent structural changes beyond the loss of RSNO and the hypothesized formation of disulfide (resulting in impaired solubility). Furthermore, the P=N backbone repeating unit has a total mass of only 45 Da, compared to a mass of 58 Da for the repeating unit of the simplest polyester, poly(glycolic acid). Consequently, the contribution of RSNO substituents to the overall mass and physicochemical properties of the polymer is vastly greater in the case of polyphosphazenes than for NO-releasing polyesters prepared from the conjugation of thiols. As such, the polyphosphazene backbone represents *a platform for nitric oxide release* (or other useful functions) in a much more literal sense than any other existent polymer system. As an example, poly(bis(3-mercapto-3-methylbut-1-yl glycinyl)phosphazene) (POP-Gly-MMB) may

be conceptualized as an immobilized, macromolecular form of the 3-mercapto-3-methylbut-1-yl glycinyl substituents, which comprise 89% of its repeating unit mass. Although only a fraction of the theoretical thiol is converted to RSNO, this suggests the potential for remarkably high NO loading (mol NO/mass polymer).

Many of the drawbacks of the first reported NO-releasing polyphosphazene, *S*-nitrosated poly(ethyl *S*-methylthiocysteinyl-*co*-ethyl cysteinyl phosphazene) (POP-EtCys), are addressed in some form by the development of the subsequent material POP-Gly-MMB, following certain principles outlined in Section 5.1 of this chapter. As originally observed by Weikel *et al*., incorporation of the ethyl cysteinyl pendant groups of POP-EtCys required the use of an *S*-protection strategy to prevent chemoselectivity issues arising from the competitive substitution of PDCP by thiol instead of amine.[29] Because most common thiol protecting groups require deprotection conditions that are poorly tolerated by polyphosphazenes, the primary thiol ethyl cysteinate was protected as the methyl disulfide using the malodorous, expensive, and potentially toxic reagent *S*-methyl methanethiosulfonate. Following synthesis of the *S*-protected polymer, the similarly noxious disulfide-cleaving agent 2-mercaptoethanol was employed to produce free thiol groups. This process did not proceed to completion, and resulted in the retention of potentially labile (through disulfide exchange) methyl disulfide groups. In the case of POP-Gly-MMB, it was anticipated that the greater steric congestion of the tertiary thiol would favor substitution of PDCP by the amine group of 3-mercapto-3-methylbut-1-yl glycinate. This hypothesis was supported by the outcome that a single major product was observed, corresponding to covalent attachment of the amine and preservation of thiol. When immersed in pH 7.4 phosphate buffered saline (PBS) at 37 °C, the relatively rapid decay of the primary RSNO of POP-EtCys-NO (36% remaining after 24 h) slowed considerably in the case of the

tertiary RSNO groups of POP-Gly-MMB-NO (83% remaining after 24 h). This slower decomposition resulted in maintenance of physiologically-relevant NO release for 2 weeks, with 16% of the initial NO content remaining. The apparent increase in stability may be attributable to a variety of factors, however the use of tertiary RSNO groups remains the most probable explanation. Although the toxicity of POP-Gly-MMB has not been evaluated, the use of glycine and naturally-occurring, food-grade 3-mercapto-3-methylbutan-1-ol as building blocks and the elimination of protection/deprotection steps with hazardous reagents represents meaningful progress toward biomedically-useful polymers.

While their value from a purely synthetic perspective is clear, it is currently unknown whether NO-releasing polyphosphazenes are suitable for use as biomaterials. Future development in this area must emphasize the identification of practical applications for such materials and a tailored approach to their design. Because polyphosphazenes may be substituted with multiple, chemically-distinct pendant groups (frequently achieved through sequential reactions), the properties of NO-releasing polyphosphazenes may be tunable through the inclusion of new substituents. In the case of amino acid ester-substituted polyphosphazenes (such as the polymers discussed in this work), the relative fragility of these materials may be enhanced through the use of appropriate organic substituents.[30] This may permit both the retention of NO release and the ability to confer mechanical properties that are better suited to a target application, such as tissue engineering or the fabrication of medical devices. In spite of the fact that NO-releasing polyphosphazenes have yet to be assessed *in vivo* for specific biological applications, the established therapeutic effects of NO and the great synthetic versatility of the polyphosphazene architecture suggests promise for future biomedical implementation.

REFERENCES

1. Williams, D. L. H. *Chem. Commun.* **1996**, 1085-1091.
2. Keefer, L. K. *ACS Chem. Biol.* **2011**, *6*, 1147-1155.
3. Zhao, Y.-L.; McCarren, P. R.; Houk, K. N.; Choi, B. Y.; Toone, E. J. *J. Am. Chem. Soc.* **2005**, *127*, 10917-10924.
4. Hu, T.-M.; Chou, T.-C. *AAPS J.* **2006**, *8*, E485-E492.
5. Grossi, L.; Montevecchi, P. C.; Strazzari, S. *J. Am. Chem. Soc.* **2001**, *123*, 4853-4854.
6. Brisbois, E. J.; Handa, H.; Major, T. C.; Bartlett, R. H.; Meyerhoff, M. E. *Biomaterials* **2013**, *34*, 6957-6966.
7. Seabra, A. B.; Martins, D.; Simões, M. M. S. G.; Da Silva, R.; Brocchi, M.; De Oliveira, M. G. *Artif. Organs* **2010**, *34*, E204-E214.
8. Damodaran, V. B.; Joslin, J. M.; Wold, K. A.; Lantvit, S. M.; Reynolds, M. M. *J. Mater. Chem.* **2012**, *22*, 5990-6001.
9. Frost, M. C.; Meyerhoff, M. E. *J. Biomed. Mater. Res. A* **2005**, *72*, 409-419.
10. Bartberger, M. D.; Houk, K. N.; Powell, S. C.; Mannion, J. D.; Lo, K. Y.; Stamler, J. S.; Toone, E. J. *J. Am. Chem Soc.* **2000**, *122*, 5889-5890.
11. Jaffe, I. A.; Altman, K.; Merryman, P. *J. Clin. Invest.* **1964**, *43*, 1869-1873.
12. Jayakumar, R.; Prabaharan, M. Sudheesh Kumar, P. T.; Nair, S. V.; Tamura, H. *Biotechnol. Adv.* **2011**, *29*, 322-337.
13. Ravi Kumar, M. N. V. *React. Funct. Polym.* **2000**, *46*, 1-27.
14. Tamura, H.; Nagahama, H.; Tokura, S. *Cellulose* **2006**, *13*, 357-364.
15. Lu, Y.; Slomberg, D. L.; Schoenfisch, M. H. *Biomaterials* **2014**, *35*, 1716-1724.

16. Lu, Y.; Shah, A.; Hunter, R. A.; Soto, R. J.; Schoenfisch, M. H. *Acta Biomater.* **2015**, *12*, 62-69.

17. Reighard, K. P.; Schoenfisch, M. H. *Antimicrob. Agents Chemother.* **2015**, *59*, 6506-6513.

18. Shively, J. E.; Conrad, H. E. *Biochemistry* **1976**, *15*, 3932-3942.

19. Vilar, R. E.; Ghael, D.; Li, M.; Bhagat, D. D.; Arrigo, L. M.; Cowman, M. K.; Dweck, H. S.; Rosenfeld, L. *Biochem. J.* **1997**, *324*, 473-479.

20. Kirmse, W. *Angew. Chem. Int. Ed. Engl.* **1976**, *15*, 251-320.

21. Doyle, M. P.; Terpstra, J. W.; Pickering, R. A.; LePoire, D. M. *J. Org. Chem.* **1983**, *48*, 3379-3382.

22. Kast, C. E.; Bernkop-Schnürch, A. *Biomaterials* **2001**, *22*, 2345-2352.

23. Ulrich, H. *Chemistry and Technology of Carbodiimides*; John Wiley & Sons, Ltd.: Chichester, 2007, p 98.

24. Kurita, K.; Yoshino, H.; Nishimura, S.-I.; Ishii, S. *Carbohydr. Polym.* **1993**, *20*, 239-245.

25. Allen, G.; Lewis, C. J.; Todd, S. M. *Polymer* **1970**, *11*, 31-43.

26. Honeyman, C. H.; Manners, I. Morrissey, C. T.; Allcock, H. R. *J. Am. Chem. Soc.* **1995**, *117*, 7035-7036.

27. Rothemund, S.; Teasdale, I. *Chem. Soc. Rev.* **2016**, *45*, 5200-5215.

28. Nair, L. S.; Khan, Y. M.; Laurencin, C. T. Polyphosphazenes. In *An Introduction to Biomaterials*, 2nd ed.; Hollinger, J. O., Ed.; CRC Press: Boca Raton, 2012.

29. Weikel, A. L.; Owens, S. G.; Fushimi, T.; Allcock, H. R. *Macromolecules* **2010**, *43*, 5205-5210.

30. Deng, M.; Laurencin, C. T.; Allcock, H. R.; Kumbar, S. G. Polyphosphazenes as Biomaterials. In *Polymeric Biomaterials: Structure and Function*, Vol. 1; Dumitriu, S.; Popa, V., Eds.; CRC Press: Boca Raton, 2013.